DESIGN OF A SOLAR POWERED UNMANNED AIRSHIP

A THESIS SUBMITTED TO
THE GRADUATE SCHOOL OF NATURAL AND APPLIED SCIENCES
OF
MIDDLE EAST TECHNICAL UNIVERSITY

BY

ONUR SİNAN SÖNMEZ

IN PARTIAL FULFILLMENT OF THE REQUIREMENTS
FOR
THE DEGREE OF MASTER OF SCIENCE
IN
AEROSPACE ENGINEERING

SEPTEMBER 2015

Approval of the thesis:

DESIGN OF A SOLAR POWERED UNMANNED AIRSHIP

submitted by **ONUR SİNAN SÖNMEZ** in partial fulfillment of the requirements for the degree of **Masters of Science in Aerospace Engineering Department, Middle East Technical University** by,

Prof. Dr. Gülbin Dural Ünver
Director, Graduate School of **Natural and Applied Sciences** _____

Prof. Dr. Ozan Tekinalp
Head of Department, **Aerospace Engineering** _____

Prof. Dr. Nafiz Alemdaroğlu
Supervisor, **Aerospace Engineering Department, METU** _____

Examining Committee Members:

Prof. Dr. Serkan Özgen _____
Aerospace Engineering Dept., METU

Prof. Dr. Nafiz Alemdaroğlu _____
Aerospace Engineering Dept., METU

Prof. Dr. Altan Kayran _____
Aerospace Engineering Dept., METU

Prof. Dr. Kahraman Albayrak _____
Mechanical Engineering Dept., METU

Assistant Prof. Dr. Mustafa Kaya _____
Aerospace Engineering Dept., THK Uni.

Date: 04.09.2015

I hereby declare that all information in this document has been obtained and presented in accordance with academic rules and ethical conduct. I also declare that, as required by these rules and conduct, I have fully cited and referenced all material and results that are not original to this work.

Name, Last name: Onur Sinan Sönmez

Signature:

ABSTRACT

DESIGN OF A SOLAR POWERED UNMANNED AIRSHIP

Sönmez, Onur Sinan
M.S., Department of Aerospace Engineering
Supervisor: Prof. Dr. Nafiz Alemdaroğlu

September 2015, 123 pages

This thesis presents the design and analysis of a low altitude, high endurance Unmanned Airship which is capable of carrying payloads up to 70 kg to 1000 meters altitude. This UAV has an endurance of 2 weeks and can resist winds up to 90 km/h. It is completely solar powered and it uses Helium as the lifting gas and uses electric motors to change it's location.

The purpose of this thesis is to design an unmanned, completely solar powered airship to be used for various missions such as: reconnaissance missions, broadcasting, base transceiver station, forest fires, traffic control and coastal surveillance. Even there are various concepts and right hand rules about the design process of an airship, some of them have become obsolete with the improvements in material sciences and technological improvements.

An empirical approach has been used as a base while making the necessary calculations. Although for the beginning of design process, some of those right hand rules have been used, in the detailed design process a deeper study has been made and the real values have been used. Even though, this type of an UAV is not a conventional approach; compared with the aerodynamic UAV's and the other surveillance aircrafts this kind of configuration is a much cheaper (in terms of both the initial cost and the operating costs) and a much safer choice.

The empirical approach gave the chance to review the design to meet the requirements even at the latest stages of design. For example after CFD analysis, the motors to be used have been changed to meet the thrust requirement.

Keywords: UAV, Unmanned Solar Powered Airship, Detailed Design

ÖZ

GÜNEŞ ENERJİSİ İLE ÇALIŞAN İNSANSIZ ZEPLİN TASARIMI

Sönmez, Onur Sinan
Yüksek Lisans, Havacılık ve Uzay Mühendisliği Bölümü
Tez Yöneticisi: Prof. Dr. Nafiz Alemdaroğlu

Eylül 2015, 123 sayfa

Bu tezde, 70 kg'a kadar faydalı yükleri 1000 metre irtifaya çıkarabilecek alçak irtifa, yüksek uçuş süresine sahip bir İnsansız Hava Gemisi Tasarımı sunulmaktadır. Bu İHA, 2 hafta maksimum uçuş süresine sahip olacaktır ve 90 km/saat'e kadar rüzgarlara dayanabilecektir. Tamamiyle güneş enerjisi ile çalışacak olup, gerek duyulan kaldırma kuvvetini Helyum gazını kullanarak sağlayacaktır ve konum değiştirmek için de elektrik motorlarını kullanmaktadır.

Bu tezin amacı; keşif görevleri, yayın yayın yapmak, baz istasyonu alıcı/verici istasyonu, orman yangınlarını önleme, trafik kontrolü ve sahil güvenlik gibi pek çok farklı görevde kullanılabilecek olan tamamen güneş enerjisi ile çalışan, insansız bir hava gemisi tasarlamaktır. Bir hava gemisinin tasarımı süreci ile ilgili birbirinden farklı bir çok konsept ve emprik data olmasına karşın, bunlardan bazıları malzeme bilimindeki ilerlemelerden ve teknolojik ilerlemelerden ötürü démodé ve eskide kalmış olarak kabul edilir.

Gerekli hesaplamalar yapılırken temel olarak emprik bir yaklaşım kullanılmıştır. Tasrım sürecinin başlarında yukarıda da bahsedilen birtakım genel kurallar kullanılmış olsa da, detaylı tasarım sürecinde daha derin bir araştırma gerçekleştirilmiş ve bunun sonucunda çıkan değerler kullanılmıştır. Emprik yaklaşım, tasarım sürecinin en son aşamalarında dahi tasarımın yeniden gözden geçirilmesine ve gerekli değişikliklerin kolayca

uygulanmasına olanak tanımıştır. Örneğin CFD analizinin ardından daha güçlü elektrik motorlarının kullanılması gerektiği görülmüştür.

Bu tip bir İHA alışılagelmiş bir model olmamasına rağmen, ayrodinamik emsallerine kıyaslahem ilk maliyet hem de işletme maliyeti açısından çok daha ucuz bir seçenektir.

Anahtar Kelimeler: İHA, İnsansız Güneş Enerjili Hava Gemisi, Detay Tasarım

Dedicated to my dearest wife and family

ACKNOWLEDGEMENTS

I would like to express my heartfelt thanks and deepest gratitude to my supervisor Prof. Dr. Nafiz Alemdaroğlu who was a pleasure to work with. His support, guidance, advice, encouragements and insight through the study provided along the way with this thesis were invaluable. I have been fortunate to have an advisor who broadens my mind and gives the freedom space to research on my own. I owe debt to him.

I also would like to thank to all of my friends for their moral support and suggestions. Particularly, I would like to give special thanks to Güçlü Özcan and Eren Turanoğuz who never left me alone during studying on my thesis. Thank you for being with me through this difficult process.

Lastly, I wish to express my gratitude to my family who always stand next to me whenever I needed and especially my dear beautiful wife Demet Yıldıran Sönmez who never let go of my hand beginning from the first day we met next to always standing behind me throughout this thesis process. I also want to thank our daughter (!) Bızdık Yıldıran Sönmez for being so cute. Thank you so much for your endless love, understanding and patience throughout this study although I could not always create enough time to spend with you. Thank you for always being there whenever I needed and thank you for believing in me when I doubted myself. Your moral support, encouragement and the joy you gave me helped me to complete this thesis. I am also deeply grateful to each of you as being a part of my life.

TABLE OF CONTENTS

LIST OF TABLES

TABLES

LIST OF FIGURES

FIGURES

LIST OF SYMBOLS

Symbol	Description	Unit
ρ	Density of the lifting fluid	kg / m^3
g	Gravitational force	m/s^2
V	Volume of the body that has been immersed into the fluid	m^3
He_{loss}	Amount of helium that is lost	m^3
W_{total}	Total weight	kg
D	Drag	N
R_{major}	Rear ellipsoid's major radius	m
r_{major}	First ellipse's major radius (front one)	m
R_{minor}	Rear ellipsoid's minor radius	m
r_{minor}	First ellipse's minor radius	m
Re_v	Reynolds number	-
$Q_{discharge}$	Helium rate released to air	m^3/s
Λ	Permeability coefficient of which for different base materials	m^2
μ	Viscosity	Pa*s
ρ_g	Gas pressure	Pa
ρ_a	Air pressures	Pa
l	Thickness of the fabric material	m
L	Airship length	m
A_V	Vertical tail area	m^2
A_H	Horizontal tail area	m^2

Symbol	Description	Unit
A_E	Elevator area	m^2
A_R	Rudder area	m^2
C_D	Drag coefficient	-
C_L	Lift coefficient	-
C_m	Pitching moment coefficient	-
C_n	Yawing moment coefficient	-
C_l	Rolling moment coefficient	-
C_N	Side force coefficient	-
$F_{buoyancy}$	Buoyancy force	N
$A_{density\_hull}$:	Area density of the hull of airship	kg/m^2
A_{hull}:	Area of the hull of airship	m^2
$W_{balloon}$	Balloon weight	kg
$W_{balloonet}$	Ballonet weight	kg
$A_{balloonet}$	Ballonet area	m^2
$r_{ballonet}$	Ballonet radius	m
$V_{ballonet\_needed}$	Needed ballonet volume	m^3
$A_{total\_ballonet}$	Total ballonet area	m^3
W_{tail_system}	Tail system weight	kg
$A_{ControlSurfaces}$	Control surface area	m^2
W_{solar_panels}	Solar panels total weight	kg
W_{each_panel}	Weight of each solar panel	kg
N_{panels}	Number of solar panels	-

Symbol	Description	Unit
W_{solar_sys}	Solar system weight	kg
W_{MPPT_sys}	MPPT system weight	kg
N_{Serial}	Number of serial connected batteries	-
$N_{Parallel}$	Number of parallel connected batteries	-
I_{per_cell}	Current of each battery cell	A
$W_{battery}$	Weight of battery	kg
S_{count}	Serial connected battery count	-
P_{count}	Parallel connected battery count	-
$W_{battery\_configuration}$	Battery configuration weight	kg
$W_{power\_man\_sys}$	Power management system weight	kg
kV	Engine's productivity	RPM/Volt
RPM_{max}	Maximum rates per minute	RPM
$W_{engines}$	Engines weight	kg
$W_{Turnigy}$	Weight of turnigy roto max 80cc	kg
$W_{sub\_comp\_engines}$	Weight of the engine's sub-components	kg
$W_{vectoring\_rod}$	Vectoring rod weight	kg
$L_{vectoring\_rod}$	Vectoring rod length	kg
W_{engine_system}	Engine system weight	kg
$W_{sub\_comp\_vectoring}$	Vectoring sub-component weight	kg
$W_{thrust\_vectoring\_system}$	Thrust vectoring system weight	kg
$W_{propulsion\_system}$	Propulsion system weight	kg

Symbol	Description	Unit
$W_{payload}$	Payload weight	kg
$W_{gondola\_structure}$	Gondola structural weight	kg
$V_{gondola\_structure}$	Gongola volume	m^3
$W_{avionics}$	Avionics weight	Kg
$W_{GONDOLA}$	Gondola total weight	kg
$W_{suspension\_system}$	Suspension system weight	kg
$V_{airship}$	Airship volume	m^3
W_{nose_group}	Weight of the nose group	kg
$W_{access\&maintenance}$	Weight of access & maintanance	kg
V_{needed}	Needed volume	m^3
D	Density	m^3
A_{each_seam}	Area of each seam	m^2
A_{seam_total}	Total seam area	m^2
N_{seam}	Number of seams	-
A_{fabric_total}	Total fabric area	m^2
W_{fabric}	Fabric weight	kg
$A_{density\_fabric}$	Area density of fabric	kg/m^2
$W_{nose\_cone\_system}$	Nose cone system weight	kg
W_{nose_cone}	Nose cone weight	kg
$W_{nose\_cone\_battens}$	Nose cone battens weight	kg
$W_{spike\_configuration}$	Spike configuration weight	kg

Symbol	Description	Unit
W_{tail_cone}	Tail cone weight	kg
W_{spike}	Spike weight	kg
$W_{batten\_connections}$	Batten connections weight	kg
$W_{base\_ring\&support\_rods}$	Base ring and support rods weight	kg
$W_{battens\_configuration}$	Battens configuration weight	kg
$W_{battens}$	Battens weight	kg
$W_{hooks\&bonding}$	Hook and bonding weight	kg
$L_{battens\_total}$	Total length of the battens to be used	m
L_{each_batten}	length of each batten	m
$N_{battens}$	Number of battens	-
$SW_{battens}$	Specific weight of battens	kg/m
$L_{suspension\_lines}$	Suspension lines length	m
$W_{suspension\_lines}$	Weight of suspension lines	kg
SW_{ropes}	Specific weight of ropes	kg/m
$W_{seams\&patches\_suspension}$	Weight of seams and patches of suspension system	kg
$W_{suspension\_sys}$	Weight of suspension system	kg
ρ_{∞}	Free air density	m^3
V_{∞}	Free air velocity	m/s
S_{ref}	Reference area	m^2
$D_{envelope}$	Envelope diameter	m^2
D_{Total}	Total diameter	m^2

Symbol	Description	Unit
$T_{Generated}$	Generated thrust	N
V	Volume	m^3
A_{CS}	Control surface area	m^2
$A_{inverted\_tail}$	Inverted tail area	m^2
$X_{tail\_ending\_point}$	Tail ending point location	m
l_{hull}	Total length of hull	m
$X_{tail\_stating\_point}$	Tail starting point	m
C_{tip_tail}	Tail tip chord	m
C_{root_tail}	Tail root chord	m
Λ_{tail}	Taper ratio of tail	-
S	Tail planform area	m^2
AR	Aspect ratio of tail	-
b^2	Span of tail	m
L	Lift force	N
C_L	Lift coefficient	-
q_∞	Dynamic pressure	m^5/s^2
$S_{p\_airship\_0°}$	Planform area of the airship at 0° incident angle	m^2
$C_{D\_airship\_\alpha=0°}$	Drag coefficient of the airship at 0° incident angle	-
q_∞	Dynamic pressure	m^5/s^2
$D_{airship\_\alpha=0°}$	Drag of airship at 0° incident angle	N
$S_{p\_airship}$	Planform area of the airship	m^2

Symbol	Description	Unit
$S_{p\_airship\_90°}$	Planform area of the airship at 90° incident angle	m^2
$C_{D\_airship\_\alpha=90°}$	Drag coefficient of the airship at 90° incident angle	-
b_{non_moving}	Span of the non-moving section of tail	M
b_{moving_sec}	Span of the moving section of tail	m
$X_{hing\_point\_moving}$	Hing point of the moving section of the tail	m
$c_{root\_moving\_sec}$	Chord of the tail root's moving section	m
$S_{p\_airship\_15°}$	Planform area of the airship at 15° tail incident angle	m^2
$C_{D\_airship\_\alpha=15°}$	Drag coefficient of the airship at 15° tail incident angle	-
$D_{airship\_\alpha=15°}$	Drag of the airship at 15° tail incident angle	N
m_{tail}	Tail weight	kg
x_{CB}	Center Of buoyancy position	m
x_{CG_tail}	Tail CG position	m
m_{nose_sys}	Nose system weight	kg
$x_{CG\_nose\_sys}$	Nose system CG	m
m_{hull}	Hull weight	kg
x_{CG_hull}	Hull CG	m
$m_{gondola}$	Gondola weight	kg
$x_{CG\_gondola}$	Gondola CG	m
N	Yaw moment	N*m
N_{wing}	Yaw moment generated by wing	N*m
$N_{fuselage}$	Yaw moment generated by fuselage	N*m

Symbol	Description	Unit
F_{tail}	Force generated by tail	N
$X_{a.c._tail}$	Aerodynamic center of tail	M
$X_{c.g.}$	Location of CG	M
X_{rudder}	Rudder length	M
X_{chord}	Chord length	M
C_n	Yaw moment coefficient	-
D_{actual}	Actual drag	N
D_{CFD}	Drag coefficient gathered by CFD	-
T_R	Thrust required	N
$W_{annular}$	Weight per meter	kg/m
F_{tail}	Force generated by tail	N
$X_{a.c._tail}$	Aerodynamic center of tail	M
$X_{c.g.}$	Location of CG	M
X_{rudder}	Rudder length	M
X_{chord}	Chord length	M
C_n	Yaw moment coefficient	-
D_{actual}	Actual drag	N

LIST OF ABBREVIATIONS

UAV	Unmanned Aerial Vehi$_c$le
CFD	Computational fluid dynamics
NPL	National Physics Laboratory
MPPTS	Maximum Peak Power Tracking System
MMPT	Maximum Peak Power Tracking
LiPo	Lithium-ion polymer
CB	Center of Buoyancy
CG	Center of Gravity
RPM	Revolutions per Minute
CATIA	Computer Aided Three-dimensional Interactive Application (Conception Assistée Tridimensionnelle Interactive Appliquée)

CHAPTER 1

INTRODUCTION

1.1. A Brief Introduction

The airships had long been used in order to satisfy human kind's desire of flight until the well-known accident which is widely known as Hindenburg disaster. This accident not only destroyed the public confidence in rigid airships but also ended the airship era long ago [1].

The main reason of the disaster was using Hydrogen instead of Helium for buoyancy, which is very easy to achieve but highly flammable. The static electric accumulated on the airframe caused an ignition of spark whenever the ropes were held by the ground crew. And the hydrogen leakage from the airframe caused the entire airship to burn completely within a few seconds [1]. From that day on, the trend for buoyant gases has turned to Helium instead of Hydrogen, as Helium is an inert gas and it does not react with other particles easily. So beginning to use Helium restarted the airship era once again.

With the restart of the airship era; the start of the unmanned air vehicle (UAV) era coincided. As the need for their capabilities have increased dramatically, unmanned aerial vehicles are used almost in every area of our lives nowadays from sports events to armed battlefields. But mostly, they are being used for reconnaissance missions which serves for the biggest power on earth today: information.

Gathering and using this information effectively is the most influential pursuit of today's world. There are no pitched battles left nowadays; but instead guerilla warfare tactics are used as it is much cheaper and needs less material and in order to succeed against this kind of tactic, opposing forces cannot fight with their tanks or artilleries. Instead they

should act before the opposing forces, meaning that they have to be one step ahead always. And reconnaissance plays a big role in achieving this one step ahead mission all the time [2].

In today's world, ensuring national security has become the most important mission for governments to achieve. In order to achieve this mission, border patrol and security plays a big role to prevent leakages of national security or to quell with the potential terrorist attacks. Also, maritime patrol and security plays a big role in order to tackle with the illegal immigration or to follow-up with the contaminants left in offshores [3]. Surveillance is another important actor in order to maintain national security against both the terrorist attacks and potential conflicts between other countries and for surveillance uses, the high field of view ability is of utmost importance [4][5]. Civilian use of UAV's is also becoming popular in broadcasting, forest fires, traffic controls and such.

1.2. Why an Airship?

Using lighter than air technology is a much safer way to fly than compared with the aero dynamical counterparts whenever Helium is considered as the buoyant gas instead of Hydrogen. Hydrogen has more lifting capacity than Helium as Helium's density is 0.164 kg/m^3, whereas Hydrogen's density is 0.08988 kg/m^3 at 0 C° and 1 atm pressure. Hydrogen, also is much easier to achieve and it has much less tendency to escape which makes it easier to keep it inside the envelope and the envelope fabric material will be less expensive and easier to access and produce. Even if there are many positive aspects of using Hydrogen as a lifting gas in an airship; because of the highly flammable nature of the Hydrogen, Helium will be used as the buoyant gas in this thesis.

Since Archimedes have found the principle of buoyancy to find out if the crown of the king was really made up of solid gold or not, the lifting force of the fluids have been used extensively. But, using air as the lifting fluid is forming the basis of the aerostatic

forces that will allow the airship to fly. The formula for the well-known Archimedes' principle of buoyancy is:

$$F_{buoyancy} = \rho * g * V \quad (1.1)$$

Where, ρ is the density of the lifting fluid which is 1.225 kg/m^3 at 1 atm pressure at 0 C°. "g" is the gravitational force which is 9.81 m/s^2 and V the volume of the body that has been immersed into the fluid. The weight of the Helium in this case will be subtracted from the lifting capacity also with the other component weights (hull, gondola, tail, payload, etc...). And whenever weight equals lifting force, the operating ceiling condition would be satisfied for that altitude also (see equation 1.2) where W_{total} is the total weight.

$$F_{buoyancy} = W_{total} \quad (1.2)$$

Airships have become very advantageous in many aspects compared with aircrafts and helicopters, as it can be seen easily at Table 1.1 [6]. In terms of almost all branches, airships have a big advantage with regards to their monitoring abilities. They are much cheaper to operate; they make much less noise; they have much less fuel consumption; they operate under much less vibration and turbulence related issues; they have much higher endurance, vertical take-off and landing and the hovering capabilities.

Table 1.1 Comparing Various Air Vehicles [6]

Project Requirement	Airplane	Helicopter	Airship
Low operation cost	✓✓	✓	✓✓✓
Long endurance	✓✓	✓	✓✓✓
Hovering capability	✓	✓✓✓	✓✓✓
Payload to weight ratio	✓✓	✓	✓✓✓
High maneuverability	✓✓	✓✓✓	✓
Low noise and turbulence	✓	✓	✓✓✓
Vertical take-off and landing	✓	✓✓✓	✓✓✓
Low fuel consumption	✓✓	✓	✓✓✓
Low vibration	✓✓	✓	✓✓✓

✓: low or none ✓✓: medium ✓✓✓: high

Low operating costs is one of the biggest advantages that an airship has, compared with the aerodynamic counterparts of it. As aerostatic forces helps the airship to beat the gravitational forces instead of aerodynamic forces, much less noise, vibration and turbulence will exist to be dealt with meaning easier handling, lower operational costs, lower maintenance costs and lower manufacturing costs.

The high endurance capability of UAV's is a huge plus against the manned competitors as endurance is one of the main aspect for aircraft design as it limits the flight duty period. Endurance can both be increased by increasing the space available for fuel or by using renewable energy resources instead of fuel. Higher endurance means wider areas of use as longer times will be available for the given missions. Even between compatible UAV's, airships have the longest endurance capability, as it does not use aerodynamic forces, in order to lift, of which lifting with the help of aerodynamic forces can be very consuming in terms of both engineering, manufacturing, maintenance and operational

costs. As the only forces that needs to be beaten is the drag force, endurance will increase dramatically compared with aerodynamically lifted counterparts.

Another advantage of the airships is their hovering ability compared with the aerodynamic counterparts. An airplane cannot hover unless it has thrust vectoring abilities (such as Harrier). Even if it succeeds in hovering, a lot of fuel consumption will be needed in order to beat the gravitational forces. A helicopter has great hovering abilities but in return it has very high operational costs to achieve this mission. The only force that needs to be beaten in an airship, while hovering, is the drag force due to winds meaning also much less operational costs for the same hovering ability with a helicopter.

Another advantage of the airships is that they produce less noise, vibration and turbulence compared with the aerodynamically lifted counterparts again [6]. As, no aerodynamic forces are needed in order to beat the gravitational forces, no airframe velocity is needed; meaning that less engine power is needed. Less engine power means less noise produced by the propeller; and as mainly there is no other noise producing element on the airship; noise production becomes very low. This leads to better surveillance conditions as heat and noise is much less, the noticeability of the airship decreases dramatically. Turbulence again becomes a negligible issue as the airframe velocity is not significant, and even if the airframe length is high enough to put the flow into turbulence conditions; this again is negligible compared with the turbulent conditions that might arise with the aero dynamical counterparts.

Also much less fuel will be consumed as the only forces that need to be beaten are the drifting forces due to wind velocity while hovering or the drag forces while moving from one position to another. This means that less power will be needed again in order to beat the gravitational forces and the only forces that needs to be beaten are the drag forces; meaning that much less power will be enough for this mission to be accomplished.

Although, in many aspects an airship has many advantages; in terms of maneuverability, airship is not the best choice compared with an airplane or a helicopter. Due to the high power and thrust-to-weight ratios that are available for them, the specific power (the rate of increasing velocity or altitude of the aircraft) can be used in return of maneuverability which is much higher than a conventional airship. Also the hull of an airship has a huge negative effect while maneuvering due to the extensive drag forces as not the forward reference area (the smallest area available) is used in order to calculate the drag forces. So maneuverability shouldn't be expected from an airship. As the subject of this thesis, is to build an aircraft with the ability to achieve the missions such as surveillance, border patrol and security, maritime patrol and security, forest fires, traffic control and such; maneuverability is not the primary requirement.

In other words an airship has huge advantages compared with an airplane or a helicopter in order to achieve the missions such as surveillance, border patrol and security, maritime patrol and security, forest fires, traffic control and such. Because all of these missions do not need speed or maneuverability as primary requirements; instead these missions need high endurance, low noticeability, low operating costs, hovering capability and low fuel consumption. In the preceding sections these will be explained in a more detailed way.

1.3. Mission Profile

The mission profile that the airship needs to achieve is shown in Figure 1.1. According to this figure, the mission profile consists of:

1) Vertical take-off
2) Ascend to 1000 meters altitude
3) During hovering, resist headwinds up to 25m/s without losing hovering position.
4) Endure for 2 weeks
5) Vertical landing.

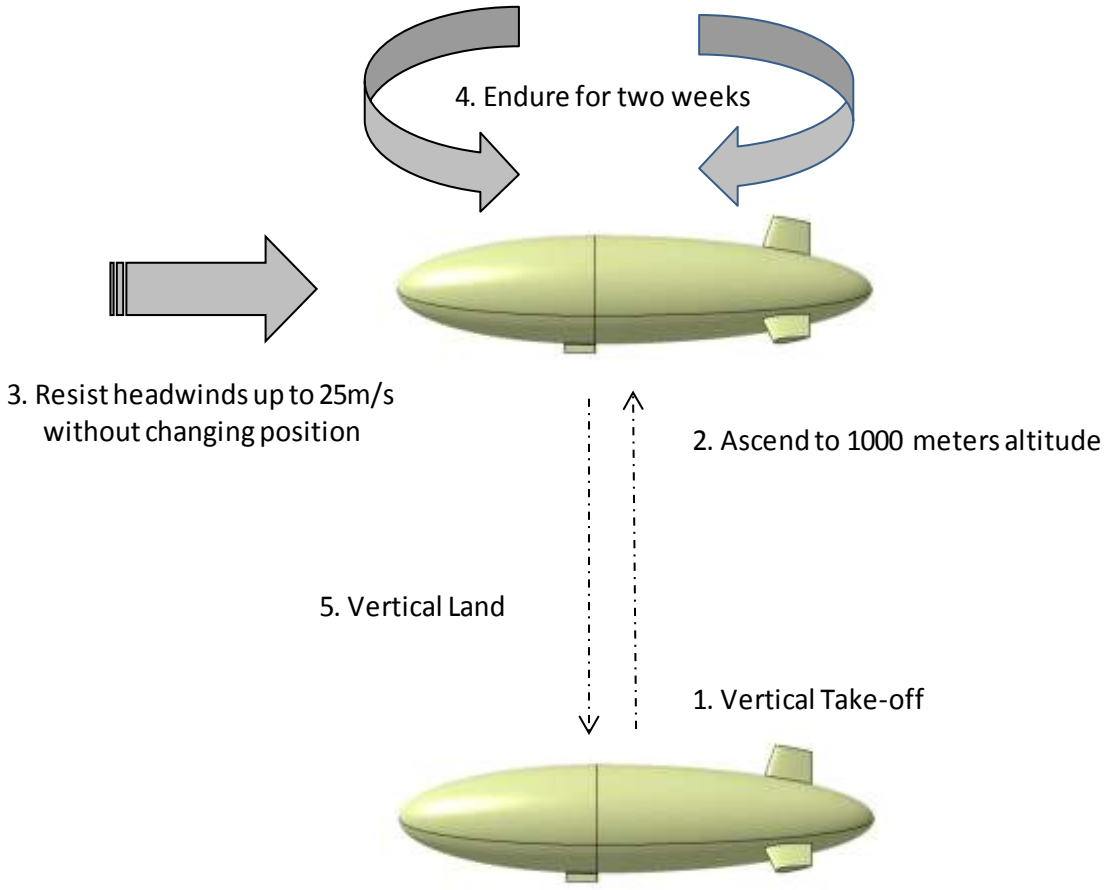

Figure 1.1 Mission Profile Representation

1.4. Design Requirements

After reviewing the literature extensively, it has been seen that there has been some examples on airships and aerostats which have been mainly concentrating on structural design, CFD analysis, control algorithm, solar design and conceptual design issues (e.g. [3], [13], [19], [20], [21], [22], [23], [24], [25]).

The competitors have been searched extensively and it is seen that although there are numerous examples of airship designs starting from half a meter to hundreds of meters in length. Also various options are available in terms of payload carrying capabilities, starting from a few grams to thousands of kilograms. But there hasn't been any example

of a solar powered, extreme endurance (2 weeks) and unmanned air vehicle that can carry payloads of up to 70 kg to 1000 meter altitude ASL (above sea level). The competitor study results that have been made according to this can easily be seen on Figure 1.2, of which the deficit has been clarified also.

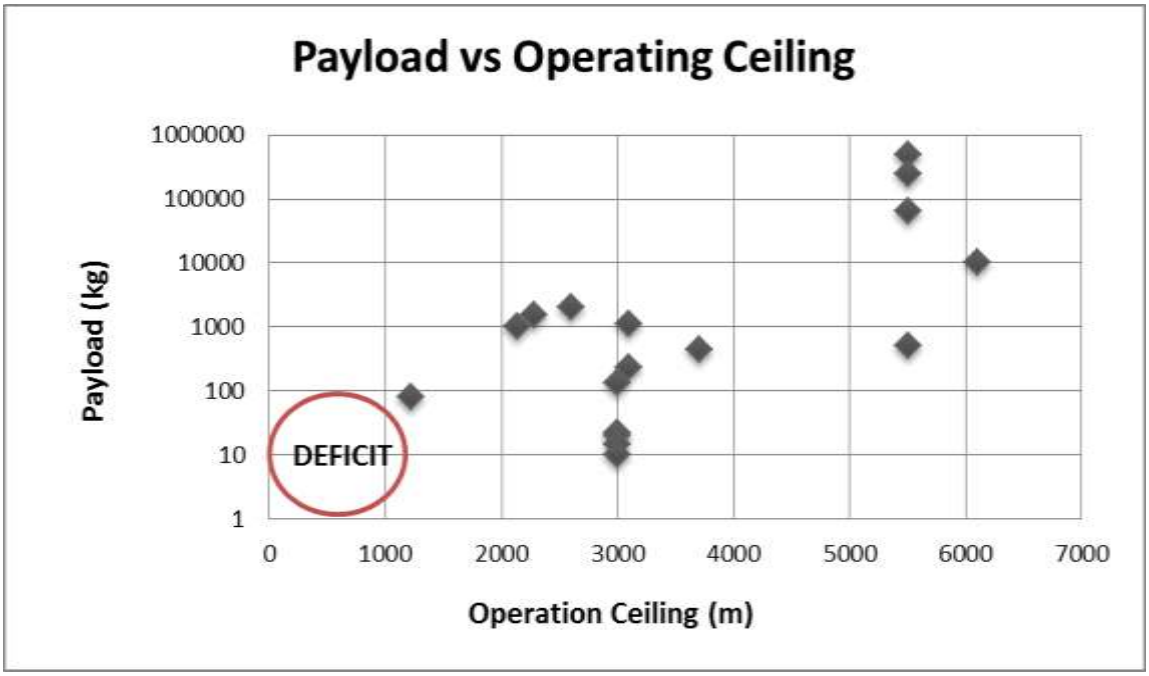

Figure 1.2 Payload vs. Operating Ceiling Between Competitors

Therefore, the design requirements to be satisfied for the airship are listed in Table 1.2 below.

Table 1.2 Design Requirements

Maximum Payload Weight	70 kg
Maximum Operating Ceiling	1000 m
Maximum Endurance	2 weeks
Temperature Range	Between -20°C & +40°C at sea level
Power Source	Solar Powered
Maximum Wind Resistance at sea level	90 km/h
Thrusting	2 electric motors with vector thrusting ability
Buoyant Gas	Helium

CHAPTER 2

CONCEPTUAL DESIGN

2.1. Conceptual Design Parameters

In the light of the design requirements introduced in Table 1.2, the best choice for the type of the lighter than air technology that will be used has been decided as non-rigid, in other words blimp type of aircraft. In order to maintain the whole system with solar power, the total weight becomes an important issue and in order to decrease the total weight as much as possible the best place to start is to eliminate the keel parts of the semi-rigid or rigid airframes.

2.2. Airship Hull Design

The envelope design, the gore types, the materials to be used for an aerostat has been explained in a very detailed way in the thesis of *The Design of Robust Helium Aerostats by Jonathan I. Miller, Department Of Mechanical Engineering, McGill University, Montreal, August 2005 [7]*. Although originally for an aerostat, most of the parts mentioned in this thesis are also applicable for an airship. The gore types to be used in designing the envelope will be cylindrical instead of conical since it is mentioned in the thesis that cylindrical single piece gores are beneficial compared with the conical ones because of the reduced number of seams [7].

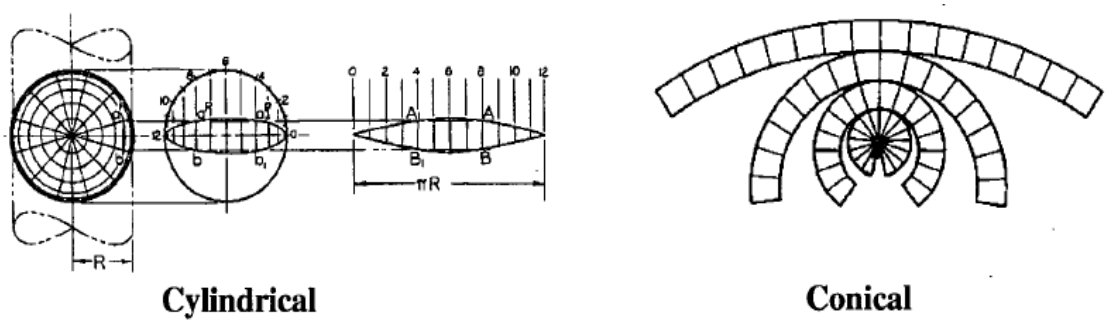

Figure 2.1 Gore Types [7]

There have been many studies made on airship hull designs. These studies mainly focus on the airship hull design in terms of aero-dynamical issues since the main limitation for the airship hull design emerges from its huge contribution to drag. Because of this reason, these studies mainly focus on reducing it as much as possible in this huge body.

There are numerous shape suggestions in terms of shape optimization processes for reducing the drag related issues, but there are three major shape optimization suggestions. First of which is the NPL (National Physics Laboratory) low drag body; which mainly consists of two ellipses meeting each other at their maximum minor diameter positions, but the second (rear) ellipsoid having major radius of 1.404 (√2) times the first ellipse's major radius (front one) [8][9][10]:

$$R_{major} = 1.404 * r_{major} \quad (2.1)$$

$$R_{minor} = r_{minor\ =R\_r} \quad (2.2)$$

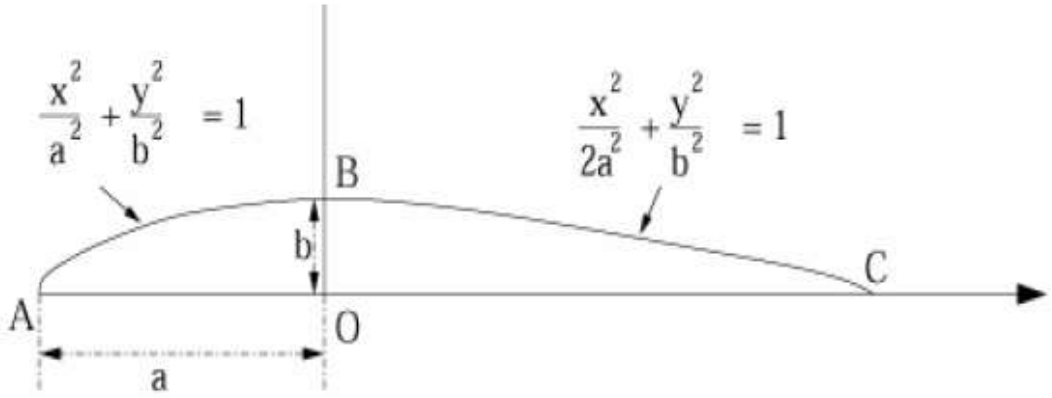

[OC] = 1.404 * [AO]

Figure 2.2 The NPL Low Drag Body [10]

The second suggestion for shape optimization is the GNVR envelope profile which combines an ellipse, a circle and a parabola as can be seen easily on Figure 2.3. This shape ensures a lower drag coefficient for aerostats or airships operating at 1000 m height and at 0.1 Mach [9]. But as 0.1 Mach is out of the operational limits for this thesis' subject the GNVR envelope profile will not be used.

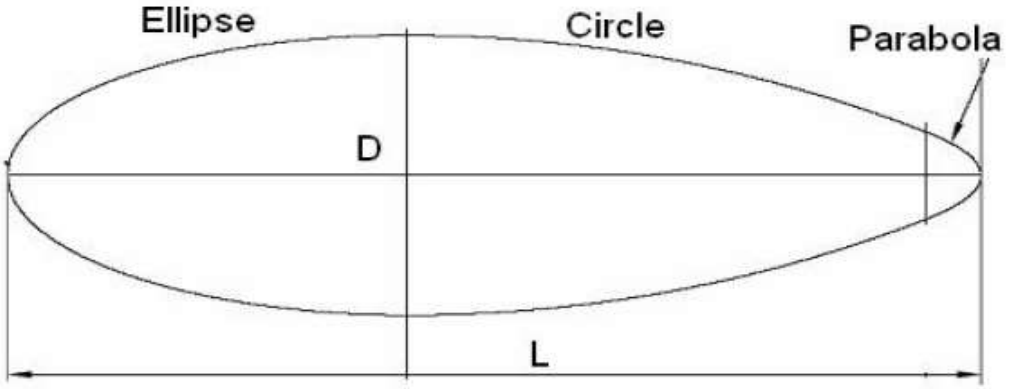

Figure 2.3 The GNVR Envelope Profile [10]

The third suggestion made by *Th. Lutz and S. Wagner* writer of the book *Drag Reduction and Shape Optimization of Airship Bodies* who stated that there are different design regimes for different volumetric Reynolds Numbers [10]. This means that, as it can also be seen at Figure 2.4, there are five different volumetric Reynolds number ranges, and for each range there is a best solution in terms of drag coefficient reduction.

$$Re_v = \frac{V_\infty V^{1/3}}{\nu} \tag{2.3}$$

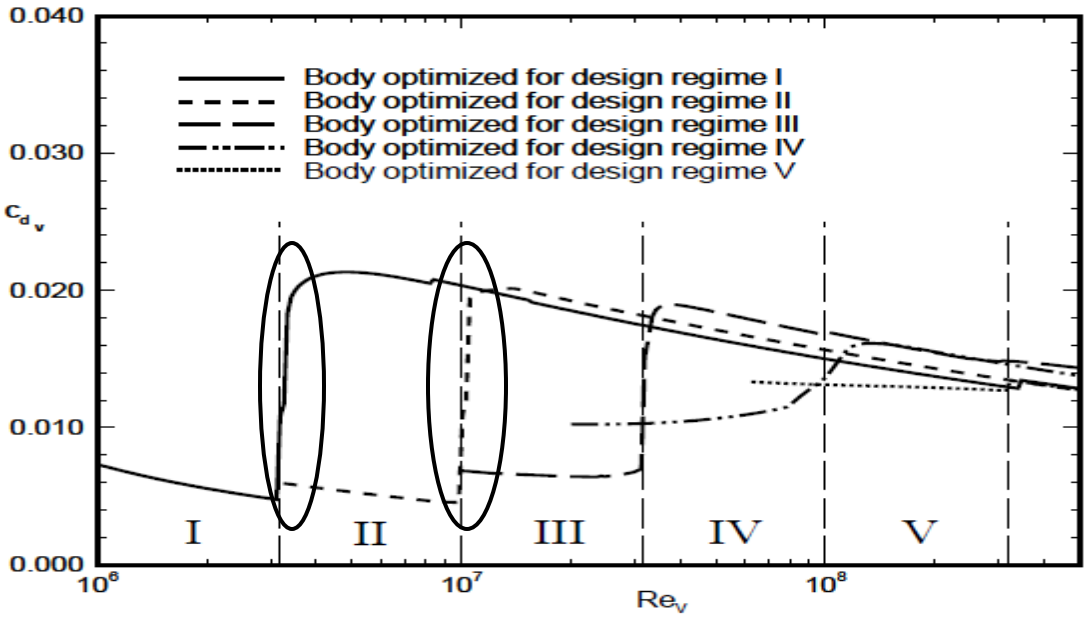

Figure 2.4 Drag Curve for Optimized Body Shapes [10]

If the volumetric Reynolds number range is between $1.0*10^6$ and $3.16*10^6$ the conventional type, or the one that can be seen on Figure 2.5 will be a good choice. But if the Reynolds number limit is above these values the best choice for the hull design changes dramatically for the examples which can be seen on Figure 2.6, which is for the design regime between $3.16*10^6 \leq Re_v \leq 1.0*10^7$ [10]. The dramatic increase of drag at the end of each design regime is due to the transition of the flow to turbulent flow.

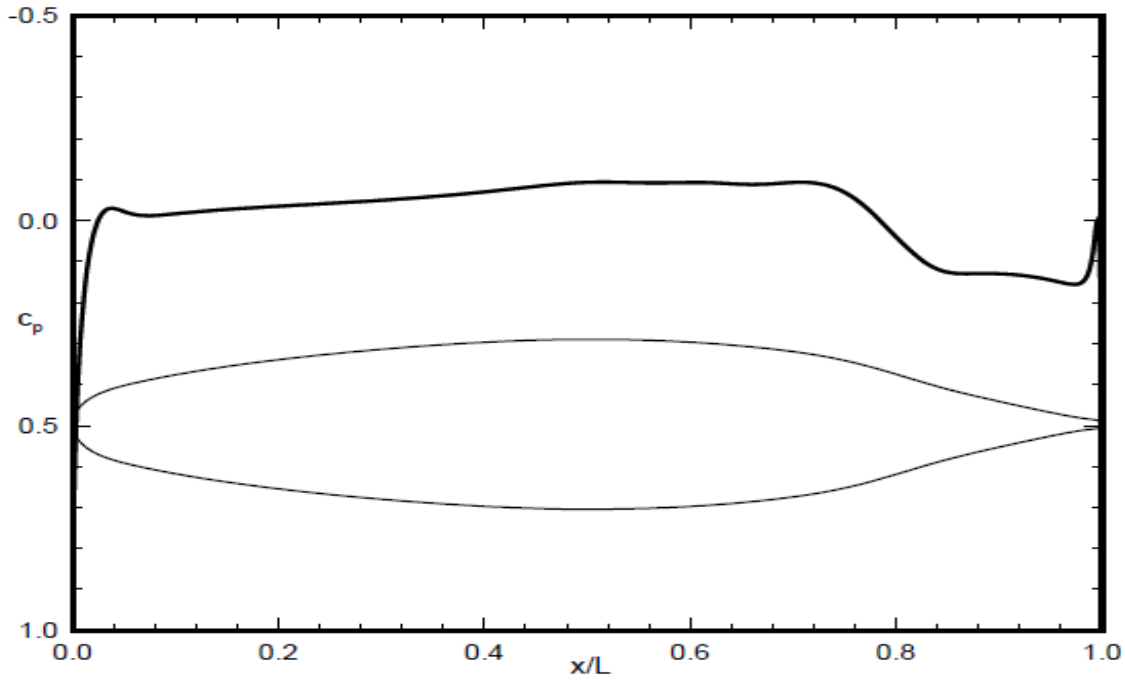

*Figure 2.5 Pressure Distribution of the Body Optimized for 1.0*106 ≤ Rev ≤ 3.16*106 [10]*

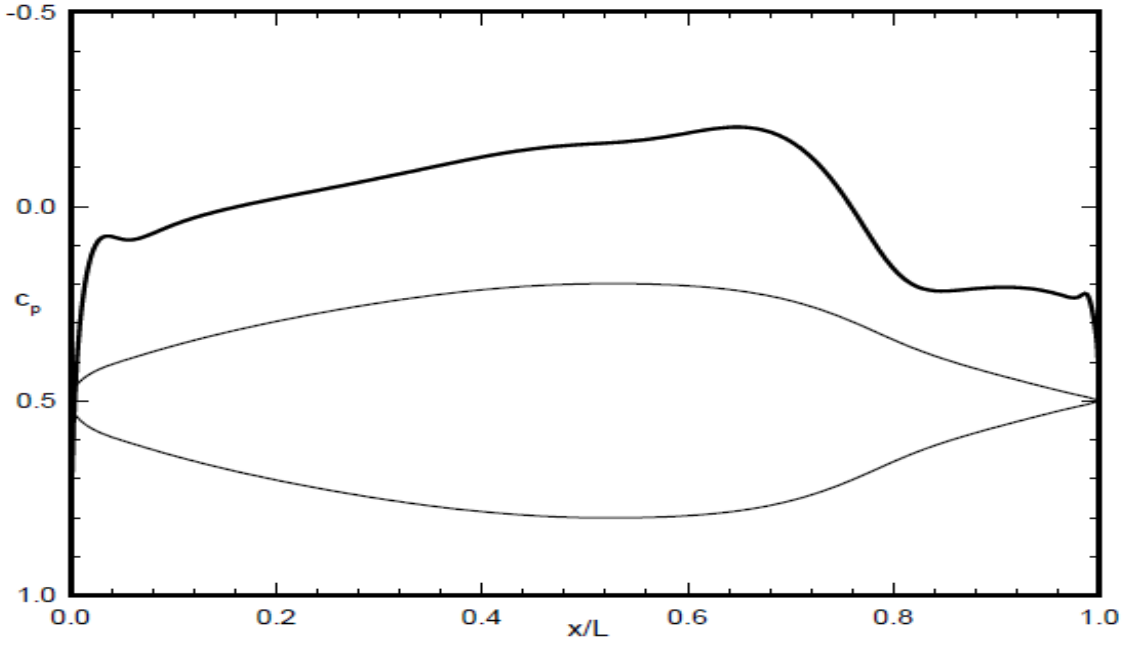

*Figure 2.6 Pressure Distribution of the Body Optimized for 3.16*106 ≤ Rev ≤ 1.0*107 [10]*

As the design regime for the volumetric Reynolds Number for this thesis is not very large; and as the related optimizations do not allow enough space for the tail configuration to be enough distant from center of gravity location, and when the existing and prospering airships are being analyzed, the NPL configuration has many advantages compared with the other configurations. Such as enough space and buoyancy force for tail configurations at the aft of the hull, prospering design, ease in manufacturing. Also there is not much difference between an NPL configuration and the best possible configuration according to *Th. Lutz and S. Wagner* [10] as the Reynolds number regime for the design specifications are not as high as informed. Due to these considerations, the NPL configuration (double ellipsoid) will be used for the hull design of this thesis.

This body will be a body of revolution, for which a given profile will be revolved around its x-axis, for the lowest drag to be achieved, the fineness ratio of the body should be determined.

Fineness Ratio = d / L (2.4)

As the forward and the aft ellipsoid lengths are known to be, *a* and *1.404*a,* and as the minor radius of the ellipsoids are equal to each other; knowing the fineness ratio (*d / L*) of the whole system will help to determine exactly the shape of the hull.

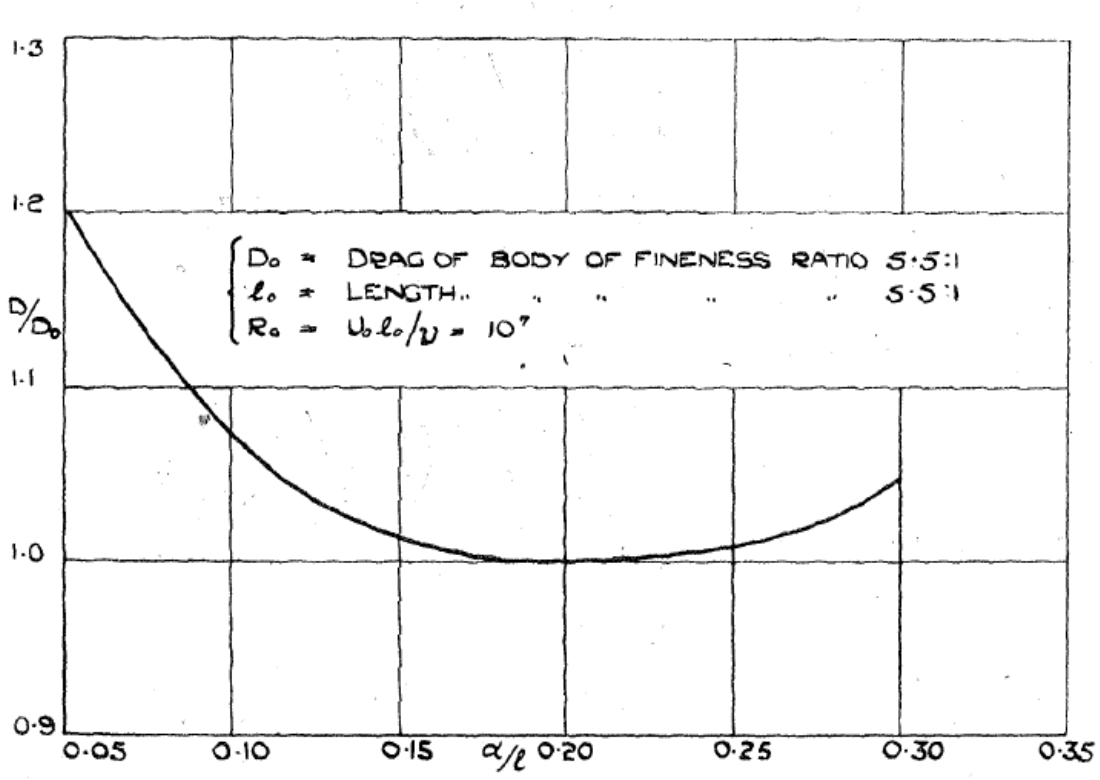

Figure 2.7 Drag of Bodies of Revolution of Equal Volume With Different Fineness Ratios [11].

As it can be seen from Figure 2.7, the best choice for the fineness ratio would be to choose the minimum ratio where D/D_0 =1. This corresponds to 0.222. The reason why the largest possible value for fineness ratio, satisfying D/D_0 = 1 requirement, has been chosen, lies behind the selection of the minimum volume/area ratio for bodies of revolution.

Table 2.1 Volume and Area Definitions for Different Bodies of Revolution

Shape	Volume	Area
Sphere	$(4/3) * \pi * r^3$	$4 * \pi * r^2$
Ellipsoid	$(4/3) * \pi * R_{major} * r_{major} * R_r$	$4\pi \left(\frac{(r_{major} * R_r)^{1.6075} + (r_{major} * R_{major})^{1.6075} + (R_{major} * R_r)^{1.6075}}{3} \right)^{\frac{1}{1.6075}}$

Also for a smooth and streamlined aerodynamic body looking like an ellipsoid in our case would be achieved simply by stretching a sphere from the two ends as can be seen in Figure 2.7. Assuming such an elastic expansion (otherwise it would not be possible), by stretching from the two ends of the spherical shape would increase the surface area while keeping the volume constant.

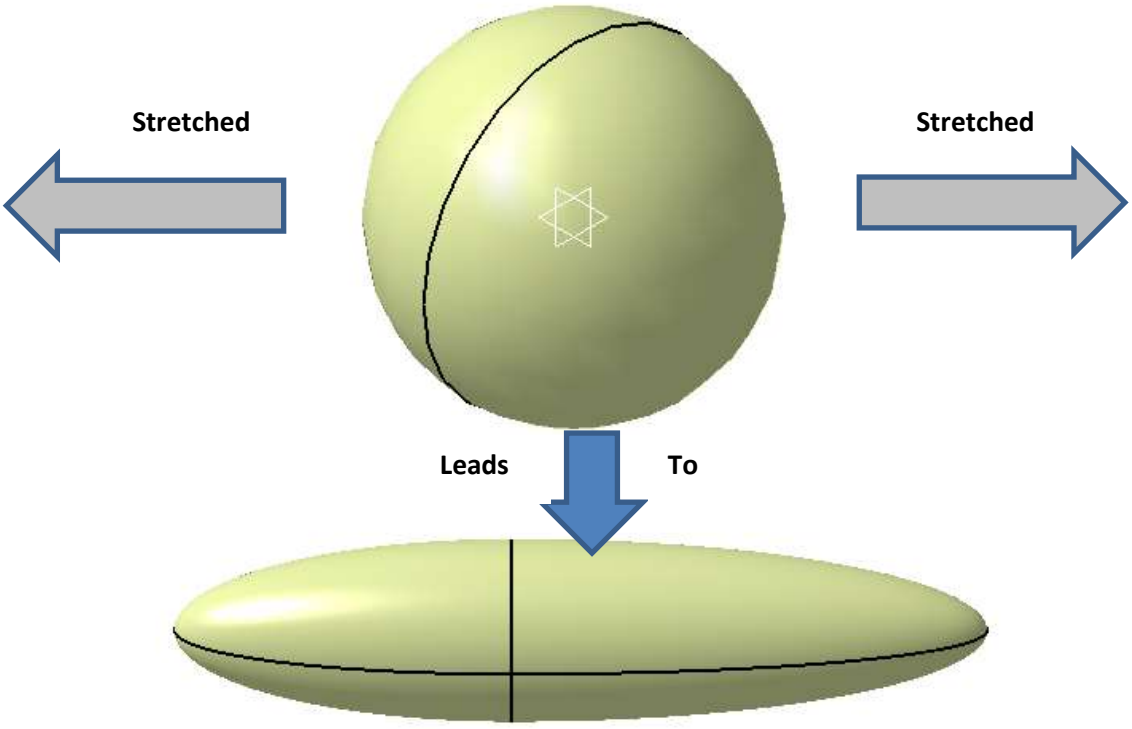

Figure 2.8 Demonstration of Stretching a Sphere to an Ellipsoid

In other words, the larger the fineness ratio gets, the smaller the surface area of the hull will become. This would mean a lighter airframe and more space for payload [11]. So the higher the fineness ratio, the better the *Airframe Weight / Hull Volume* ratio is. But the higher the fineness ratio, the more the system approaches to a spherical shape. So there is a need for a compromise between lower drag and less airframe weight. As it can be seen from Figure 2.7, when $d/L = 0.222$ the desired compromise is achieved. Although there is not an exact demonstration for an ellipsoid of revolution having two different major radii, the calculated surface area would be:

$$A_{ellipsoid} = 4\pi \left(\frac{(r_{major} * R_r)^{1.6075} + (r_{major} * R_{major})^{1.6075} + (R_{major} * R_r)^{1.6075}}{3} \right)^{\frac{1}{1.6075}} \quad (2.5)$$

This is an estimation done by empirical means to attain a given value of volume to the whole system. The r_{major} would be calculated from the volume information with the help of the following equation:

Since d / L = 0.222,

$$r_{major} = (3 * V / 4.808 / \pi / (0.222)^2)^{(1 / 3)} \quad (2.6)$$

$$R_{major} = 1.404 * r_{major} \quad (2.7)$$

$$L = R_{major} + r_{major} \quad (2.8)$$

$$R\_r = d/2 \quad (2.9)$$

$$R\_r = (R_{major} + r_{major}) * 0.111 \quad (2.10)$$

As soon as a desired value is assigned for the volume of the hull with the help of an excel table provided at the end of Chapter 2, in Appendix A), the R_{major}, r_{major} and the R_r values are calculated for the best configuration. This will also calculate the corresponding surface area (in m^2) and the corrsponding hull weight, using the detailed design procedure given in this section.

2.3. Balloon Design

With the help of this calculation, the hull weight is determined. While determining the weight it should be kept in mind that the biggest contribution to the weight is coming from the weight of the envelope fabric. While determining the weight of the fabric, as a

rule of thumb, it is also calculated by considering the contribution for the seams and patches done on the balloon during manufacturing [8]:

$$0.35\ kg/m^2 \leq A_{density\_hull} \leq 0.53\ kg/m^2 \quad (2.11)$$

The smaller figure is used for the calculations of bigger volume of airship hulls, whereas the heavier value is generally for a higher area density of fabric choice.
Then the total weight of the balloon would be calculated as:

$$W_{balloon} = 0.35\ (kg/m^2) * A_{hull} \quad (2.12)$$

As can be understood from the previous discussion, choosing a proper fabric material for the balloon is one of the most important topics in airship design. However, there are many other limitations regarding the hull design, such as the aerodynamical design limitations as well as the consideration of preserving the Helium inside the airship body. That is the problem of leakage.

Helium atom is the smallest diameter atom in size. Although Hydrogen is the smallest atom in nature, due to the fact that Hydrogen atoms are usually attached to another Hydrogen atom they are not the smallest size molecules in nature. Therfore He atoms are the smallest possible atoms available in nature. Besides He is an inert gas which makes it more preferable over very active and oxidizing (explosive) Hydrogen gas. Although He is more preferable because it is an inert gas and not very explosive as Hydrogen, due the fact that its diameter is very small makes it very prone to leakşng from even the smallest hole. Therefore sealing and leakage from fabric becomes a very series problem against He storage. The main reason for the sealing is to eliminate the loss of Helium through the stretched fabric as much as possible Because, losing He gas from the balloon is a very series problem and loss of large amounts of Helium gas is not desired if one considers that this system will be in the air for at least 2 weeks continuously. So the design constraint for Helium loss is limited to 1% of total Helium

mass available per day. Therefore some of the properties of the materials used for envelope, ballonet and adhesive materials are listed below [8]

The envelope material desirable properties are listed at below Table 2.2:

Table 2.2 Envelope Material Desirable Properties

- High strength to weight ratio for minimizing weight while maximizing strength
- Resistant to environmental effects such as humidity, temperature, sunlight increases the durability and lifetime of the envelope
- High tear resistance for damage tolerance as some impact may occur during landing or small accidents may occur also
- Flexible as envelope will be inflated and deflated during its life cycle.
- Low permeability to minimize the loss of Helium during operation, in order to increase the endurance and to decrease the operating costs as Helium is very expensive.

Due to the recent improvements on fabric materials compared with the ones already used reduced significantly the leakage loss as well as reduced the weight of the hull. Some of the main material types that are available from various manufacturers are listed in Table 4. It has to be noticed that lower the permeability function, the less the Helium to be lost. In other words, while going down the list in Table 2.3; the fabric material's permeability characteristics are improved.

The Darcy's law (see equation 2.13) can provide an insight about how the balloon envelope material is important and how the permeability coefficient will have an effect on the material choice in order to achieve the design criteria of maximum 1% of total Helium mass loss per day. $Q_{discharge}$ is the Helium rate released to air, of which the unit is in m^3/s. λ is the permeability coefficient (m^2) of which for different base materials have

been listed on Table 4. μ is the viscosity (Pa*s), $A_{balloon}$ the total balloon area, ρ_g and ρ_a are the gas and air pressures respectively and l is the thickness of the fabric material.

$$Q_{discharge} = -\left(\frac{\lambda * A_{balloon}}{\mu}\right) * \left(\frac{\rho_g - \rho_a}{l}\right) \quad (2.13)$$

The so-called Darcy's law gives an insight to us while choosing the best option for the base material by evaluating the pros and cons in terms of the permeability, weight and availability.

Table 2.3 Permeability Coefficients of Heat Resistant Films against Helium [12]

Baloon Envelope Material	Permeability Coefficient
Teflon	1.71×10^{-17}
Nylon 6	1.71×10^{-18}
High-strength polyester	2.00×10^{-18}
Polyimide a	2.28×10^{-18}
Polyimide b	2.29×10^{-18}
Polyethylene	7.16×10^{-18}
PBO	1.43×10^{-19}
Liquid crystal polymer	2.86×10^{-19}
Ethylene vinyl alcohol	4.29×10^{-19}

Nylon based materials have been chosen as they provide a good compromise between permeability, availability and weight as mentioned earlier. There are many reasons for choosing nylon based materials. First of all they have proven themselves with the use of

Helium balloons also in other endurance demanding areas (such as in inflatable military specification items). Then they are easy to reach than many other materials.

So, a value of 0.142 kg/m^2 will be used for determining the present airship hull weight calculations. The fabric material that is selected to be used during the design is Lamcotec's Heat Sealable 70 Denier Urethane-Coated Nylon Taffeta whose physical properties are detailed in Table 2.4.

As it can clearly be seen from Table 2.4, the total weight of the fabric (area density) is much less compared with the ones listed in the rule of thumb options for which the best available option was limited to 0.35 kg/m^2. Also the permeability values are of great importance since the design criteria limits the maximum loss of Helium to only 1 % is total Helium mass contained in the hull. For example, a 1000 m^3 of hull volume of a similar kind of airship designed here would correspond to 815 m^2 of hull area which can easily be seen from the formula used for the area calculations of the ellipsoid (see equation 2.5):

r_{major} = (3 * 1000 / 4.808 / π / (0.222) ^{2})$^{(1/3)}$ = 15.9 m

R_{major} = 1.404 * 15.9 m = 22.3 m

d / L = 0.222

L = R_{major} + r_{major}

R_r = d / 2

R_r = (38.3 m) * 0.111 = 4.2 m

$$A_{hull} = 4\pi \left(\frac{(15.9 * 4.2)^{1.6075} + (15.9 * 22.3)^{1.6075} + (22.3 * 4.2)^{1.6075}}{3} \right)^{\frac{1}{1.6075}}$$

$A_{hull} = 816\ m^2$

Thus, it was found as 816 m^2 of fabric material area with the relation given at Table 2.4 below [7].

For an endurance of 2 weeks, the total Helium loss (He_{loss}) will be:

$He_{loss} = \Lambda_{He} * A_{hull} * days * weeks$ (2.14)

He_{loss} = 2.0 (L / m^2. 24 hrs) * 816 (m^2) * 7 (days / 24 hrs) * 2 (weeks / flight) = 23 m^3 / flight

Thus, according to the equations;

23 m^3 / 1000 m^3 = 2.3 % of total Helium mass will be lost in a period of two weeks.

The above result shows that the airship easily satisfies the bottleneck of 2 weeks endurance. Allowed Helium loss would be 14 % in total, and with only 2.3% of Helium loss, the mission will be accomplished.

Table 2.4 Lamcotec's Heat Sealable 70 Denier Urethane-Coated Nylon Taffeta Specifications [7]

Basic Fabric Weight	59.3 g/m^2 (1.8 oz/yd^2)	Elongation at Break	38 % Warp 54 % Weft
Total Weight	142 g/m^2 (4.2 oz/yd^2)	Thickness	0.15 mm
Tongue Tear	8.9 N Wrap 7.6 Weft	Strip Adhesion (Heat Sealed) Film to Film	48 N / 25 mm
Breaking Strength	679 N Warp %69 N Weft	Permeability to Helium	1.5-2.0 L/m^2/24 hrs

Test Reference: Mil-C-83489, Fed-STD 191A, Mil-STD 810D, ASTM, Cal. Bulletin 117, CFR, NFPA

2.4. Ballonet

Ballonet is the component of the airship, which ensures for the airship to ascend and descend safely. Ballonets achieve this mission by inhaling and exhaling atmospheric air, as they can be identified as the lunges of a human. Whenever the ballonets are filled with air, with the help of a pump, the airship becomes heavier than air and the balloon descend. As the ballonets takes away the volume intended for Helium and it will also increase the weight of the ship by adding the weight of the inhaled air. The density of Helium will increase, the lifting capability of the Helium will decrease and the ship will become a much heavier vehicle than it used to be as the weight of the air is also going to be included in the total weight calculation. The ballonet weight should also be estimated in a similar concept with the hull. The general rule for ballonets indicates that, the area density of the ballonets should be between:

$$0.275 \text{ kg/m}^2 \leq A_{density\_ballonet} \leq 0.305 \text{ kg/m}^2 \quad (2.15)$$

The only difference between ballonet calculation and the hull fabric weight estimation is that while using these area densities for weight estimation, this time the larger the ballonet volume is the smaller the area density of the fabric material that is going to be used or vice versa. In other words, as the ballonet volume is much smaller than the ones determining this rule of thumb, 0.305 kg/m^2 would be used while determining the ballonet weight (including seams and patches as well):

$$W_{balloonet} = 0.305\ (kg/m^2) * A_{balloonet} \quad (2.16)$$

The ballonet material desired characteristics are listed in Table 2.5 below:

Table 2.5 Ballonet Material Desired Characteristics

- Low permeability to air and Helium both to minimize Helium contamination and loss
- Light weighted in order to eliminate the extra weight added to the total weight
- Flexible to support many inflation and deflation cycles

As Lamcotec's Heat Sealable 70 Denier Urethane-Coated Nylon Taffeta achieves all the requirements listed above and also much lighter than the corresponding competitors, it will also be used for the ballonets. The new weight calculation with the new fabric materials will be:

$$W_{balloonet} = 0.142\ (kg/m^2) * A_{balloonet} \quad (2.17)$$

The reason of choosing the same material for the ballonette as the one used for the hull fabric is its low permeability. If the fabric material that is going to be used for the ballonet fabric would be of a higher permeablity, the loss of Helium, due to the binging and purging processes happening inside the ballonet, would have been of a much higher

value. As Helium would be going inside the ballonet volume and being disposed with air the Helium loss would occur. This fabric material is a special laminate fabric which is especially used for Helium balloons because of its high strength and low permeability.

Two ballonets would be used in total; one of which would be just in front and the other one would be just behind the CG. So that, in times of need, pitch-up and pitch-down characteristics would be achieved by varying the air volume inside those ballonets. The ballonet shapes are going to be two spheres as sphere provides the highest volume for the given area within revolved bodies (meaning minimum weight for the ballonets).

$$r_{ballonet} = ((3/4) * (V_{ballonet\_needed} / 2) * \pi)^{(1/3)} \quad (2.18)$$

$$A_{total\_ballonet} = (4 * \pi * r^2_{ballonet}) * 2 \quad (2.19)$$

2.5. Airship Fins' Design and Analysis

Airship fins are one of the most important segments of the design process, because they will ensure that the airship will be taking its smallest reference area of the hull body against the headwinds at all times. As the lowest drag producing part of such a huge body is the forward facing reference area of the hull body, the most important job of the fins is to ensure the lowest possible drag creation by trimming the airship relative to the wind direction. Also, as this is an airship not an aerostat, some missions may require mobility rather than patrolling services only. In these aspects, airship fins also do have an important role in controlling and maneuvering.

Although there are researches made about finless counterparts [13], they are much more inefficient compared with the conventional approaches. Since all the maneuvers needed to be achieved are being generated by vector thrusting, this resulted in very large energy consumption. Finless configuration is also much harder to control and the equations of motions become much more complex. Also since the subject of this thesis is to design an airship using the solar approach, no excess power will be available and power

consumption should be as low as possible in order to get the systems running and accomplish all the mission.

The hull-fin interactions should also be observed in order to choose the best solution to see whether the related configuration would be prosperous enough. Research has also been made with respect to this issue [14]; and it has clearly been seen that related fluid analysis is necessary for this kind of interactions since this analysis will reveal the facts between the drag, lift, and moment coefficients with respect to different angles of attack [15].

Airfoil choice is not a very big issue as this is not supposed to be a very maneuverable aircraft. A symmetric airfoil for the tail configuration would prove enough stability [16]. This should be kept in mind that the more complex the airfoil section is, the more expensive it would cost by all means: from constructing the related airfoil sectioned tail to attaching the tail to the body and attaching the moving surfaces to the tail surface.
As tail positioning and tail configuration is also an issue that needs to be taken into account seriously, such as if the fins are being positioned way behind then they might lie within wakes meaning less control and efficiency or if they are positioned way ahead they would not have any considerable effect as the moment arm will not be long enough to affect the positioning of the aircraft [8]. Tail configuration is also an important issue whether to use a conventional type of tail or an inverted-Y configuration is an important issue while taking into account the efficiency of the tails [17]. Tail area calculation and designing according to these calculations is also important and there have been criteria and rules of thumbs related to this issue [18].

The tail group weight estimation is a bit more complex than the ones listed above as the tail area needed is to be calculated carefully. But, the area density that is going to be used for small airship tail structures is presumed to be:

$$W_{tail\_system} = 4.9\ kg/m^2 * A_{ControlSurfaces} \quad (2.20)$$

The total tail area, as a rule of thumb, that is going to be needed is going to be calculated according to Burgess' [19] statement for control surfaces (2.20).

$$A_{\text{Control Surfaces}} = 0.13 * (V^{\frac{2}{3}}) \quad (2.21)$$

According to this statement the vertical and the horizontal control surface areas are taken to be equal to each other. When compared with the Blakemore's statement [20], which can also be seen at Figure 2.9 and Figure 2.10 where:

L : Airship Length (m)
A_V : Vertical Tail Area (m^2)
A_H : Horizontal Tail Area (m^2)
A_E : Elevator Area (m^2)
A_R : Rudder Area (m^2)

The two approaches are found to be very close to each other and as the Burgess' statement is a much less complex approach compared with the Blakemore's, for future conceptual design calculations Burgess' approach for fin-tail configuration is going to be used. In the excel table, there will also be a Control Surface Area column and a Control Surface Weight column which will automatically be calculated for the figures.

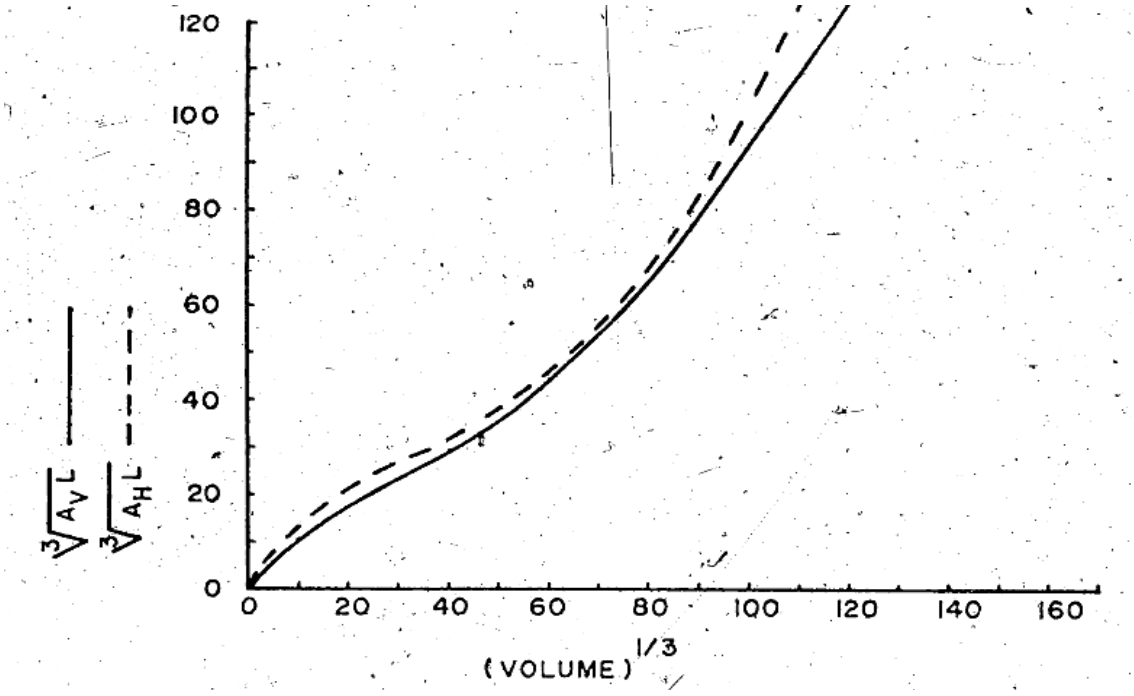

Figure 2.9 Blakemore's Statement of Tail Fixed Portion Area

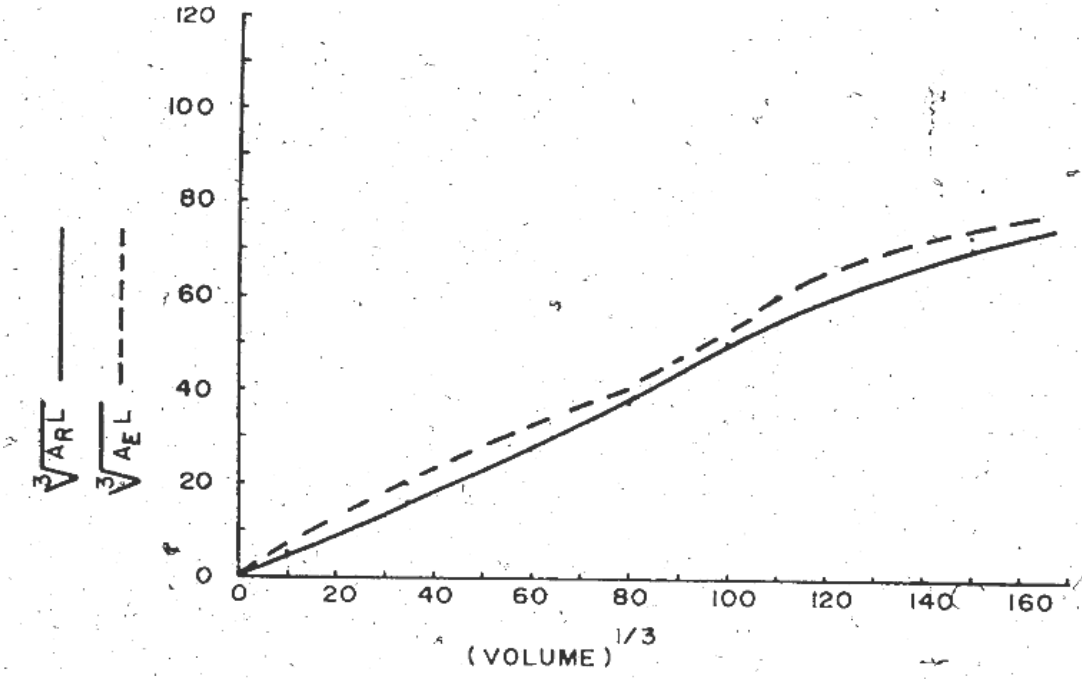

Figure 2.10 Blakemore's Statement of Elevator and Rudder Area

While making the necessary calculations both figures would be used for comparison.

2.6. Solar Power Systems for Airships

A solar system of an airship is mainly consisting of Solar Panels, Maximum Peak Power Tracking System (MPPTS), batteries that needed to be charged in order to use the stored energy at night and whenever excess power consumption is needed, and the cabling required to support the whole system [21]. The main problem for the system to overcome is the solar panel settlement due to the curved surface availability for solar panel application and the huge weight increase due to batteries and the system engineering that needs to be applied for these systems.

A solar cell or a photovoltaic cell is a device used for converting the solar energy coming from the sun into electrical energy by p-n junction concept [22]. Solar cell's working principle can best be summarized in this way: When photons have enough energy electrons will be raised from the valance band to the conduction band and whenever a load is connected between the positive and the negative contacts the current will flow through this load as can be seen easily in Figure 2.11 below [23]:

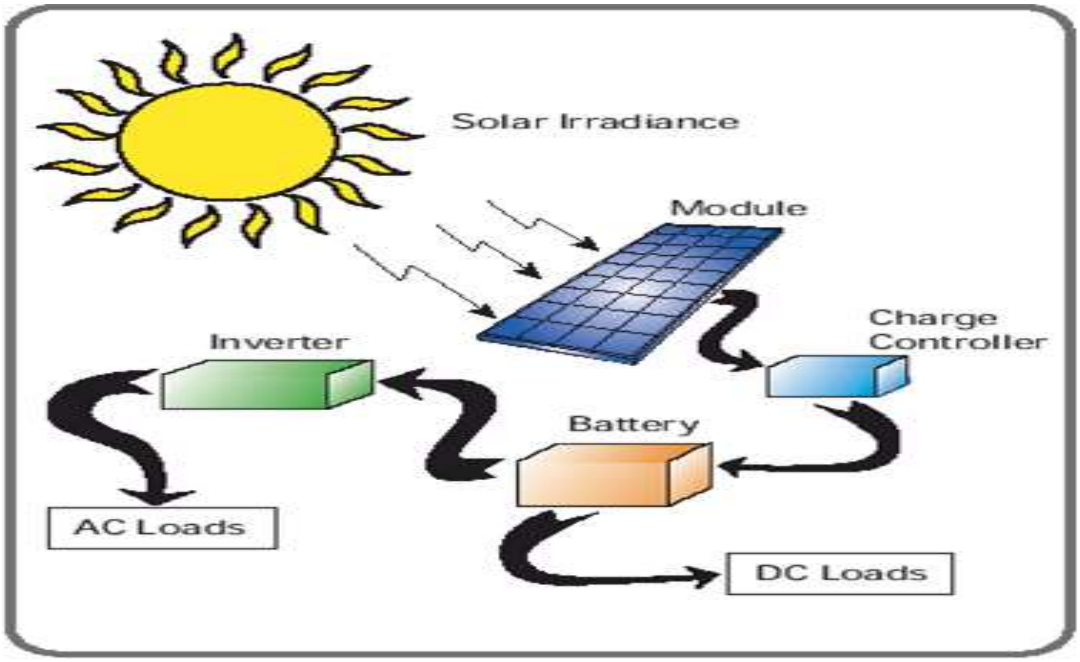

Figure 2.11 Summary of Photovoltaic (PV) Cell Operation [23]

There are various photovoltaic cell options when compared in terms of their efficiencies, weight, flexibility, cabling options and price. But the best choice should be made between these options taking into consideration efficiency, price and flexibility. One of the most important criterion that has to be taken into consideration is the flexibility of the cells, since the surface used for these photovoltaic cells is a curved one and therefore, the photovoltaic cells must be elastic enough to be put onto the shape of that surface without harming both the surface of the hull and the photovoltaic cell. Therefore the best choice for the solar cells is the Solbian SP137 solar panels: These cells are capable of producing up to 137 Watts of peak power, have 23 % of efficiency Sunpower solar cells and are both very thin (1/16") and very flexible (up to 30 degrees). We should keep in mind that weight is a very important factor in our applications. An example of Solbian SP137 cells, which is applied on a marine craft, are seen in Figure 2.12. Twenty pieces of these panels are going to be installed on the system in order to produce 3.74 kW/h in peak operating conditions [24].

Figure 2.12 SP 137 Installed Marine Craft [25]

The total solar panel weight would be:

$$W_{solar\_panels} = W_{each\_panel} * N_{panels} \quad (2.22)$$

That leads to

W_{solar_panels} = 2.2 kg * 20 = 44 kg

Assuming 20 % of the solar panel weight for the connections and for the cabling would correspond to:

$W_{solar\_sys} = W_{solar\_panels} * 1.2 = 53$ kg

A Maximum Peak Power Tracking System (MMPTS) is also needed to connect these solar panels to the batteries in order to effectively use the already variable power (due to incident angles of the sunlight) acquired from the sun [26]. As the solar panels will be laid perpendicular to the airship front zone, only one Maximum Peak Power Tracking System (MMPTS) will be enough because only one incident angle will be available at all times. This means that only one current output will exist nearly all the time. The most efficient way of connecting these solar panels to the batteries will be by using only one MPPT instead of using 5 or 6 MPPT's. As the solar panels will have only one incident angle with the sun, 1 MPPT is going to be enough instead of installing these panels to tail surfaces and such other surfaces as well [22]. The two solar panels will be connected in series made up of ten groups made up of two Solbian SP 137 solar panels connected in series that will be connected in parallel having a configuration of 48 Volts and 60 Amperes. They will be connected with each other just before the cables are taken into the airship hull. As the shortest way for the cables from the panels placed at the top to the MPPT system and the batteries located inside the gondola (at the bottom) is by getting inside the hull instead of turning around the hull diameter, the merged cable configuration will be transported inside the airship hull thus shortening as much as possible the path of the cabling.

The cables that will be connected to the MPPT and the Power Tracking System are in turn connected to the batteries tol store the excess power. Both the MPPT System and the batteries are needed to be stored in the gondola together as they can be affected by the outside conditions. The weight of the MPPT system is assumed to be:

$W_{MPPT\_sys} \approx 3kg$

Lithium-ion polymer (LiPo) batteries will be used to store the excess power. Lithium-polymer batteries are used to store the excess power. These batteries are lighter and thinner and therefore occupy sufficiently small volume. This is why they are more frequently used in radio controlled applications when compared to the lithium-ion batteries. They are more trustworthy. Furthermore using them means a lighter configuration which is also an important aspect in order to increase the endurance. 14S 96P Li-Po (14 Serial, 96 Parallel) battery configuration made up of Panasonic NCR-18650B 3350 mAh battery cells will be used. This is a 1C/2C battery configuration. The reason for choosing this type of configuration is that a high discharge rate is not needed for an airship. Instead of this a very long discharge time is expected in order to increase the endurance. In other words the system must have a very long endurance and with 96 P configurations the time of staying alive for the system is extended as much as possible with the lowest possible weight. They will provide:

$N_{Serial} * 3.7\ V = 14 * 3.7\ V \approx 51.8$ Volts

$N_{Parallel} * I_{per\_cell} = 96 * 3350\ mAh = 321.6$ Amperes maximum

And they will weigh around:

$$W_{battery} = S_{count} * P_{count} * W_{each\_cell} \quad (2.23)$$

That leads to

$W_{battery} = 14 * 96 * 40\ g = 53.8\ kg$

Leaving 10 % of the battery weight for the casing and the connections of the batteries would mean:

$W_{battery\_configuration} = W_{battery} * 1.1 = 59.2$ kg

The total power management system weight is calculated by:

$$W_{power\_man\_sys} = W_{MPPT\_sys} + W_{battery\_configuration} \quad (2.24)$$

Thus, summing the weight of the MPPT and the weight of battery would give us:

$W_{power\_man\_sys} = 3$ kg + 59.2 kg = 62.2 kg

2.7. Propulsion System

In order to support the system, two low kV brushless dc electric motors (Turnigy Roto Max 80cc size, 195 kV, brushless out runner motors) will be used, which have the ability to produce 6.6 kW of power at 150 A and weighing 2kg each.

$$kV = RPM_{max} / Volts \quad (2.25)$$

In our case:

195 kV * 51.8 Volts ≈ 10,000 RPM maximum

The reason for choosing lower kV value is to increase the efficiency for very low speed aircraft such as the airships.

As two electrical motors will be used, the total weight of the engines would be:

$W_{engines} = 2 * W_{Turnigy} = 4$ kg

The propeller weight and the cabling of the engines are estimated to be:

$W_{sub\_comp\_engines} = 0.25 * W_{engines} = 0.25 * 4\ kg = 1\ kg$

Thus, the total engine system weight would be calculated by:

$$W_{engine\_system} = W_{engines} + W_{sub\_comp\_engines} \quad (2.26)$$

That leads to;

$W_{engine\_system} = 4\ kg + 1\ kg = 5\ kg$

The thrust vectoring system that is going to be used is a rod attached to a servo turning the rod 270 ° and by doing this the electric engines are also used for vector thrusting. The rod length is 3 meters and its weight is:

$W_{vectoring\_rod} = L_{vectoring\_rod} * W_{annular} = 3\ m * 1\ kg/m = 3kg$

The servo and the related connections are used to reducing the weight around:

$W_{sub\_comp\_vectoring} \approx 1.5\ kg$

The total thrust vectoring system weight is calculated by:

$$W_{thrust\_vectoring\_system} = W_{vectoring\_rod} + W_{sub\_comp\_vectoring} \quad (2.27)$$

Which leads to;

$W_{thrust\_vectoring\_system} = 3\ kg + 1.5\ kg = 4.5\ kg$

In total, the propulsion system weigh is calculated by:

$$W_{propulsion\_system} = W_{engine\_system} + W_{thrust\_vectoring\_system} \quad (2.28)$$

Thus, the propulsion system will weigh:

$W_{propulsion\_system} = 5 + 4.5 = 9.5$ kg

2.8. Payload and Gondola Weight

As indicated in Table 1.2, the payload capacity of the system is estimated to be:

$W_{payload} = 70$ kg

No paint, pilot and fuel weight exists as this is a solar powered unmanned airship. The gondola weight will be determined from the manned versions for the conceptual design process. This will not be a wrong approach since in this case instead of a human, the gondola will carry a huge load of batteries which will eventually equate itself to a human's weight. For the gondola weight:

$$W_{gondola\_structure} = 10.5 \text{ kg/m}^3 * V_{gondola\_structure} \quad (2.29)$$

The above equation (see equation 2.28) will be used as the components that are to be carried will need at least the same structural capability compared with the manned gondola designs. 1 m^3 of volume for the gondola will be enough for the first estimation.

$W_{gondola\_structure} = 10.5 \text{ kg/m}^3 * 1 \text{ m}^3 = 10.5$ kg

The total avionics weight used in this system is estimated to be:

$W_{avionics} \approx 10$ kg

And they will also be stored inside the gondola.

If we sum up all the component weights, that are located inside the gondola or directly attached to gondola itself:

$$W_{GONDOLA} = W_{gondola\_structure} + W_{avionics} + W_{payload} + W_{propulsion\_system} + W_{power\_man\_sys} \quad (2.28)$$

That leads us to a total gondola weight of:

$$W_{GONDOLA} = 10.5\ kg + 10\ kg + 70\ kg + 9.5\ kg + 62.2\ kg = 162.2\ kg$$

2.9. Suspension System

The suspension system's weight estimation has been made according to the empirical data as 10 to 13 kg of weight for per 1000 m^3 should be given available with respect to the shape and the complexity of the system. In other words 1.0 to 1.3 percent of the hull volume should be spared for the suspension system's weight estimation. As in this case, the system doesn't need a complicated suspension design, the weight estimation would be:

$$W_{suspension\_system} = 0.010 * V_{airship} \quad (2.30)$$

The exact weight estimation will be found from the iteration results given below as the final volume of the system would outcome at that point only.

2.10. Nose Reinforcement Group

The nose reinforcement can be summarized as the part to be attached to the ground station (a mooring probe). This part is also the rigid part where the fabric gores are going to be attached together. This section will be maintaining the structure shape as the nose cone battens and the nose cone itself are the first components to be standing against wind and wind related forces. This group can be estimated as 17 to 21 kg per 1000 m^3

hull volume and as the ballonet weight configuration determination. The less the hull volume is, the higher the group weight estimation will be or vice versa. In other words:

$$W_{nose\_group} = 0.021 * V_{airship} \quad (2.31)$$

The exact weight estimation will again be found from the iteration results given below as the final volume of the system would come at that point only.

2.11. Access and Maintenance

As maintenance will be needed after a long term use of this kind of vehicle or in the case of an accident, accessing inside the airship hull or the gondola will not be needed While designing the access needed for the maintenance and such, the most important things that are needed to be considered are listed in Table 2.6 below:

Table 2.6 Design Considerations for Access and Maintenance

- In case of any damage occurs to the suspension lines
- In case of any damage occurs or maintenance is needed for the ballonet configuration
- If the payload attached into the gondola should be changed or accessing inside the gondola for the maintenance or renovating the batteries or the avionics

1 percent of the total hull volume will be considered while estimating the access/maintenance weight.

$$W_{access\&maintenance} = 0.01 * V_{airship} \quad (2.32)$$

2.12. Iteration Results and Component Weights

The iteration results gathered from the Excel data can be seen at Table 2.7. The buoyancy force ($F_{buoyancy}$) has been intentionally left below the W_{total} + 10 % value to make sure that the vehicle won't be out of control even at peak operating conditions for ground handling.

According to the iteration results the hull volume is found to be around:

$V_{needed} \approx 500\ m^3$

All the component weights related to the final volume estimation are calculated according to the equations 2.12, 2.17, 2.20, 2.22, 2.24, 2.29, 2.30, 2.31 and 2.32 and below equations:

r_{major} = (3 * 500m^3 / (4.808 * π * 0.222^2) $^{(1/3)}$ = 12.63 meters

$R_{major} = 1.404 * r_{major} = 12.63\ m * 1.404 = 17.73$ meters

d / L = 0.222

$L = R_{major} + r_{major} = 12.63\ m + 17.73\ m = 30.36$ meters

R_r = d/2

$R\_r = (R_{major} + r_{major}) * 0.111 = 30.36\ m * 0.111 = 3.37$ meters

$$A_{balloon} = 4\pi \left(\frac{(12.63 * 3.37\ m)^{1.6075} + (12.63\ m * 17.73\ m)^{1.6075} + (17.73\ m * 3.37\ m)^{1.6075}}{3} \right)^{\frac{1}{1.6075}}$$ so;

$A_{balloon} = 514\ m^2$, $W_{balloon} = 0.142\ (kg/m^2) * 514\ m^2 = 73$ kg

$r_{ballonet} = ((3 / (4 * \pi)) * (200\ m^3 / 2))^{(1/3)} = 2.88$ m so;

$A_{total_ballonet} = (4 * \pi * (2.88)^2) * 2 = 208.5\ m^2$and

$W_{balloonet} = 0.142\ (kg/m^2) * 208.5\ m^2 = 29.6$ kg

$A_{ControlSurfaces} = 0.13 * 500^{(2/3)} = 8.2\ m^2$

$W_{tail\_system} = 4.9\ kg/m^2 * 8.2\ m^2 = 40.2$ kg

$W_{suspension\_system} = 0.010 * 500 = 5$ kg

$W_{nose\_group} = 0.021 * 500 = 10.5$ kg

$W_{access\&maintenance} = 0.01 * 500 = 5$ kg

Table 2.7 Iteration Results for -20 C° at Ground Level for Conceptual Design

W_{solar_sys}	$W_{propulsion\_system}$	$W_{ballonet\_system}$	$A_{ControlSurfaces}$	$W_{access\&maintenance}$	$A_{balloon}$	$W_{balloon}$	W_{nose_group}
53.000	**9.500**	**183.669**	**8.189**	**0.729**	**513.871**	**72.969**	**10.500**
53.000	9.500	182.385	8.178	0.728	513.186	72.872	10.479
53.000	9.500	181.101	8.167	0.727	512.500	72.775	10.458
53.000	9.500	179.817	8.156	0.726	511.814	72.677	10.437
53.000	9.500	178.533	8.145	0.725	511.127	72.580	10.416

Table 2.7 Iteration Results for -20 C° at Ground Level for Conceptual Design (continued)

V_{hull}	W_{total}	$L_{airship}$	R_{major}	r_{major}	W_{Helium}	$W_{suspension\_system}$	$D_{airship}$	R_r
500.000	**610.197**	**30.363**	**17.733**	**12.630**	**82.000**	**5.000**	**6.744**	**3.372**
499.000	608.566	30.343	17.721	12.622	81.836	4.990	6.740	3.370
498.000	606.935	30.323	17.709	12.613	81.672	4.980	6.735	3.367
497.000	605.304	30.303	17.697	12.605	81.508	4.970	6.731	3.365
496.000	603.673	30.282	17.685	12.596	81.344	4.960	6.726	3.363

Table 2.7 Iteration Results for -20 C° at Ground Level for Conceptual Design (continued)

$F_{buoyancy}$ (N)	$F_{buoyancy}$ (kg)	W_{total} + 10%	$W_{GONDOLA}$	$W_{balloonet}$	W_{tail_system}	$V_{ballonet\_filled}$
6298.020	**642.000**	**671.217**	**162.200**	**29.589**	**40.128**	**120.000**
6285.423	640.716	669.423	162.200	29.589	40.074	119.000
6272.827	639.432	667.629	162.200	29.589	40.021	118.000
6260.231	638.148	665.835	162.200	29.589	39.967	117.000
6247.635	636.864	664.040	162.200	29.589	39.914	116.000

CHAPTER 3

DETAILED DESIGN

In the detailed design chapter, all of the sub-systems and their components actual weight will be estimated and 4 iterations will be calculated in order to re-size the airship and prove that the airship satisfies the necessary requirements for peak operating conditions. The hull shape, tail configuration, gondola design, propulsion estimation, solar cell estimation, battery alignment and the suspension line design will also be revised and their weight estimation will also be recalculated.

3.1. Hull Configuration

The hull shape has been envisioned to be an NPL low-drag configuration as the most trustworthy option was thought to be the NPL low-drag configuration and the hull length has been found to be around 30 meters.

The system will consist of 12 gores each of which has been revolved 30 degrees around the central axis and which will be laser cut and attached together with an adhesive material. Less number of gores would be used in order to reduce the seaming material amount and to gain from their weight. For example 2 gores, which would be revolved 90 degrees around its axis, would only need two seaming sections. But, in terms of manufacturing easiness, it would be nearly impossible to handle such huge portions. Not only cutting the desired shape, but also seaming these two pieces by ensuring the correct surface shape would be extremely hard. A compromise has been taken into consideration between reducing the weight or the manufacturing easiness and shape optimization. And, according to that compromise, the best solution was found to use 12 identical gores. The gores will be folded and then attached together. The folded gores are being represented in Figure 3.1.a; and the unfolded gores which will be laser cut are being represented in Figure 3.1.b. These representations are true images of the airship model.

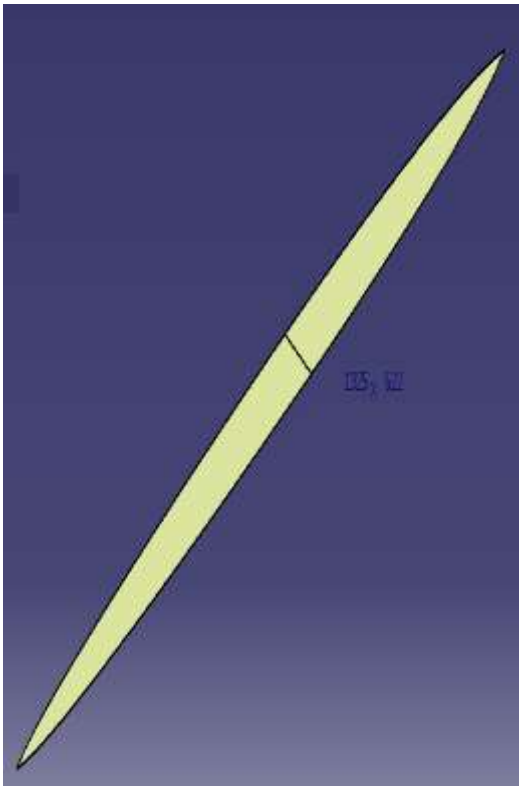

Figure 3.1.a Folded Gore

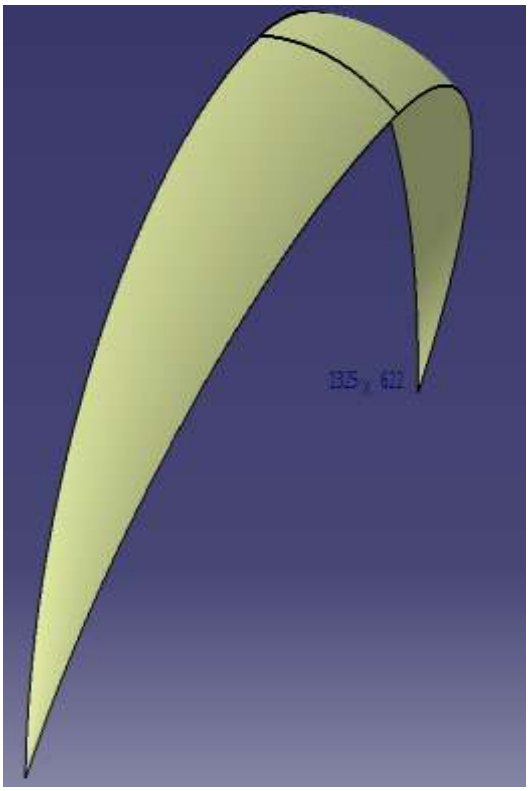

Figure 3.1.b Unfolded Gore

The hull weight will also be estimated taking into account the extra fabric that will be used in order to stick two gores together by using the fabric's heat-sealing ability. The two pieces will be affiliated to each other and the two gores will be sticked together with an extra piece of fabric (seams and patches) getting 5 centimeters wider to each gore of which the configuration can be seen at Figure 3.2.a where all the 12 gores of the airship body were sticked together. The model on Figure 3.2.b is a real model of the airship that has been outlined in the conceptual design process with the dimensions given as 30.4 meters in total length and 6.7 meters in diameter.

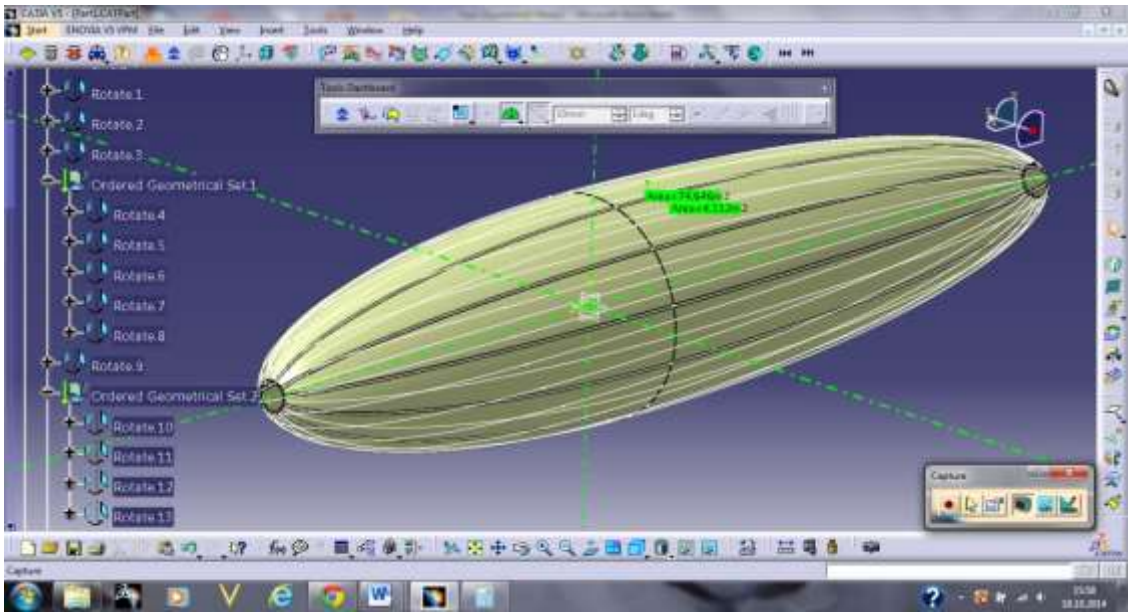

Figure 3.2.a Hull Configuration with 12 Gores and Extra 12 Connective Fabrics Which were Dimensioned According to the Conceptual Design

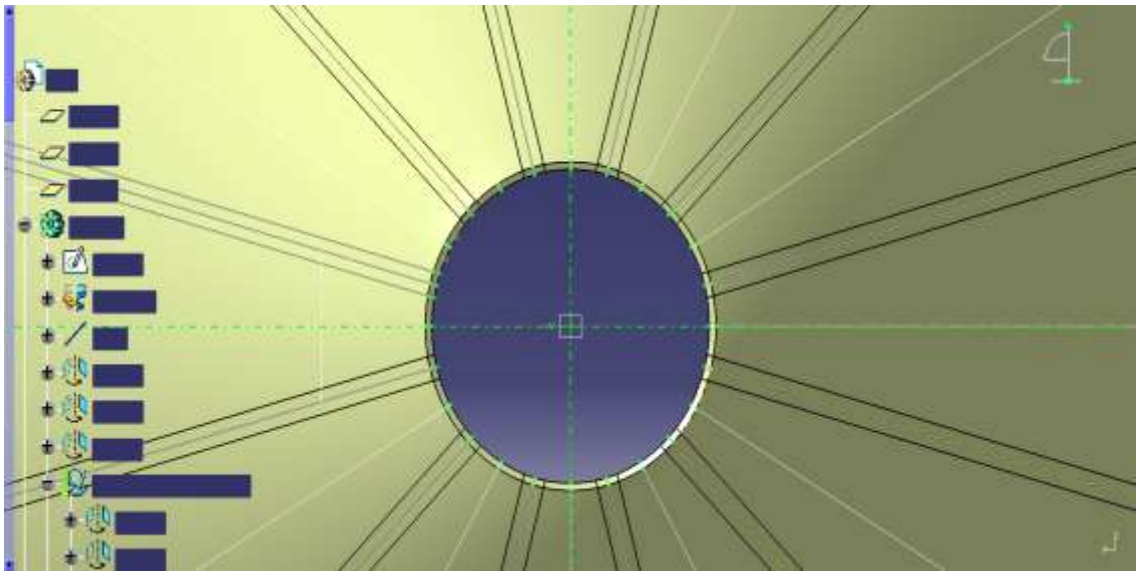

Figure 3.2.b Gore and Connective Fabric Material Configuration

These 12 gores are revolved bodies around central axis for 30 degrees. They are sticked together with 12 pieces of seaming material which ensures that those 12 pieces are connected to each other without losing any Helium. The seaming material area is:

$A_{each\_seam} = 4.112\ m^2$

Thus, the total seaming area is calculated by:

$$A_{seam\_total} = A_{each\_seam} * N_{seam} \quad (3.1)$$

That is;

$A_{seam\_total} = 4.112\ m^2$ / piece * 12 pieces = $49.344\ m^2$

The seaming material desired characteristics are listed in Table 3.1 below:

Table 3.1 Seaming and Patching Material Desired Characteristics

- Long term aging properties
- Improved gas and vapour barrier properties
- Good flexibility and wear resistance
- Heat seal or RF-weldable
- Excellent weatherability
- Functional flame retardance and static dissipation
- Low creep

The same material that is being used for the airship hull (Lamcotec's Heat Sealable 70 Denier Urethane-Coated Nylon Taffeta) satisfies all the requirements above. As this

material is heat sealable also, it is very easy to seam the fabric pieces together. Whenever the fabric that is intended to be attached is heated on top of the other piece with the help of a special iron, it bonds to the other piece and becomes seams the two pieces together.

It has been seen that the total fabric area for the body will be equal to 513.9 m^2 according to Table 2.7. The fabric material that is going to be used including the quantity for seaming and patching purposes is calculated by:

$$A_{fabric\_total} = A_{balloon} + A_{seam\_total} \quad (3.2)$$

That is;

$$A_{fabric\_total} = 513.9\ m^2 + 49.3\ m^2 = 563.2\ m^2$$

The total weight of the fabric material to be used calculated by:

$$W_{fabric} = A_{fabric\_total} * A_{density\_fabric} \quad (3.3)$$

That is,

$$W_{fabric} = 563.2\ m^2 * 0.142\ kg/m^2 = 80\ kg$$

This fabric weight should be allocated for the hull weight if NPL- low drag contribution type is used. The value has been calculated to be around 73 kg. The difference is to be accounted for the seams and the patches.

3.2. Nose Cone and Tail Cone System

The nose cone and the tail cone configuration are to be computed with the help of the drawings which have been prepared in CATIA V5. The related weight estimation will

also be made according to these 3-D drawings. The main material that is going to be used for the nose cone and tail cones is going to be aluminum, and after using the "Apply Material" command of CATIA, the total weight will be found out accordingly. The nose cone and the tail cone has been dimensioned according to where the hull fabric ends, the nose cone is laced to the hull gores. It is an important part which makes sure that the whole system will stay stable, whenever an unexpected wind load occurs. It will also withstand the loads whenever the system is moored into the mast. The tail cone is used to ensure that the fabric gores are slicked together properly. The nose cone and the tail cone can be seen at Figure 3.3.a and 3.3.b respectively, which were dimensioned with respect to the findings gathered at conceptual design chapter.

The nose cone system is consisting of three major elements:

- Nose cone
- Nose Cone battens
- Spike

These three elements come together to compose the nose cone system. The total weight of the nose cone system would be:

$$W_{nose\_cone\_system} = W_{nose\_cone} + W_{nose\_cone\_battens} + W_{spike\_configuration} \quad (3.4)$$

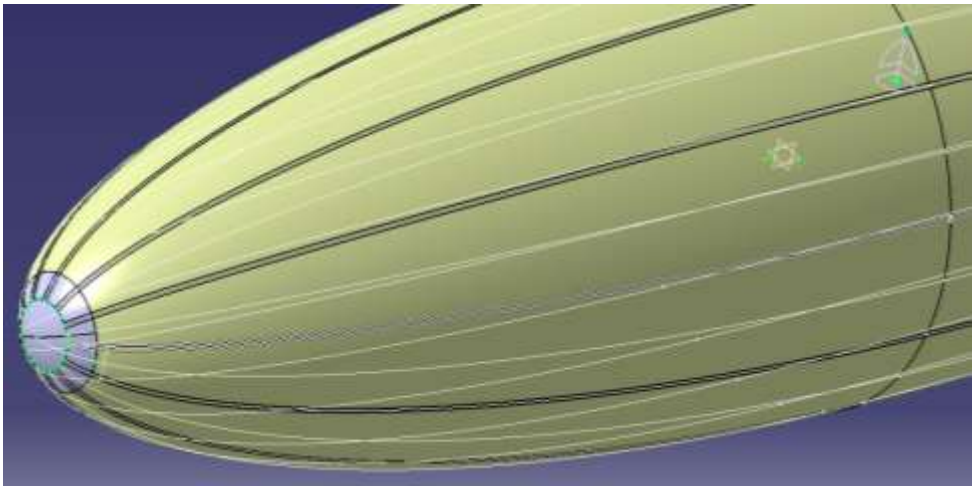

Figure 3.3.a Nose Cone Design According to the Conceptual Design Results

The same profile of the fore ellipse has been used while designing the nose cone and this profile has been revolved along the central axis. The nose cone has been designed to be made up of aluminum of 1mm thickness and goes beyond 50 centimeters where the fabric ends. This extra length has been put in order to be sure that the system is capable of withholding the Helium inside the volume.

The reason why aluminum has been chosen lies behind aluminum's perfect Helium keeping ability inside of it. And as gores are lid together inside this nose cone, a very good Helium insulator is needed to be used as the biggest losses occur at the seams and patches generally. And at the nose cone there will be 12 seams attached together. The total weight of the nose cone itself has come out to be:

$W_{nose\_cone} = 11.1$ kg

This weight calculation result is found excluding the nose cone batten weights and the spike weight.

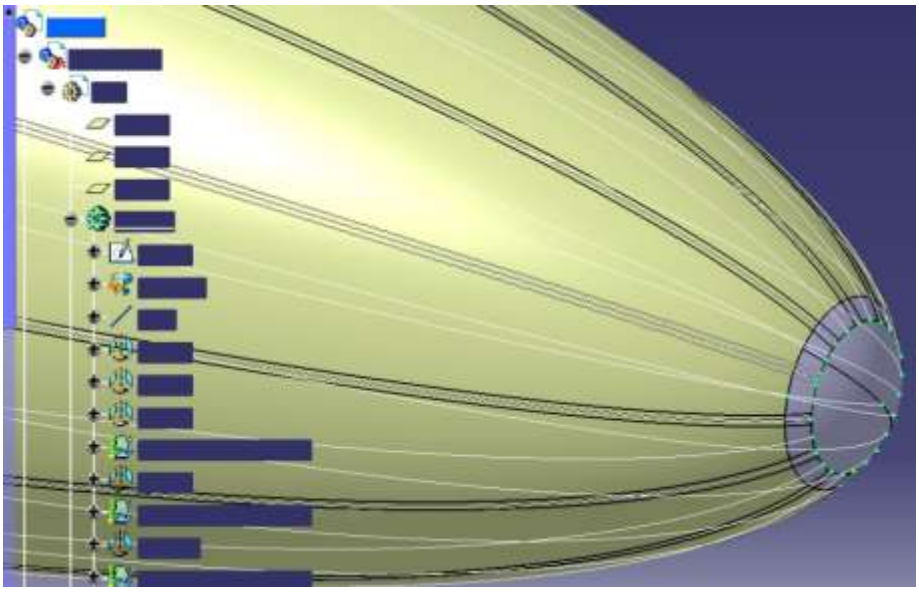

Figure 3.3.b Tail Cone Design According to the Conceptual Design Results

The tail cone is again made up of the same profile with the aft ellipse revolved around the central axis. But it was made from 0.5 mm thickness aluminum instead of 1 mm thickness aluminum which was used for the nose cone. As the nose cone will be exposed to much more severe loads than the tail cone and as there will be battens attached to the nose cone with the help of a spike which will also be used to moor the ship to the mast, there needs to have enough thickness in order to weld the system together.

This time the cone goes beyond 20 centimeters only, as there are not that much extra forces that needs to be withstanded and as there are no battens stretching backwards. Again this part is made up of aluminum as aluminum is the best keeper of Helium. There will not be any battens at the rear side by the reason of lack of forces that needs to be withstanded. Totally the tail cone weighs about:

$W_{tail\_cone} = 3.6$ kg

The nose cone battens and the spike that will allow the airship to be moored to the mooring mast will be positioned at the front end of the airship. The design of the spike that will be used to moor the airship can be seen at Figure 16. It is made up of aluminum

profiles which were welded together in order to provide the shape of the airship stable even in extreme wind conditions or when the whole airship is moored. The spike weight distribution is:

$$W_{spike\_configuration} = W_{spike} + W_{batten\_connections} + W_{base\_ring\&support\_rods} \quad (3.5)$$

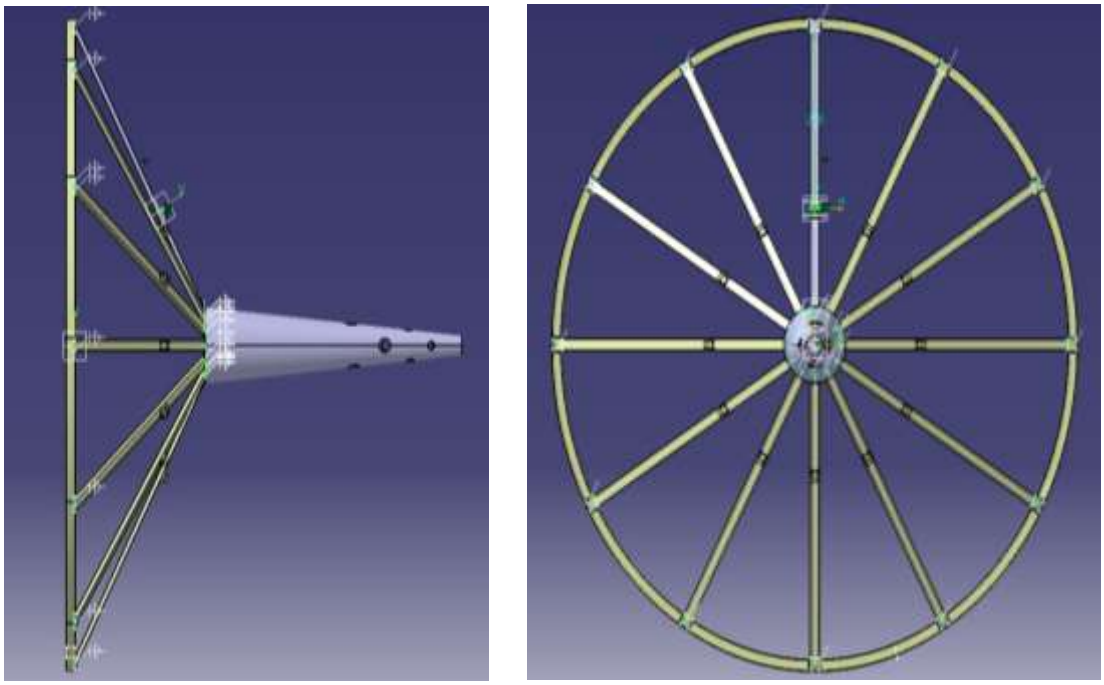

Figure 3.4 Nose Cone Spike and the Nose Cone Batten Holder

There are 12 pieces of support bars, which are used to hold the battens and to distribute the loads. These bars were welded to both the base ring and to the spike that can be seen above. The spike is especially designed to stay inside the moor with holes distributed around it which are to keep the spike inside the moor. According to Catia Add Material function the spike weighs around:

$W_{spike} = 2$ kg

The connection parts of the battens weigh around:

$W_{batten\_connections} = 1.2$ kg

The support rods and the base ring weigh around:

$W_{base\_ring\&support\_rods} = 1.5$ kg

In other words, according to the equation 3.5, the spike configuration weighs about:

$W_{spike\_configuration} = W_{spike} + W_{batten\_connections} + W_{base\_ring\&support\_rods}$

Thus,

$W_{spike\_configuration} = 2$ kg + 1.2 kg + 1.5 kg = 4.7 kg

This weight is the total weight excluding the other structures such as the nose cone battens and the nose cone itself. The details of the drawings (technical drawings in 2-D) can also be found in Appendix B

The nose cone battens are the main reason why all of these components listed above have been designed. These components' main aim is to supplement the needed support to the battens in order to keep the airship's shape stable to hold the drag forces in the lowest possible values and to ensure that the system is safely carrying the payload. 12 battens have been used for the 12 gores of the body. These battens are being bonded to both the hull and to the batten holders on the fore end. They are positioned at the middle of each fabric gore where each one of the battens extend up to 8 meters rearwards from the very beginning of the airship. 8 meters of extension has been decided from the rule of thumb of the batten extension (8) where "L_{each_batten}" is the length of each batten and "L" equals to total length of the airship body in x-direction

$$L_{each\_batten} = 0.2 * L \quad (3.6)$$

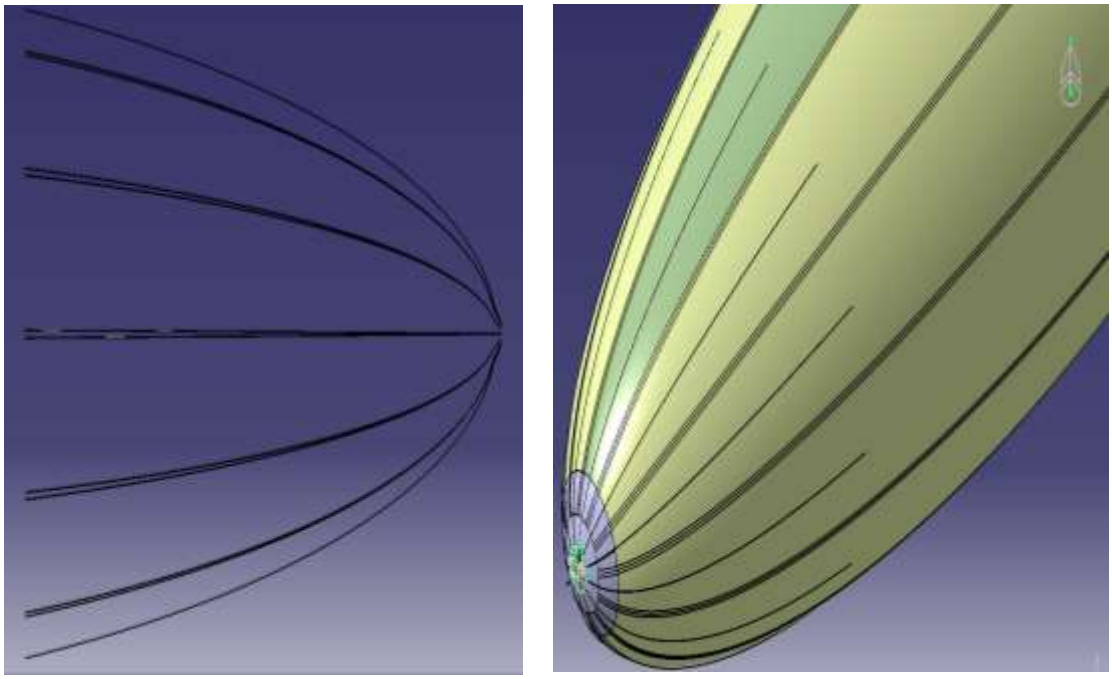

Figure 3.5 The Nose Cone Batten Configuration

The nose cone batten configuration can be seen at Figure 17. At the first picture, only the battens are shown, but at the second picture, the whole configuration is being shown respectively. The batten configuration weight breakdown has been made accordingly:

$$W_{battens\_configuration} = W_{battens} + W_{hooks\&bonding} \quad (3.7)$$

The battens that are going to be used are "Surelift Performance Series 620 which has a diameter of 6 mm" and they have an annular weight of 120g/m. Each rope's length is 8.4 meters and 12 battens are totally used. Thus, for calculating the total length of the battens the related equation was applied:

$$L_{battens\_total} = L_{each\_batten} * N_{battens} \quad (3.8)$$

Thus, the total length used becomes;

$L_{battens\_total}$ = 8.4 m/piece * 12 pieces = 100.8 m in length.

As 120 g/m is the specific weight of the battens, the total weight of the battens is calculated by the equation below:

$$W_{battens} = SW_{battens} * L_{battens\_total} \quad (3.9)$$

That leads to;

$W_{battens} = 0.12$ kg/m * 100.8 = 12.1 kg.

Moreover, since the hooks and their bonding totally weighs about 2.4 kg, the total weight for battens is calculated by the equation 3.7:

$$W_{battens\_configuration} = W_{battens} + W_{hooks\&bonding}$$

Meaning;

$W_{battens\_configuration}$= 12.1 kg + 2.4 kg = 14.5 kg

The nose cone system total weight is calculated by:

$$W_{nose\_cone\_system} = W_{nose\_cone} + W_{battens\_configuration} + W_{spike\_configuration} \quad (3.10)$$

Thus, the total weight would be:

$W_{nose\_cone\_system}$ = 11.1 kg + 14.5 + 4.7 = 30.3 kg.

When nose and tail system weights are added together, the total weight of the nose and the tail cone system is found to be 33.9 kg where it was estimated to be 24.15 before in the conceptual design process and with a 10% of safety factor, 26.4 kg was left for the nose and tail system together. But, even if the manifested weight is different than what was expected, a difference of 7 kg is not a very big deal to deal with in such an airship.

But again the calculations about the nose cone and the tail cone will be revised accordingly and in the detailed design, they will be kept separated to ensure that the CG calculations are to be made in a correct order.

3.3. Suspension Lines' Design

Suspension lines are the mainframe elements putting the whole system and the gondola (payload carrying unit) together. As this is a blimp not a rigid or a semi-rigid airship, the whole system is standing together as a whole with the help of inside and outside pressure difference [8]. But this system needs to be supported in order to avoid the loads to be concentrated at one point and endangering the systems' reliability and durability. These supporting units are being called as suspension lines and these lines are to be designed carefully by taking into account the gains and the losses such as weight, structural load distributions, complexity of design and manufacturing processes and deformation of the hull body while carrying the gondola and its related components such as batteries, payloads, receivers and the gondola structure itself [21].

There are mainly two configurations related to suspension line design; one of which is the conventional type, where many suspension lines lie down inside the hull volume from the top of the hull body up to the gondola which can also be seen on Figure 3.6 [27].

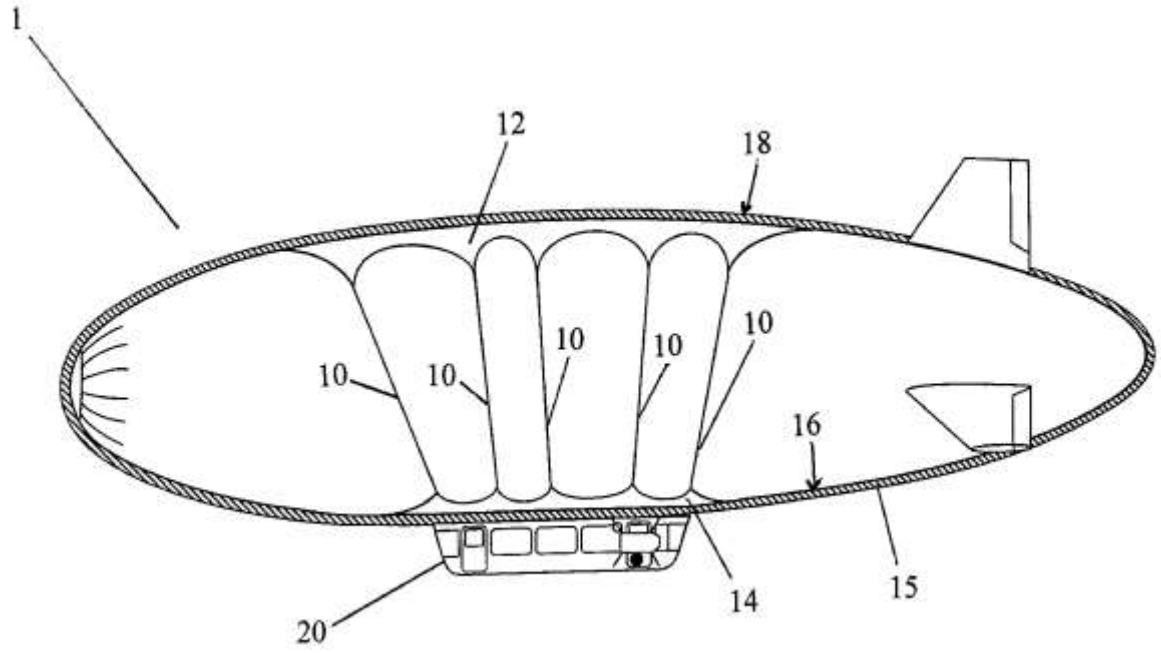

Figure 3.6 Conventional type of a suspension line design [27]

And the other configuration is the two rope rings, being braced to the gondola at two ends and at the hull body completely, which are mainly distributing the loads that are being generated by the gondola weight. Even though this kind of attachment is distributing the loads generated by the gondola less efficiently than the conventional type, it is much less complex to manufacture, support and attach. Also the risk of these ropes to interlace together would be eliminated by this way and for small loads, this kind of load distribution unit will be enough. This type of suspension lines can be seen at Figure 3.7 [21].

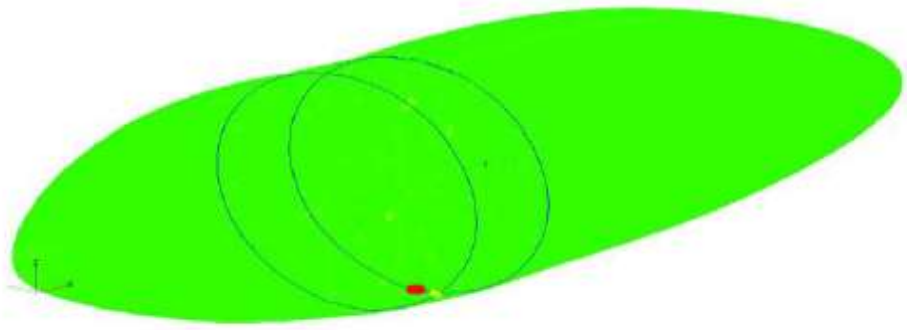

Figure 3.7 Deformation and Force of Airship Model [21]

The same ropes that are being used in the nose cone battens which are "Surelift Performance Series 620" would be used for the suspension lines. Assuming the section for the largest diameter for the rope length calculation as some extras would be needed also, the length of the lines would be:

$$L_{suspension\_lines} = 2 * (2 * \pi * R\_r) \quad (3.11)$$

That is;

$L_{suspension\_lines}$ = 2* (2 * π * 3.37 m) = 42.3 meters of suspension lines are to be used.

The total weight of these lines would be calculated by:

$$W_{suspension\_lines} = SW_{ropes} * L_{suspension\_lines} \quad (3.12)$$

So that, it is calculated as:

$W_{suspension\_lines}$ = 0.12 kg/m * 42.3 m = 5.1 kg

Allowing 20% of the line weight for the seams and patches leads to the related equation:

$$W_{seams\&patches\_suspension} = 20\ \% * W_{suspension\_lines} \quad (3.13)$$

So that, the calculation result becomes;

$$W_{seams\&patches\_suspension} = 0.2 * 5.1\ kg = 1\ kg$$

Then, the total weight of the suspension system would be calculated by the equation below:

$$W_{suspension\_sys} = W_{suspension\_lines} + W_{seams\&patches\_suspension} \quad (3.14)$$

Thus, the total weight is;

$W_{suspension\_sys}$ = 5.1 kg + 1 kg = 6.1 kg in total.

3.4. Drag Calculations and Preliminary CFD Results

Although it is nearly impossible to predict the exact drag of a body, many approaches exist to have a model for the flow and also to at least have an approximation for the forces inside the flow. The best and the most efficient way is to use CFD calculations.

As the shape of the airship has not yet been finalized, only the hull body has been used for the preliminary CFD calculations. The CFD analysis approach to calculate the drag force of the airship is using a constant velocity inlet and constant pressure outlet. As no supercritical values are needed for the analysis, inviscid flow has been chosen for the preliminary calculations. According to those calculations the hull would be creating a drag coefficient of:

$C_D = 0.0224$

This would mean:

$$D = 0.5 * \rho_{\infty} * V^2_{\infty} * S_{ref} * C_D \quad (3.15)$$

Thus, it is calculated as:

$$D = 0.5 * 1.0\ kg/m^3 * (25\ m/s)^2 * 35.7\ m^2 * 0.0224 = 250\ N$$

This 250 N is calculated for 90 km/h wind speeds. But, as this estimation has been made only for the hull of the airship this calculation will be extended for the rest of the airship with a rule of thumb [8]. According to the rule of thumb, the envelope drag is calculated by the equation below:

$$D_{envelope} = 40\ \% * D_{Total} \quad (3.16)$$

Then the total drag for the airship would be:

$$D_{Total} = 2.5 * D_{envelope} = 2.5 * 250\ N = 625\ N$$

3.5. Propulsion System Calculations

A special type of propeller is needed to be chosen also to overcome the drag value of the design specification. The propeller diameter will be 22 inches and the pitch of it will be 12 inches made by carbon-fiber [28], producing around 65 kg of thrust (in total) at peak conditions. This will ensure that the chosen configuration of envelope and design criteria is going to be achieved.

The thrust generated has to be equal to drag at peak operating conditions in order to satisfy the design requirements. In other words:

$$T_{Generated} \geq D_{Total} \quad (3.17)$$

Then, which is calculated as:

$T_{Generated} = 65 * 9.81 = 638\ N \geq 625N$

Since $T_{Generated}$ is found to be higher than D_{Total}, the requirement has been satisfied for the current configuration as it can be seen above. The weight estimation to be used is the same as in the conceptual design process as the system still satisfies the requirements.

3.6. Detailed Design Iteration Results

The final iteration results for the detailed design calculations can be seen at Tables 3.3, 3.4, 3.5 and 3.6. The reason of having four different tables is to simulate the four peak operating conditions for the airship and to conclude that the system would satisfy the requirement for peak operating temperatures which are listed below at Table 3.2.

Table 3.2 Peak Operating Temperatures and Altitude Ranges vs. the Requirement Satisfaction Criteria

Peak Operating Temperatures and Altitude Ranges	Requirement Satisfaction Criteria
0 meters altitude at 40 C°	No excess lifting force with air inside the ballonets
1000 meters altitude at 34 C°	$F_{buoyancy} \geq W_{total}$
0 meters altitude at -20 C°	No excess lifting force with air inside the ballonets
1000 meters altitude at -30 C°	$F_{buoyancy} \geq W_{total}$

Only the successive sections of the tables have been listed below; the complete table results have been given in Appendix A.

Table 3.3 Weight Calculation Iteration Results for 0 Meters Altitude and 40 C° after Detailed Design Process

W_{solar_sys}	$W_{propulsion\_system}$	$W_{ballonet\_system}$	$A_{ControlSurfaces}$	$W_{access\&maintenance}$	$A_{balloon}$	$W_{balloon}$	W_{nose_group}
53.000	9.500	108.269	8.189	0.729	513.871	72.969	30.300
53.000	9.500	107.145	8.179	0.728	513.186	72.872	30.300
53.000	9.500	106.021	8.168	0.727	512.500	72.775	30.300
53.000	9.500	104.897	8.157	0.726	511.814	72.677	30.300
53.000	9.500	103.773	8.146	0.725	511.127	72.580	30.300

Table 3.3 Weight Calculation Iteration Results for 0 Meters Altitude and 40 C° after Detailed Design Process (cont'd)

V_{hull}	W_{total}	$L_{airship}$	R_{major}	r_{major}	W_{Helium}	$W_{suspension\_system}$	$D_{airship}$	R_r
500.000	562.597	30.363	17.733	12.630	82.000	6.100	6.744	3.372
499.000	561.157	30.343	17.721	12.622	81.836	6.100	6.740	3.370
498.000	559.717	30.323	17.709	12.613	81.672	6.100	6.735	3.367
497.000	558.277	30.303	17.697	12.605	81.508	6.100	6.731	3.365
496.000	556.837	30.282	17.685	12.596	81.344	6.100	6.726	3.363

Table 3.3 Weight Calculation Iteration Results for 0 Meters Altitude and 40 C° after Detailed Design Process (cont'd)

$F_{buoyancy}$ (N)	$F_{buoyancy}$ (kg)	$W_{GONDOLA}$	$W_{balloonet}$	W_{tail_system}	$V_{ballonet\_filled}$	W_{tail_cone}
5513.220	562.000	165.500	29.589	40.128	70.000	3.600
5502.193	560.876	165.500	29.589	40.074	69.000	3.600
5491.167	559.752	165.500	29.589	40.021	68.000	3.600
5480.140	558.628	165.500	29.589	39.967	67.000	3.600
5469.114	557.504	165.500	29.589	39.914	66.000	3.600

Table 3.4 Weight Calculation Iteration Results for 1000 Meters Altitude and 34 C° after Detailed Design Process

W_{solar_sys}	$W_{propulsion\_system}$	$W_{ballonet\_system}$	$A_{ControlSurfaces}$	$W_{access\&maintenance}$	$A_{balloon}$	$W_{balloon}$	W_{nose_group}
53.000	9.500	41.517	8.189	0.729	513.871	72.969	30.300
53.000	9.500	41.517	8.178	0.728	513.186	72.872	30.300
53.000	9.500	41.517	8.167	0.727	512.500	72.775	30.300
53.000	9.500	41.517	8.156	0.726	511.814	72.677	30.300
53.000	9.500	41.517	8.145	0.725	511.127	72.580	30.300

Table 3.4 Weight Calculation Iteration Results for 1000 Meters Altitude and 34 C° after Detailed Design Process (cont'd)

V_{hull}	W_{total}	$L_{airship}$	R_{major}	r_{major}	W_{Helium}	$W_{suspension\_system}$	$D_{airship}$	R_r
500.000	495.845	30.363	17.733	12.630	82.000	6.100	6.744	3.372
499.000	495.529	30.343	17.721	12.622	81.836	6.100	6.740	3.370
498.000	495.213	30.323	17.709	12.613	81.672	6.100	6.735	3.367
497.000	494.897	30.303	17.697	12.605	81.508	6.100	6.731	3.365
496.000	494.581	30.282	17.685	12.596	81.344	6.100	6.726	3.363

Table 3.4 Weight Calculation Iteration Results for 1000 Meters Altitude and 34 C° after Detailed Design Process (cont'd)

$F_{buoyancy}$ (N)	$F_{buoyancy}$ (kg)	$W_{GONDOLA}$	$W_{balloonet}$	W_{tail_system}	$V_{ballonet\_filled}$	W_{tail_cone}
4875.570	497.000	165.500	29.589	40.128	12.000	3.600
4865.818	496.006	165.500	29.589	40.074	12.000	3.600
4856.067	495.012	165.500	29.589	40.021	12.000	3.600
4846.316	494.018	165.500	29.589	39.967	12.000	3.600
4836.565	493.024	165.500	29.589	39.914	12.000	3.600

Table 3.5 Weight Calculation Iteration Results for 0 Meters Altitude and -20 C° after Detailed Design Process

W_{solar_sys}	$W_{propulsion\_system}$	$W_{ballonet\_system}$	$A_{ControlSurfaces}$	$W_{access\&maintenance}$	$A_{balloon}$	$W_{balloon}$	W_{nose_group}
53.000	9.500	251.989	8.189	0.729	513.871	72.969	30.300
53.000	9.500	250.599	8.178	0.728	513.186	72.872	30.300
53.000	9.500	249.209	8.167	0.727	512.500	72.775	30.300
53.000	9.500	247.819	8.156	0.726	511.814	72.677	30.300
53.000	9.500	246.429	8.145	0.725	511.127	72.580	30.300

Table 3.5 Weight Calculation Iteration Results for 0 Meters Altitude and -20 C° after Detailed Design Process (cont'd)

V_{hull}	W_{total}	$L_{airship}$	R_{major}	r_{major}	W_{Helium}	$W_{suspension\_system}$	$D_{airship}$	R_r
500.000	706.317	30.363	17.733	12.630	82.000	6.100	6.744	3.372
499.000	704.611	30.343	17.721	12.622	81.836	6.100	6.740	3.370
498.000	702.905	30.323	17.709	12.613	81.672	6.100	6.735	3.367
497.000	701.199	30.303	17.697	12.605	81.508	6.100	6.731	3.365
496.000	699.493	30.282	17.685	12.596	81.344	6.100	6.726	3.363

Table 3.5 Weight Calculation Iteration Results for 0 Meters Altitude and -20 C° after Detailed Design Process (cont'd)

$F_{buoyancy}$ (N)	$F_{buoyancy}$ (kg)	$W_{GONDOLA}$	$W_{balloonet}$	W_{tail_system}	$V_{ballonet\_filled}$	W_{tail_cone}
6817.950	695.000	165.500	29.589	40.128	160.000	3.600
6804.314	693.610	165.500	29.589	40.074	159.000	3.600
6790.678	692.220	165.500	29.589	40.021	158.000	3.600
6777.042	690.830	165.500	29.589	39.967	157.000	3.600
6763.406	689.440	165.500	29.589	39.914	156.000	3.600

Table 3.6 Weight Calculation Iteration Results for 1000 Meters Altitude and -30 C° after Detailed Design Process

W_{solar_sys}	$W_{propulsion\_system}$	$W_{ballonet\_system}$	$A_{ControlSurfaces}$	$W_{access\&maintenance}$	$A_{balloon}$	$W_{balloon}$	W_{nose_group}
53.000	9.500	183.669	8.189	0.729	513.871	72.969	30.300
53.000	9.500	182.385	8.178	0.728	513.186	72.872	30.300
53.000	9.500	181.101	8.167	0.727	512.500	72.775	30.300
53.000	9.500	179.817	8.156	0.726	511.814	72.677	30.300
53.000	9.500	178.533	8.145	0.725	511.127	72.580	30.300

Table 3.6 Weight Calculation Iteration Results for 1000 Meters Altitude and -30 C° after Detailed Design Process (cont'd)

V_{hull}	W_{total}	$L_{airship}$	R_{major}	r_{major}	W_{Helium}	$W_{suspension\_system}$	$D_{airship}$	R_r
500.000	637.997	30.363	17.733	12.630	82.000	6.100	6.744	3.372
499.000	636.397	30.343	17.721	12.622	81.836	6.100	6.740	3.370
498.000	634.797	30.323	17.709	12.613	81.672	6.100	6.735	3.367
497.000	633.197	30.303	17.697	12.605	81.508	6.100	6.731	3.365
496.000	631.597	30.282	17.685	12.596	81.344	6.100	6.726	3.363

Table 3.6 Weight Calculation Iteration Results for 1000 Meters Altitude and -30 C° after Detailed Design Process (cont'd)

$F_{buoyancy}$ (N)	$F_{buoyancy}$ (kg)	$W_{GONDOLA}$	$W_{balloonet}$	W_{tail_system}	$V_{ballonet\_filled}$	W_{tail_cone}
6298.020	642.000	165.500	29.589	40.128	120.000	3.600
6285.423	640.716	165.500	29.589	40.074	119.000	3.600
6272.827	639.432	165.500	29.589	40.021	118.000	3.600
6260.231	638.148	165.500	29.589	39.967	117.000	3.600
6247.635	636.864	165.500	29.589	39.914	116.000	3.600

As it was seen in Tables 3.3, 3.4, 3.5 and 3.6; all the requirements given in Table 3.2 above have been satisfied.

CHAPTER 4

STABILITY

4.1. Tail Configuration

Tail configuration is an important aspect of the airship design. This is an entirely solar powered airship meaning that no other source of energy is available which also means that there isn't much excess power available in this system. This increases the importance of the efficiency of the tail configuration. Even further, as the biggest energy consuming unit in an aircraft is its engine and in order to decrease the energy consumed by the engine; the least drag encountering position against the wind must be attained which is the forward facing position against the wind. To achieve this mission, tail is an important part of the design.

Tail configuration is important as this is not a tethered system, the mission may include patrolling an area or using the moving ability of the airship from one place to another or in order to avoid excessive weather conditions, maneuvering might be needed. Although, the maneuvering ability that would be expected is not of the same kind of its aerodynamic counterparts, the best compromise with weight, efficiency and the cost should be made very carefully. Because not, much efficiency is expected, but inefficiency is also not wanted; weight is an important aspect while making decisions about the configuration of the tail, but while decreasing weight, high cost options should also be avoided such as the complex composite materials. Although the composite materials can decrease the weight of the component up to 20%, the increase in price and complexity while manufacturing instead of other options would overcome the advantages of using them.

The position where the tail needs to stand is another big issue because, if the tail is too forward, the moment arm will be too little to enable the moments needed or if the tail is

too rearwards then the weight of the tail will become a huge burden for the rear side to provide the buoyancy needed. In order to stabilize this force, the gondola also would be needed to move too much forward which may eventually cause some structural problems.

There are numerous configuration options for tails such as the V-tail, H-tail, conventional types etc. (Appendix B). But when it comes to airships, the most efficient types of tail configurations are the inverted-Y configuration and the conventional tail configurations. The conventional tail configuration is used in almost 70% of the aircrafts designed up to date and they do provide enough stability and control [17]. The inverted-Y configuration on the other hand has been used extensively in the aerostats especially. Although the conventional type of tails are more trustworthy as they are time-tested, the increase in the efficiency of the inverted-Y configuration against the conventional type is a good compromise that needs to be taken under consideration seriously as in the other criteria, to increase the efficiency of the tail section, much more effort needs to be taken in terms of both the cost and the manufacturing complexity.

This specific configuration is a good responder for low air speeds and it has clearly been seen that although increasing anhedral decreases longitudinal stability, it has a positive effect on directional stability. At the paper named as "Aerodynamic Design of KARI-Mid Sized Aerostat", the tail-body configuration of an aerostat, with similar dimensions, has been investigated. Even though the paper is mainly focusing on aerostats, the mission objectives are not very apart from each other.

An inverted Y-configuration will be used with some degree of anhedral to increase the efficiency of the tail section. Two different types of fin-body configurations mainly for the anhedral degree has been deeply investigated and found different results for both the 30° and 45° anhedral types. In terms of drag coefficient (C_d), they both had similar ranking. But it has been clearly seen that, in terms of lift coefficient (C_L) and pitching moment coefficient (C_m), 30° anhedral tail configuration has the lead. But, in terms of, yawing moment coefficient (C_n), rolling moment coefficient (C_l), and side force

coefficient (C_N), 45° anhedral type of tail configuration has the lead as it can easily be seen on Table 4.1 below:

Table 4.1 Coefficients vs Anhedral Types for Different Angles of Anhedral

	C_l	C_L	C_m	C_n	C_N
30° anhedral type	X	O	O	X	X
45° anhedral type	O	X	X	O	O

O: Preferable **X:** Non-Preferable

The lift coefficient and pitching moment coefficients can be important for aero dynamical counterparts as for nearly all of them to take-off, land, increase or decrease altitude, they need the pitching moment to create angle of attack. But for an airship, these are not important, as the airship will almost never need to pitch-up or down. And to increase or decrease altitude, the airship does not need to give any angle of attack, take in or leave some air from the ballonets would do what is necessary. Also the thrust vectoring of the electrical motors increase the ability to land and/or take-off.

The yawing moment coefficient, side force coefficient and the rolling moment coefficient are much more important for the efficiency of the entire system. As the biggest handicap of this system is its low maneuverability, which makes the system vulnerable to rapid climate changes. To sustain the efficiency of the system in long term (as the system is named as high endurance system, it needs to endure for 2 weeks continuously), maneuverability at least to some extent is needed. For the airship to change its location in the best route possible maneuverability to some extent is needed. The most important thing is the drag, as this kind of a system with a huge hull can be dragged easily if it can't take the wind from its front face, where the smallest projection area is achieved. In order to take the wind from the front position the yawing moment and the side force coefficient is the most important aspects. And with the light of this

information, the anhedral type of 45° is chosen to be used as it shows the best characteristics for very low airspeeds.

While cambered airfoils create nose down pitching moment, symmetric airfoils have zero pitching moment ($C_{m,0}$) at zero angle. In the below Table 4.2, different airfoil profile investigations have been listed:

Table 4.2 Specifications of Different Airfoil Profiles

Airfoil	Thickness (%)	$C_{l,max}$	Design C_t	C_{m0}	C_{d0} at Design C_1	C_{d0},min	Re (10^6)
NACA 0009	9	1.25	-	0	-	0.0052	3
NACA 0012	12	1.5	-	0	-	0.0057	3
NACA 001264	12	1.35	-	0	-	0.005	3
NACA 0012 64Mod	12	1.5	-	-0.05	-	0.0042	3
NACA 1408	8	1.35	-	-0.025	-	0.005	3
NACA 1410	10	1.5	-	-0.0015	-	0.0055	3
NACA 1410	12	1.6	-	-0.0025	-	0.006	3
NACA 23012	12	1.6	0.3	-0.00125	0.0068	0.0065	3

Because of this reason, a symmetric airfoil is going to be used in order to be sure that the best compromise is being gathered between cost, manufacturing ease and efficiency as to produce a symmetric airfoil is much easier than to produce a cambered one and to manufacture it, is much easier. As in the future if composites were to be used for tail manufacturing, only one mold will be needed for the symmetric profile. Also they are much more efficient than a flat plate, meaning that the best compromise is achieved. As a result, NACA 0018 airfoil profile has been chosen between symmetric airfoils to ensure stability and to increase maneuverability as much as possible.

The sweep of the tail is another issue that needs to be decided and as Raymer mentioned in his book “Aircraft Design: A Conceptual Approach”, for low speed aircrafts there is no reason to have a vertical tail sweep beyond 20 degrees other than aesthetics, we will also be using 20 degrees of sweep in order to be sure that the tail profile will be out of the wake and as there is no way to achieve the critical Mach number, the profile isn’t needed to stay inside the Mach Cone, also meaning that no excess tail sweep is needed [17].

The size and the location of the tail is an important aspect also, which needs to be taken into account very carefully. In order to decide the location of the tail, a CFD analysis with inviscid flow over it has been simulated. The orthogonal quality of the mesh was around 0.23 and assumed simple velocity inlet and pressure outlet. The reason of choice for such a method was only to determine the tail location and to provide an insight into the drag calculations. In the following sections a deeper analysis have been made. The ending location of the tails (26.4 meters from the nose tip) has been chosen according to the CFD calculations which can also be seen at Figure 18. These calculations have been made for the peak values, which have been set to be 90 km/h (25m/s). As it can be seen easily the flow becomes unsteady around 27 m hull length. To increase the efficiency of the tails, the flow around them should be regular and uniform. The moment arm is also needed to be as long as possible, to increase the effectiveness of the tails.

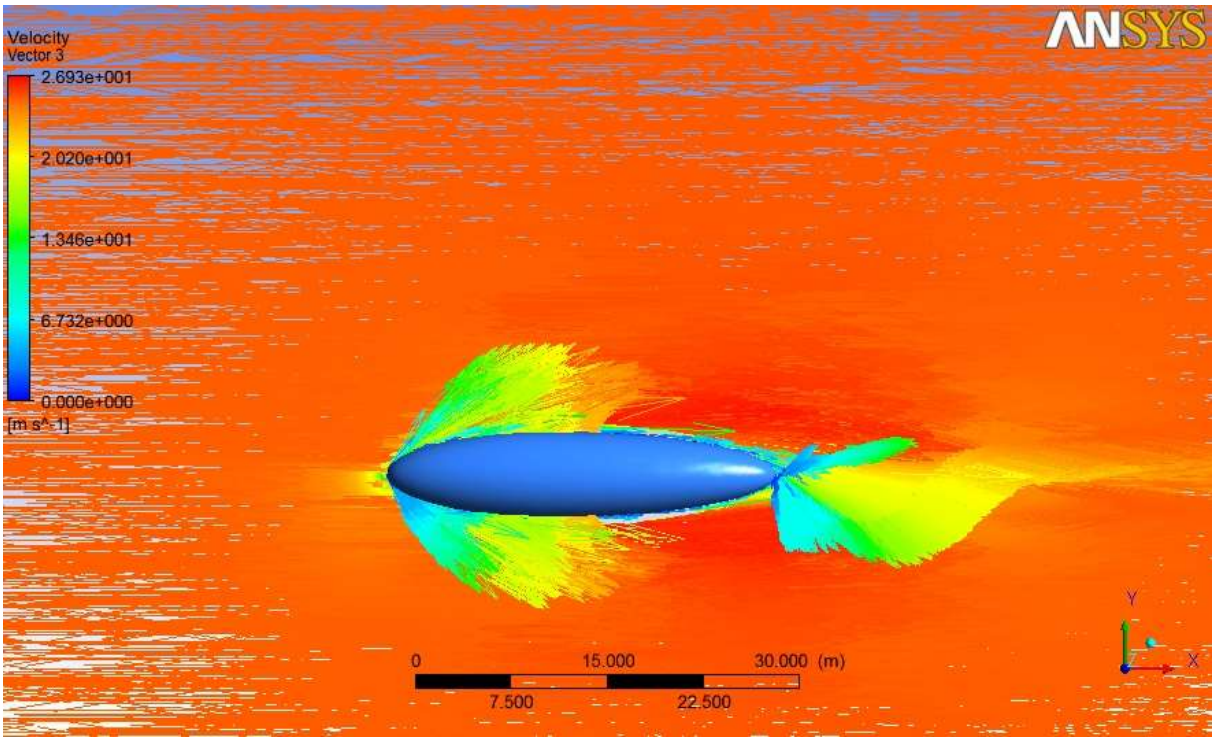

Figure 4.1 CFD Results Showing the Flow (25m/s) Around the 3D Model of Airship Hull

About the determination of tail size, Kleiner [29] has a suggestion which can also be used as a rule of thumb (see equation 4.1). This figure can be used for both the vertical and the horizontal tails' control surfaces.

$$A_{CS} = 0.13 \times V^{(2/3)} \quad (4.1)$$

Thus,

$$A_{CS} = 0.13 \times 500^{(2/3)} = 8$$

According to the equation 4.1, 8 m^2 of surface area for both the vertical and horizontal control surfaces is needed. As the tail configuration is inverted-Y configuration with 45 degrees anhedral, the total control surface would be 16 m^2. According to these calculations, the inverted tail areas (the ones with 45° of anhedral) are found to be as:

$$A_{inverted\_tail} = A_{CS} / \sin(\pi/4) \quad (4.2)$$

That is,

$8\ m^2 / \sin(\pi/4) = 11.3\ m^2$

That each individual fin needs to have around 5.5 m^2 of control surface area (projection area) as a rule of thumb. This figure will be applied for the diagonal fins. In order to achieve extra yaw control, the same tail size will also be used for the vertical fins to ensure maneuverability.

So, the best compromise between the moment arm and the efficiency of the airship has been made and the tail ending location (including the control surfaces), have been set to be just before the wake development section.

$$26.4\ m = (X_{tail\_ending\_point} / l_{hull}) * l_{hull} \quad (4.3)$$

$$X_{tail\_ending\_point} / l_{hull} = 26.4\ m / 30.4\ m = 77\ \% \quad (4.4)$$

$$23.4\ m = (X_{tail\_stating\_point} / l_{hull}) * l_{hull} \quad (4.5)$$

$$X_{tail\_starting\_point} / l_{hull} = 23.4\ m / 30.4\ m = 87\ \% \quad (4.6)$$

The root of the tail has been chosen to be around 3 meters and the 0.77 times the total hull length has been chosen as this value is within the limits for the competitors also [21].

The taper ratio of the tail profile is calculated by:

$$\Lambda_{tail} = C_{tip\_tail} / C_{root\_tail} \quad (4.7)$$

That is;

Λ_{tail} = 2356 mm / 3000 mm = 0.79

To calculate the aspect ratio of the vertical tail profile, one vertical tail plus the two 45 degree anhedral tails' vertical projection should be added together:

$S = 2 * (5.5\ m^2 * \sin \pi/4) + 5.5\ m^2 = 13.28\ m^2$ of vertical tail area (4.8)

$AR = b^2 / S$ (4.9)

That is;

$AR = 2^2 / 13.28 = 0.3$

This would correspond to an Aspect Ratio of 0.3 and a taper ratio of 0.79 in total.

The same tails are going to be used for both the vertical and the inverted-Y tails to simplify the assembly condition. As it has been mentioned before, if the tails would be manufactured from composites, having identical tails is a big advantage for manufacturing easiness also. A demonstration of the 3D model of the airship with tails can be seen at Figure 4.2 below.

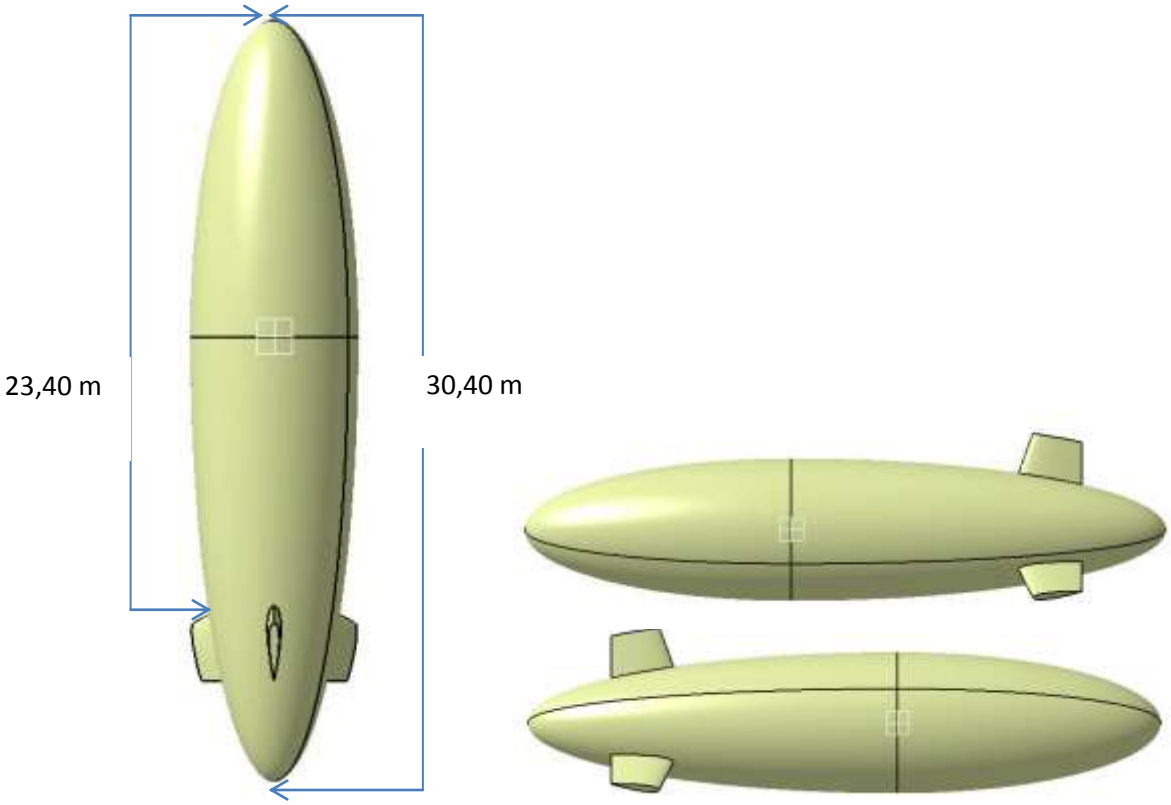

Figure 4.2 Top, Right and Left Views of the Airship Hull + Tail Configuration

4.2. Drag Calculations

As symmetrical airfoils have been used, and as the airship hull is a completely symmetric body also, no pitching moment or aerodynamic lift is being produced while at zero incidence angle.

$$L = C_L * S * q_\infty \quad (4.10)$$

$$\text{As } C_L \approx 0 \quad (4.11)$$

$$L \equiv 0 \quad (4.12)$$

The meshing properties and the models used in CFD calculations for this section are listed below in Table 4.3.

Table 4.3 Mesh Properties and the Models Used

Propulsion System Specifications	
Count of Elements	4 million
Minimum Orthogonal Quality	0.14
Minimum element size	1 mm
Assembly Meshing	Tetrahedrons
Triangle Surface Mesher	Advancing Front
Viscous Model	SST k-omega
Boundary Conditions	Velocity Inlet – Pressure Outlet

As the CFD analysis from now on has been made with the full model of the airship (assembled with tails and gondola), the assembly meshing has been used in order to improve the quality of the mesh. An advancing front triangle surface mesher has been used also. The SST k-omega model has been used as it has been used and found to be the best viscous model for the aircrafts like airships and aerostats [30]. SST k-omega solver is a good solver for aero-dynamic flows.

For the rest of the CFD analysis also the same viscous model with the same boundary conditions will be used. Special care has been shown in order to be sure that the minimum orthogonal quality is at least above 0.1 and the y+ values to stay between 30 & 300 [30].

The CFD calculations have been made accordingly for the peak operating conditions (25 m/s). And the C_D value for zero incidence angles for both the airship body, tail configuration and the gondola for the direct head winds is found to be equal to:

$S_{p\_airship\_0°} = 40\ m^2$

$C_{D\_airship\_\alpha=0°} = 0.063$

$$D_{airship\_\alpha=0°} = (½) * \rho_\infty * V_\infty^2 * S_{p\_airship} * C_{D\_airship\_\alpha=0°} \quad (4.13)$$

That is;

$D_{airship\_\alpha=0°} = (1/2) * (1.225\ kg/m^3) * (25\ m/s)^2 * (40\ m^2) * 0.063 = 965\ N$

The Table 4.4 taken from the Fluent calculations can also be seen below. As it can be seen from this figure, the viscous forces are not negligible. The small difference of the total drag forces between the calculations and the Fluent result is due to the 4th decimal of drag coefficient.

Table 4.4 Drag Force Estimation from CFD Results for 0° Incidence Angle

Forces – Direction Vector (1 0 0)						
	Forces (n)			Coefficients		
	Pressure	Pressure	Total	Pressure	Viscous	Total
Zone airship	598.316	368.501	966.818	0.045	0.018	0.063
Net	598.316	368.501	966.818	0.045	0.018	0.063

The airship needs to withstand the side-wind force also for peak operating conditions (25m/s). The Drag calculations for the 90° side-wind is found to be:

$S_{p\_airship\_90°} = 170\ m^2$

$C_{D\_airship\_\alpha=90°} = 0.681$

$$D_{airship\_\alpha=90°} = (½) * \rho_\infty * V_\infty^2 * S_{p\_airship} * C_{D\_airship\_\alpha=90°} \quad (4.14)$$

That is;

$D_{airship\_\alpha=90°} = (1/2) * (1.225\ kg/m^3) * (25\ m/s)^2 * (170\ m^2) * 0.681 = 44317N$

Table 4.5 Drag Force Estimation from CFD Results for 90° Incidence Angle

Forces – Direction Vector (0 1 0)						
	Forces (n)			Coefficients		
	Pressure	Viscous	Total	Pressure	Viscous	Total
Zone airship	44077.563	217.337	44294.9	0.677	0.003	0.681
Net	44077.563	217.337	44294.9	0.677	0.003	0.681

When Table 4.5 is analyzed, it can be seen that there is a huge difference for the same operating conditions between 90° and 0° wind incidence angle. When the 90° side wind clashes directly to the airship the force that would be created is nearly 45 times higher than the direct wind. It is a dramatic example to show the importance of the airship while it has to localize itself directly heading to the headwinds always.

As airships suffer from bad maneuverability, in order to eliminate this negative aspect an all-moving tail configuration is going to be used. In this configuration, the root portion of the tail would be non-moving, the rest of the tail would be all-moving tail which will be rotating just behind the m.a.c of the tail profile.

$b_{non\_moving} = 0.2\ m$

$b_{moving\_sec} = 1.8\ m$

$X_{hing\_point\_moving} = 0.3 * c_{root\_moving\_sec} = 24.3\ m$ from the nose-tip (4.15)

The demonstration of the arrangement with 15° of tail incidence angle can be seen in Figure 4.3 below:

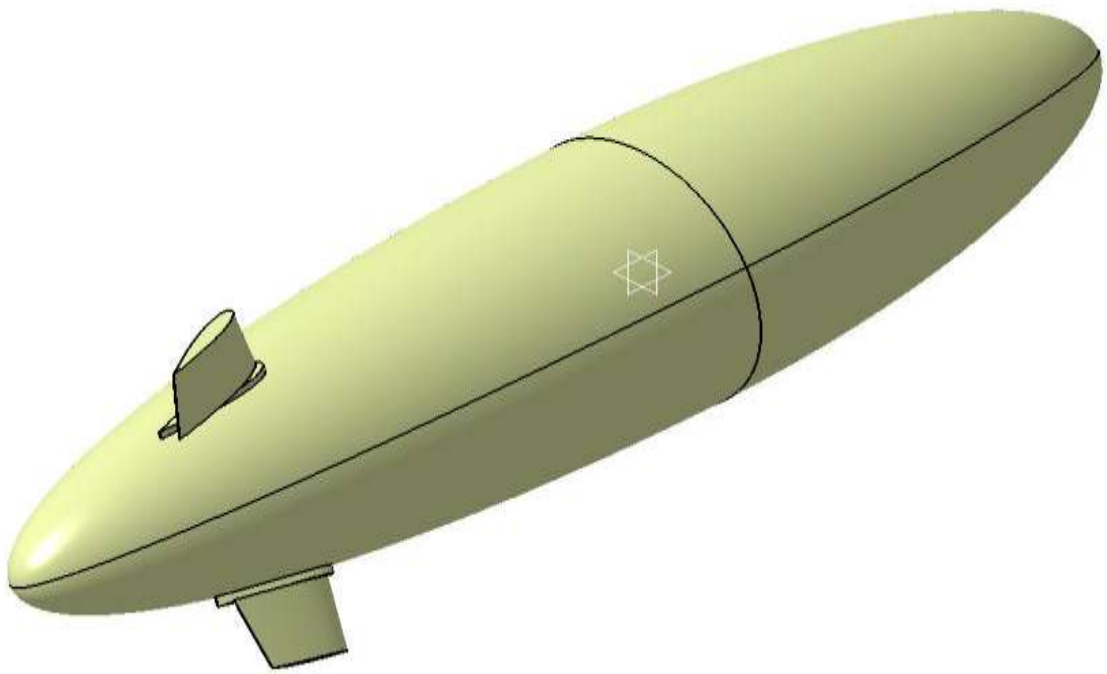

Figure 4.3 Representation of the Airship with All Moving Tail Configuration (with 15° Tail Incidence Angle)

The drag calculations for such a configuration have been made below:

$S_{p\_airship\_15°} = 40.5m^2$

$C_{D\_airship\_\alpha=15°} = 0.0978$

$$D_{airship\_\alpha=15°} = (½) * \rho_{\infty} * V_{\infty}^{2} * S_{p\_airship\_15°} * C_{D\_airship\_\alpha=15°} \quad (4.16)$$

That is;

$D_{airship\_\alpha=15°} = (1/2) * (1.225\ kg/m^3) * (25\ m/s)^2 * (40.5\ m^2) * 0.0978 = 1516\ N$

Moreover, the results of CFD calculation can be seen below in Table 4.6:

Table 4.6 Drag Calculations for 15° Tail Incidence Angle

Forces – Direction Vector (1 0 0)						
	Forces (n)			Coefficients		
	Pressure	Viscous	Total	Pressure	Viscous	Total
Zone airship-shadow	1066.218	431.799	1498.017	0.070	0.028	0.098
Net	1066.218	431.799	1498.017	0.070	0.028	0.098

According to Table 4.6, it can be seen that for the airship to have the ability to maneuver at 15° tail incidence angle, at least 1500 N of thrust is needed for peak operating conditions.

4.3. Center of Buoyancy (CB) and Center of Gravity (CG) Calculations

The Center of Buoyancy of the system is found to be at 14.55 meters from the nose tip, just ahead the middle of the hull. CG location will be adjusted to be at the same location with the CB to ensure stability of the system. The tail and the hull positions and magnitude have already been set. To keep the CB and the CG locations on top of each other, we will adjust the location of the gondola. All the components' effect on CG has been calculated as it is mentioned in 4.17 and 4.18.

$$m_{tail} * (x_{CB} - x_{CG\_tail}) + m_{nose\_sys} * (x_{CB} - x_{CG\_nose\_sys}) + m_{hull} * (x_{CB} - x_{CG\_hull}) + m_{gondola} * (x_{CB} - x_{CG\_gondola}) = 0 \quad (4.17)$$

$$x_{CG\_gondola} = \{[m_{tail} * (x_{CB} - x_{CG\_tail}) + m_{nose\_sys} * (x_{CB} - x_{CG\_nose\_sys}) + m_{hull} * (x_{CB} - x_{CG\_hull})] / m_{gondola}\} + x_{CB} \quad (4.18)$$

The effect of Helium mass, ballonets and the air weight inside the ballonets have not been added into this calculation as their CG has already been on top of the CB location meaning that they won't have any effect on CG location. According to equations 4.17 and 4.18, the resulting location for gondola CG is found to be:

$x_{CG\_gondola} = \{[40.12 * (14.55 - 25.00) + 30.00 * (14.55 - 3.55) + 87.38 * (14.55 - 14.76)] / 165.5\} + 14.55 = 13.59$ meters from the nose-tip

The resulting 3D model with the gondola added according to the information above, is represented below in Figure 4.4. The same model will be used in the CFD calculations in order to check whether the resulting body will satisfy the requirements or not.

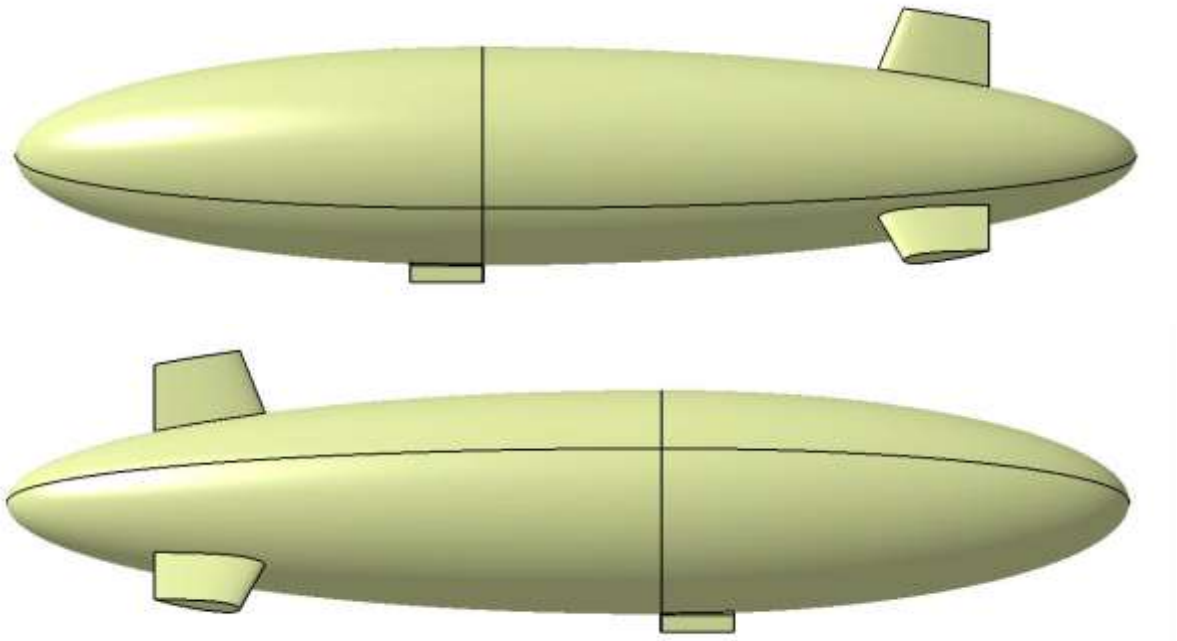

Figure 4.4 3D Representation of the Model for CFD Calculations

4.4. Yaw Moment Calculations

There are 2 main directional stability moments which are taken into consideration for flying vehicles: the rolling moment and the yaw moment. The rolling moment is not an important aspect that needs to be calculated for an airship but the yaw moment is very important to ensure directional stability for aerostatic maneuvering.

As the tail profile is a symmetrical airfoil, during 0° incidence flight, the tails won't be producing any pitch, yaw or roll coefficients. Ignoring the prop-wash and the side-wash effect, the yaw moment on the airship is found by the related equation below:

$$N = N_{wing} + N_{fuselage} + F_{tail} (X_{a.c.\_tail} - X_{c.g.}) \quad (4.19)$$

When $N_{wing} = 0$ and $N_{fuselage} = 0$, then the equation becomes:

$$N = F_{tail} (X_{a.c.\_tail} - X_{c.g.}) \quad (4.20)$$

For 15° tail incidence angle, F_{tail} is found from the Fluent results which can be seen below in Table 4.7 below:

Table 4.7 F_{tail} Fluent Results for 15° of Tail Incident Angle

Moments – Moments Center (-0.96 0 0) Moment Axis (0 1 0)			
	Moments (n-m)		
	Pressure	Viscous	Total
Zone airship	-205.218	-16.398	-221.616
Net	-205.218	-16.398	-221.616

Since, $N = F_{tail} (X_{a.c._tail} - X_{c.g.})$; N becomes:

N = 221 * (24.3 m - 13.59 m) = -2366.9 N*m

The resulting yaw moment for 15° incident angle gathered from Fluent can be seen in Table 8.

Table 4.8 Resulting Yaw Moment Due to CFD Results for 15° of Tail Incident Angle

Moments – Moments Center (-0.96 0 0) Moment Axis (1 1 0)			
	Moments (n-m)		
	Pressure	Viscous	Total
Zone airship	-2360.063	-3.956	-2364.019
Net	-2360.063	-3.956	-2364.019

The resulting yaw moment for 10° incident angle gathered from Fluent can be seen in Table 9.

Table 4.9 Resulting Yaw Moment Due to CFD Results for 10° of Tail Incident Angle

Moments – Moments Center (-0.96 0 0) Moment Axis (1 1 0)			
	Moments (n-m)		
	Pressure	Viscous	Total
Zone airship	-1489.839	-19.378	-1509.217
Net	-1489.839	-19.378	-1509.217

The resulting yaw moment for 5° incident angle gathered from Fluent can be seen in Table 4.10.

Table 4.10 Resulting Yaw Moment Due to CFD Results for 5° of Tail Incident Angle

Moments – Moments Center (-0.96 0 0) Moment Axis (1 1 0)			
	Moments (n-m)		
	Pressure	Viscous	Total
Zone airship	-1476.194	-12.864	-1489.057
Net	-1476.194	-12.864	-1489.057

The reason why an all-moving tail is being used underlies behind those Figure 4.9. If a classical type of tail configuration has been used, the moment that would be created would be much less for the same angle of incidence.

Assume that a conventional type of tail configuration would be used and assume that:

$X_{rudder} / X_{chord} = 25\ \%$

For rudder deflection of 15° for a conventional type tail the yawing moment would be:

$C_n = -0.156$

$N = q_\infty * S * b * C_n$

$0.5 * (1.225\ kg/m^3) * (25\ m/s)^2 * 5.5\ m^2 * 2m * (-0.161) = -678\ N$

As it can be seen easily from the calculations made for the conventional type of rudder, there is a dramatic increase (3.5 times) on directional stability, when an all-moving tail is to be used.

4.5. Propulsion and Thrusted Vectoring Configuration

The propulsion unit needs to keep the airship stable at 25 m/s head-wind conditions due to design parameters. According to the CFD calculations made and shown at Table 12, the airship produces 967N drag for the maximum operating velocity at head-wind position. Adding 20% of safety factor for the interference drag with the components that could not be counted inside the CFD, such as the ropes hanging around the airship, the engines and the solar panels, drag would be a better estimation for the required thrust determination.

$$D_{actual} = D_{CFD} + 20\% \text{ Safety Factor} \quad (4.21)$$

Thus D_{actual} becomes:

$$D_{actual} = 967 \text{ N} + (20\%) * 967\text{N} = 1160 \text{ N}$$

This will be taken as reference:

$$T_R = W / (L/D_{actual}) \quad (4.22)$$

As L = W for floating objects,

$$T_R = D_{actual} \quad (4.23)$$

According to the previous calculations, two Turnigy Roto-Max 80 cc Brushless DC Electrical motors with a 22 x 12 inches propeller [28] configuration would be used. The calculations have shown that this kind of configuration is capable of producing 65 kg of thrust at peak conditions. But according to the latest CFD results the need has been increased to:

$$1160 \text{ N} / 9.81 \text{ (kg/m}^2\text{s}^2\text{)} = 118 \text{ kg} = T_R$$

According to the latest data, a new engine (Hacker A200-8) with a similar weight and operating conditions (14S LiPo configuration and 180A of current) would be used. This new type of engine weighs around 2.5 kg each and produces 9090 W of power at 4600 RPM [30]. This engine is again a very low Kv (110 Kv) engine.

$$Kv = RPM / Volt \quad (4.24)$$

$$RPM = Kv * Volt \quad (4.25)$$

That is;

$$RPM = 110 * 50.5 = 5555$$

With the battery configuration we can provide up to 5555 RPM in times of need, but generally it would be turning in much lower rates. A much bigger custom-made propeller would be used to provide the necessary thrust which would be 34" x 8.5"= It would be providing 60.3 kg of thrust in 4600 RPM and would be needing 9 kW of power.

Table 4.11 Propulsion System General Specifications

Propulsion System Specifications		
Engine	9.1 kW	@ 4600 RPM
Propeller	Static pitch carbon fiber	34" x 8.5"
Generated Max. Thrust	60.3 kg * 2 = 120.6 kg	
Required Max. Thrust	118 kg	

With this kind of configuration, the system will be able to withstand 90 km/h winds at least for 1 hour even at night conditions (no solar radiation to charge the batteries). This would allow the airship to maneuver in order to get away or land if the bad weather

conditions would continue. This means that in normal conditions, the system will get through the night easily.

According to the recent information, the airship has satisfied the requirement which is important for stability analysis:

$T_{generated} \geq D_{actual}$

CHAPTER 5

CONCLUSION

In the thesis, the design of an unmanned, completely solar powered airship which has the ability to lift 70 kg of payload up to 1000 meters altitude has been carried out. The airship has a maximum endurance of 2 weeks time and uses Helium as the lifting gas. Two electrical engines (each of which has the ability to generate 9.1 kW of power) are to be used to generate the thrust required to achieve the design requirements.

The required thrust has been calculated by setting the generated drag by the airship for the headwind case for maximum operating conditions which is 25 m/s air velocity. The drag calculations have been made via a CFD analysis. Firstly, a CFD analysis just for the airship hull has been performed and the rule of thumbs have been used to make an assumption for the rest of the system. But then, a complete CFD analysis for the whole system have been performed and it has been seen that there has been a huge difference with the rule of thumbs, so the engines to be used had to be changed to achieve the design requirement.

The airship also has the ability to take-off and land vertically which ensures the airship to operate easily (like a helicopter) for any geographic region. As all the airship's soft spot is its low maneuverability compared with the aerodynamic counterparts, to overcome this issue at least to some extent, the airship designed here can also use thrusted vectoring for increased maneuverability.

To ensure the 2 weeks of endurance, the fabric of the hull was not the only limiter. It has two electrical engines, an avionic system and the payload, all of which needs electrical energy to operate. In conventional systems, this kind of energy need is compensated directly from the battery and indirectly from the internal combustion engines. But as this

airship is completely solar powered, huge batteries and huge solar panel configurations have been used in order to answer this kind of system's energy needs.

To improve the stability of the system, inverted-Y tail configuration with 45 degrees anhedral has been used. And also instead of using a conventional type of tail with rudders and elevators, an all moving tail configuration has been used to compensate the low maneuverability of the system.

All the weight of the sub-components and the volume need of the system have been calculated with an empirical approach. This kind of an approach is quite hard at the first phases of the calculations as not enough inputs were available to use. At the preliminary design and at some parts of the conceptual design some rule of thumbs of the conventional designs have been used for a bulletproof system. Then all the items have been calculated individually in the detailed design process. Although, this kind of an approach needs too much research to be conducted at the beginning of the preliminary and conceptual design, and too much resources to prepare the necessary model (in Excel in our case); it is the safest way for the continuity of the process. As design is a never-ending path, even at the latest stages of design some modifications might be needed. Empirical approach allowed maneuverability for the design process itself.

Even though there are various innovative approaches within the thesis, the hull design has been performed according to conventional approaches. Even though other approaches might prove to be much less drag producing options, this kind of path has been followed to ensure the safety of the system. As the other approaches left so less volume at the aft locations, this might have created a risk when the tail configuration is attached to that location. The other reason for choosing the conventional type was to ensure the airworthiness of the system. The aim in this approach was to ensure the safety of the hull no matter the cost is. Because, even if all the other components of the airship is necessary and useful, the most important and vital component of the airship is its lift generating body. Because of that reason, only for the hull design and its sub-

components, we always preferred to stay on the safe side and used the conventional approach.

The listed items below can be considered as a future work:

- Structural analysis of the suspension lines, tail configuration and the airship hull may be performed.
- A 1:3 scaled prototype production by installing the autopilot, avionics and weather radar station inside the gondola can be carried out.
- Thrust vectoring ability can be increased to lateral and longitudinal directions also in order to improve maneuverability.
- Using hydrogen as the lifting gas instead of Helium can be implemented as Hydrogen is a much cheaper option.
- Electronic System Integration can be made and improved.
- The Solar Cell Arrangement and battery management can be improved to increase efficiency and endurance even more.
- Aerodynamic improvement study can be performed.

REFERENCES

[1] Daily News (2013). *Hindenburg mystery solved 76 years after historic catastrophe: static electricity caused the airship to explode*. Retrieved from http://www.dailymail.co.uk/news/article-2287608/Hindenburg-mystery-solved-76-years-historic-catastrophe-static-electricity-caused-airship-explode.html on June 2013.

[2] Butler, A., DiMascio, J. (2012). *Looking East.* Aviation Week & Space Technology, Vol. 174, Issue 2.

[3] Homeland Security (2012). *Written testimony of U.S. Customs and Border Protection for a House Homeland Security Subcommittee on Border and Maritime Security hearing titled "Measuring Border Security: U.S. Border Patrol's New Strategic Plan and the Path Forward"*. Retrieved from http://www.dhs.gov/news/2012/05/08/written-testimony-us-customs-and-border-protection-house-homeland-security on July 2013.

[4] Caldwell, A.A. (2014). *DHS has lent border drones hundreds of times*. Washington Times. Retrieved from http://www.washingtontimes.com/news/2014/jan/15/dhs-has-lent-border-drones-hundreds-of-times on May 2014.

[5] Phang, N., S. (2006). *Tethered Operation Of Autonomous Aerial Vehicles To Provide Extended Field Of View For Autonomous Ground Vehicles*. Masters Thesis. Naval Postgraduate School, Monterey, California.

[6] Elfes, A., Bueno,S.S, Bergerman, M. and Ramos, J.J.G.(1998). A Semi Autonomous Robotic Airship For Environmental Monitoring Missions. In *Proceedings of the IEEE International Conference on Robotics and Automation*, Volume 4, pp. 3449-3455, Leuven, Belgium. IEEE Press.

[7] Miller, J.I. (2005). *The Design of Robust Helium Aerostats*. Masters Thesis. McGill University, Montreal.

[8] Khoury, G.A. (2012). *Airship Technology*. Cambridge Aerospace Series: 10, Cambridge University Press, Cambridge.

[9] Kale, S.M., Joshi, P. and Pant, R.S. (2005). A generic methodology for determination of drag coefficient of an aerostat envelope using CFD. In *Proceedings of 5thAIAA\ATIOand 16th Lighter-Than-Air Systems Technology Conference and Balloon System Conference*, Crystal City, Arlington,USA.

[10] Lutz, T. and Wagnery, S. (1998). Drag Reduction and Shape Optimization of Airship Bodies. *Journal of Aircraft,* Vol 35, No. 3, pp 345-351.

[11] De Young, A. (1939). The Calculation of the Total and Skin Friction Drags of Bodies of Revolution at Zero Incidence. *Air Ministry Reports and Memoranda No.* 1874. Aeronautical Research Council, London, England.

[12] Dosselaer, I.V. (2014). *Buoyant Aerobot Design and Simulation Study*. Masters Thesis. Delft University, Holland.

[13] Peddiraju, P. (2010). Development and validation of a dynamics model for an unmanned finless airship. Masters Thesis. McGill University, Montreal,Quebec.

[14] Liu, J., Lu, C. And Xue, L. (2010) Numerical Investigation On The Aeroelastic Behavior Of An Airship With Hull-Fin Configuration. *Journal of Hydrodynamics*, Issue 2 , pp. 207-213.

[15] Funk, P. Lutz, T. And Wagner, S. (2003). Experimental investigations on hull-fin interferences of the LOTTE airship. Aerospace Science and Technology, Volume 7, Issue 8, pp. 603–610.

[16] Jacobs, E.N. and Albert, S. (1937). *Airfoil Section Characteristics As Affected By variations of The Reynolds Number*. National Advisory Committee for Aeronautics Report, vol. 586., USA.

[17] Raymer, D.P. (2013). *Aircraft Design: A Conceptual Approach (5th Edn.)*. American Institute of Aeronautics and Astronautics.

[18] U. S. Department Of Transportation, Federal Aviation Administration (2007). *Airship Design Criteria*. CreateSpace Independent Publishing Platform.

[19] Burgess, C. P. (2004). *Airship Design*. University Press of the Pacific, Honolulu, Hawaii, 2004.

[20] Blakemore, T. L., and Pagon, W. W. (2003). *Pressure Airships*. University Press of the Pacific.

[21] Mei, Q. (2011). A solar power system for high altitude airships. Doctoral Thesis, The University of Toledo, USA.

[22] Özyetiş, E. (2013). Design and Manufacturing of A High Speed Jet Powered Target Drone. Masters Thesis. Middle East Technical University, Ankara, Turkey.

[23] High Output SP Panels. Retrieved from http://www.bruceschwab.com/uploads/2014-solbian-handout-wsxp.pdf on September 2014.

[24] SP Panel. Retrieved from http://www.shop.ilportaledelsole.com/WebRoot/ce_it/Shops/990116484/5130/D35E/EF19/B968/18E6/C0A8/8008/AD90/6-317-800-600-80.jpg on December 2014.

[25] Jiang, J., Huang, T., Hsiao, Y. and Chen, C. (2005). Maximum Power Tracking for Photovoltaic Power Systems. Tamkang Journal of Science and Engineering, vol. 8, no. 2, pp. 147–153.

[26] Chen, W. J., Zhang, D. X., Duan, D. P. and Fu, G. Y. (2011). *Equilibrium Configuration Analysis of Non-rigid airship subjected to weight and bupoyancy*. In Proceedings of 11th AIAA Aviation Technology, Integration, and Operations Conference. *Virginia Beach*, pp. 1–12.

[27] Hankinson, J., Bewley, J., Hankinson, R. and Spyrou, G. (2001). *Airship Gondola Suspension System and Method of Making Same*. US Patent 6,290,176.

[28] Mejzlik Modelbau Catalog, *Propeller 22"x12"–3B* Retrieved from http://www.mejzlik.eu/electro-3-bladed/propeller-20-x-13-e-l-3b on February 2015.

[29] Kleiner, H., J. (1974). *Aspects Of Airship Design*. Masters Thesis. McMaster University, Canada.

[30] Shields, K. (2010*). CFD Applications in Airship Design.* Masters Thesis. West Virginia University, USA.

APPENDIX A

ITERATION RESULTS

Table A.1 Iteration Results for 0 Meters Altitude and 40°C

W_{solar_sys}	$W_{propulsion\_system}$	$W_{ballonet\_system}$	$A_{ControlSurfaces}$	$W_{access\&maintenance}$	$A_{balloon}$	$W_{balloon}$	W_{nose_group}
53.000	10.500	108.269	8.189	0.730	513.872	72.970	30.300
53.000	10.500	107.145	8.179	0.729	513.186	72.872	30.300
53.000	10.500	106.021	8.168	0.728	512.500	72.775	30.300
53.000	10.500	104.897	8.157	0.727	511.814	72.678	30.300
53.000	10.500	103.773	8.146	0.726	511.127	72.580	30.300
53.000	10.500	102.649	8.135	0.725	510.440	72.482	30.300
53.000	10.500	101.525	8.124	0.724	509.752	72.385	30.300
53.000	10.500	100.401	8.113	0.723	509.064	72.287	30.300
53.000	10.500	99.277	8.102	0.722	508.376	72.189	30.300
53.000	10.500	98.153	8.091	0.721	507.687	72.091	30.300
53.000	10.500	97.029	8.080	0.720	506.997	71.994	30.300
53.000	10.500	95.905	8.069	0.719	506.307	71.896	30.300
53.000	10.500	94.781	8.058	0.718	505.616	71.798	30.300
53.000	10.500	93.657	8.047	0.717	504.925	71.699	30.300
53.000	10.500	92.533	8.036	0.716	504.234	71.601	30.300
53.000	10.500	91.409	8.025	0.715	503.542	71.503	30.300
53.000	10.500	90.285	8.012	0.714	502.850	71.405	30.300
53.000	10.500	89.161	8.003	0.713	502.157	71.306	30.300
53.000	10.500	88.0373	7.992	0.712	501.463	71.208	30.300
53.000	10.500	86.913	7.981	0.711	500.770	71.109	30.300
53.000	10.500	85.789	7.970	0.710	500.0753	71.011	30.300
53.000	10.500	84.665	7.959	0.709	499.381	70.912	30.300
53.000	10.500	83.541	7.947	0.708	498.685	70.813	30.300
53.000	10.500	82.417	7.936	0.707	497.990	70.715	30.300

,

Table A.2 Iteration Results for 0 Meters Altitude and 40°C (cont'd)

V_{hull}	W_{total}	$L_{airship}$	R_{major}	r_{major}	W_{Helium}	$W_{suspension\_system}$	$D_{airship}$
500.000	562.597	30.364	17.733	12.631	82.000	6.100	6.745
499.000	561.158	30.344	17.722	12.622	81.836	6.100	6.740
498.000	559.718	30.323	17.710	12.614	81.672	6.100	6.736
497.000	558.278	30.303	17.698	12.605	81.508	6.100	6.731
496.000	556.837	30.283	17.686	12.597	81.344	6.100	6.727
495.000	555.397	30.262	17.674	12.588	81.180	6.100	6.722
494.000	553.957	30.242	17.662	12.580	81.016	6.100	6.718
493.000	552.516	30.222	17.650	12.571	80.852	6.100	6.7137
492.000	551.076	30.201	17.638	12.563	80.688	6.100	6.709
491.000	549.635	30.181	17.626	12.554	80.524	6.100	6.704
490.000	548.195	30.160	17.614	12.546	80.360	6.100	6.699
489.000	546.754	30.140	17.602	12.537	80.196	6.100	6.695
488.000	545.313	30.119	17.590	12.529	80.032	6.100	6.690
487.000	543.872	30.098	17.578	12.520	79.868	6.100	6.686
486.000	542.430	30.078	17.566	12.512	79.704	6.100	6.681
485.000	540.989	30.057	17.554	12.503	79.540	6.100	6.677
484.000	539.548	30.037	17.542	12.494	79.376	6.100	6.672
483.000	538.106	30.016	17.530	12.486	79.212	6.100	6.667
482.000	536.665	29.995	17.518	12.477	79.048	6.100	6.663
481.000	535.223	29.974	17.506	12.469	78.884	6.100	6.658
480.000	533.781	29.954	17.494	12.460	78.720	6.100	6.654
479.000	532.339	29.933	17.482	12.451	78.556	6.100	6.649
478.000	530.897	29.912	17.469	12.443	78.392	6.100	6.644
477.000	529.455	29.891	17.457	12.434	78.228	6.100	6.640

Table A.3 Iteration Results for 0 Meters Altitude and 40°C (cont'd)

R_r	$F_{buoyancy}$ (N)	$F_{buoyancy}$ (kg)	$W_{GONDOLA}$	$W_{balloonet}$	W_{tail_system}	$V_{ballonet\_filled}$	W_{tail_cone}
3.372	5513.220	562.000	165.500	29.589	40.128	70.000	3.600
3.370	5502.194	560.876	165.500	29.589	40.075	69.000	3.600
3.368	5491.167	559.752	165.500	29.589	40.021	68.000	3.600
3.366	5480.141	558.628	165.500	29.589	39.968	67.000	3.600
3.363	5469.114	557.504	165.500	29.589	39.914	66.000	3.600
3.361	5458.088	556.380	165.500	29.589	39.861	65.000	3.600
3.359	5447.061	555.256	165.500	29.589	39.807	64.000	3.600
3.357	5436.035	554.132	165.500	29.589	39.753	63.000	3.600
3.354	5425.008	553.008	165.500	29.589	39.699	62.000	3.600
3.352	5413.982	551.884	165.500	29.589	39.645	61.000	3.600
3.350	5402.956	550.760	165.500	29.589	39.592	60.000	3.600
3.347	5391.929	549.636	165.500	29.589	39.538	59.000	3.600
3.345	5380.903	548.512	165.500	29.589	39.484	58.000	3.600
3.343	5369.876	547.388	165.500	29.589	39.430	57.000	3.600
3.341	5358.850	546.264	165.500	29.589	39.376	56.000	3.600
3.338	5347.823	545.140	165.500	29.589	39.322	55.000	3.600
3.336	5336.797	544.016	165.500	29.589	39.268	54.000	3.600
3.334	5325.771	542.892	165.500	29.589	39.214	53.000	3.600
3.331	5314.744	541.768	165.500	29.589	39.160	52.000	3.600
3.329	5303.718	540.644	165.500	29.589	39.105	51.000	3.600
3.327	5292.691	539.520	165.500	29.589	39.051	50.000	3.600
3.324	5281.665	538.396	165.500	29.589	38.997	49.000	3.600
3.322	5270.638	537.272	165.500	29.589	38.943	48.000	3.600
3.320	5259.612	536.148	165.500	29.589	38.888	47.000	3.600

Table A.4 Iteration Results for 1000 Meters Altitude and 34°C

W_{solar_sys}	$W_{propulsion\_system}$	$W_{ballonet\_system}$	$A_{ControlSurfaces}$	$W_{access\&maintenance}$	$A_{balloon}$	$W_{balloon}$	W_{nose_group}
53.000	10.500	41.517	8.189	0.730	513.872	72.970	30.300
53.000	10.500	41.517	8.179	0.729	513.186	72.872	30.300
53.000	10.500	41.517	8.168	0.728	512.500	72.775	30.300
53.000	10.500	41.517	8.157	0.727	511.814	72.678	30.300
53.000	10.500	41.517	8.146	0.726	511.127	72.580	30.300
53.000	10.500	41.517	8.135	0.725	510.440	72.482	30.300
53.000	10.500	41.517	8.124	0.724	509.752	72.385	30.300
53.000	10.500	41.517	8.113	0.723	509.064	72.287	30.300
53.000	10.500	41.517	8.102	0.722	508.376	72.189	30.300
53.000	10.500	41.517	8.091	0.721	507.687	72.091	30.300
53.000	10.500	41.517	8.080	0.720	506.997	71.994	30.300
53.000	10.500	41.517	8.069	0.719	506.307	71.896	30.300
53.000	10.500	41.517	8.058	0.718	505.616	71.798	30.300
53.000	10.500	41.517	8.047	0.717	504.925	71.699	30.300
53.000	10.500	41.517	8.036	0.716	504.234	71.601	30.300
53.000	10.500	41.517	8.025	0.715	503.542	71.503	30.300
53.000	10.500	41.517	8.014	0.714	502.850	71.405	30.300
53.000	10.500	41.517	8.003	0.713	502.157	71.306	30.300
53.000	10.500	41.517	7.992	0.712	501.463	71.208	30.300
53.000	10.500	41.517	7.981	0.711	500.770	71.109	30.300
53.000	10.500	41.517	7.970	0.710	500.075	71.011	30.300
53.000	10.500	41.517	7.959	0.709	499.381	70.912	30.300
53.000	10.500	41.517	7.947	0.708	498.685	70.813	30.300
53.000	10.500	41.517	7.936	0.707	497.990	70.715	30.300

Table A.5 Iteration Results for 1000 Meters Altitude and 34°C (cont'd)

V_{hull}	W_{total}	$L_{airship}$	R_{major}	r_{major}	W_{Helium}	$W_{suspension\_system}$	$D_{airship}$
500.000	495.845	30.364	17.7335	12.631	82.000	6.100	6.745
499.000	495.530	30.345	17.722	12.622	81.836	6.100	6.740
498.000	495.214	30.323	17.710	12.614	81.672	6.100	6.736
497.000	494.898	30.303	17.698	12.605	81.508	6.100	6.731
496.000	494.581	30.283	17.686	12.597	81.344	6.100	6.727
495.000	494.265	30.262	17.674	12.588	81.180	6.100	6.722
494.000	493.949	30.242	17.662	12.580	81.016	6.100	6.718
493.000	493.632	30.222	17.650	12.571	80.852	6.100	6.713
492.000	493.316	30.201	17.638	12.563	80.688	6.100	6.709
491.000	492.999	30.181	17.626	12.554	80.524	6.100	6.704
490.000	492.683	30.160	17.614	12.546	80.360	6.100	6.699
489.000	492.366	30.140	17.602	12.537	80.196	6.100	6.695
488.000	492.049	30.119	17.590	12.529	80.032	6.100	6.690
487.000	491.732	30.098	17.578	12.520	79.868	6.100	6.686
486.000	491.414	30.078	17.566	12.512	79.704	6.100	6.681
485.000	491.097	30.057	17.554	12.503	79.540	6.100	6.677
484.000	490.780	30.037	17.542	12.494	79.376	6.100	6.672
483.000	490.462	30.016	17.530	12.486	79.212	6.100	6.667
482.000	490.145	29.995	17.518	12.478	79.048	6.100	6.663
481.000	489.827	29.974	17.506	12.469	78.884	6.100	6.658
480.000	489.509	29.954	17.494	12.460	78.720	6.100	6.654
479.000	489.191	29.933	17.482	12.451	78.556	6.100	6.649
478.000	488.873	29.912	17.469	12.443	78.392	6.100	6.644
477.000	488.555	29.891	17.457	12.434	78.228	6.100	6.640

Table A.6 Iteration Results for 1000 Meters Altitude and 34°C (cont'd)

R_r	$F_{buoyancy}$ (N)	$F_{buoyancy}$ (kg)	$W_{GONDOLA}$	$W_{balloonet}$	W_{tail_system}	$V_{ballonet\_filled}$	W_{tail_cone}
3.372	4875.570	497.000	165.500	29.589	40.128	12.000	3.600
3.370	4865.819	496.006	165.500	29.589	40.075	12.000	3.600
3.368	4856.068	495.012	165.500	29.589	40.021	12.000	3.600
3.366	4846.317	494.018	165.500	29.589	39.968	12.000	3.600
3.363	4836.565	493.024	165.500	29.589	39.914	12.000	3.600
3.361	4826.814	492.030	165.500	29.589	39.861	12.000	3.600
3.359	4817.063	491.036	165.500	29.589	39.807	12.000	3.600
3.357	4807.312	490.042	165.500	29.589	39.753	12.000	3.600
3.354	4797.561	489.048	165.500	29.589	39.699	12.000	3.600
3.352	4787.810	488.054	165.500	29.589	39.645	12.000	3.600
3.350	4778.059	487.060	165.500	29.589	39.592	12.000	3.600
3.347	4768.307	486.066	165.500	29.589	39.538	12.000	3.600
3.345	4758.556	485.072	165.500	29.589	39.484	12.000	3.600
3.343	4748.805	484.078	165.500	29.589	39.430	12.000	3.600
3.341	4739.054	483.084	165.500	29.589	39.376	12.000	3.600
3.338	4729.303	482.090	165.500	29.589	39.322	12.000	3.600
3.336	4719.552	481.096	165.500	29.589	39.268	12.000	3.600
3.334	4709.801	480.102	165.500	29.589	39.214	12.000	3.600
3.331	4700.049	479.108	165.500	29.589	39.160	12.000	3.600
3.329	4690.298	478.114	165.500	29.589	39.105	12.000	3.600
3.327	4680.547	477.120	165.500	29.589	39.051	12.000	3.600
3.324	4670.796	476.126	165.500	29.589	38.997	12.000	3.600
3.322	4661.045	475.132	165.500	29.589	38.943	12.000	3.600
3.320	4651.294	474.138	165.500	29.589	38.888	12.000	3.600

Table A.7 Iteration Results for 0 Meters Altitude and -20°C

W_{solar_sys}	$W_{propulsion\_system}$	$W_{ballonet\_system}$	$A_{ControlSurfaces}$	$W_{access\&maintenance}$	$A_{balloon}$	$W_{balloon}$	W_{nose_group}
53.000	10.500	251.989	8.189	0.730	513.872	72.970	30.300
53.000	10.500	250.599	8.179	0.729	513.186	72.872	30.300
53.000	10.500	249.209	8.168	0.728	512.500	72.775	30.300
53.000	10.500	247.819	8.157	0.727	511.814	72.678	30.300
53.000	10.500	246.429	8.146	0.726	511.127	72.580	30.300
53.000	10.500	245.039	8.135	0.725	510.440	72.482	30.300
53.000	10.500	243.649	8.124	0.724	509.752	72.385	30.300
53.000	10.500	242.259	8.113	0.723	509.064	72.287	30.300
53.000	10.500	240.869	8.102	0.722	508.376	72.189	30.300
53.000	10.500	239.479	8.090	0.721	507.687	72.092	30.300
53.000	10.500	238.089	8.080	0.720	506.997	71.994	30.300
53.000	10.500	236.699	8.069	0.719	506.307	71.896	30.300
53.000	10.500	235.309	8.058	0.718	505.616	71.798	30.300
53.000	10.500	233.919	8.047	0.717	504.925	71.699	30.300
53.000	10.500	232.529	8.036	0.716	504.234	71.601	30.300
53.000	10.500	231.139	8.025	0.715	503.542	71.503	30.300
53.000	10.500	229.749	8.014	0.714	502.850	71.405	30.300
53.000	10.500	228.359	8.003	0.713	502.157	71.306	30.300
53.000	10.500	226.969	7.992	0.712	501.463	71.208	30.300
53.000	10.500	225.579	7.981	0.711	500.770	71.109	30.300
53.000	10.500	224.189	7.970	0.710	500.075	71.011	30.300
53.000	10.500	222.799	7.959	0.709	499.381	70.912	30.300
53.000	10.500	221.409	7.947	0.708	498.685	70.813	30.300
53.000	10.500	220.019	7.937	0.707	497.990	70.715	30.300

Table A.8 Iteration Results for 0 Meters Altitude and -20°C (cont'd)

V_{hull}	W_{total}	$L_{airship}$	R_{major}	r_{major}	W_{Helium}	$W_{suspension\_system}$	$D_{airship}$
500.000	706.317	30.364	17.733	12.631	82.000	6.100	6.745
499.000	704.612	30.344	17.722	12.622	81.836	6.100	6.740
498.000	702.906	30.323	17.710	12.614	81.672	6.100	6.736
497.000	701.200	30.303	17.698	12.605	81.508	6.100	6.731
496.000	699.493	30.283	17.686	12.597	81.344	6.100	6.727
495.000	697.787	30.262	17.674	12.588	81.180	6.100	6.722
494.000	696.081	30.242	17.662	12.580	81.016	6.100	6.718
493.000	694.374	30.222	17.650	12.571	80.852	6.100	6.713
492.000	692.668	30.201	17.639	12.563	80.688	6.100	6.709
491.000	690.961	30.181	17.626	12.554	80.524	6.100	6.704
490.000	689.255	30.160	17.614	12.546	80.360	6.100	6.699
489.000	687.548	30.140	17.602	12.537	80.196	6.100	6.695
488.000	685.841	30.119	17.590	12.529	80.032	6.100	6.690
487.000	684.134	30.098	17.578	12.520	79.868	6.100	6.686
486.000	682.426	30.078	17.566	12.512	79.704	6.100	6.681
485.000	680.719	30.057	17.554	12.503	79.540	6.100	6.677
484.000	679.012	30.037	17.542	12.494	79.376	6.100	6.672
483.000	677.304	30.016	17.530	12.486	79.212	6.100	6.667
482.000	675.597	29.995	17.518	12.477	79.048	6.100	6.663
481.000	673.889	29.974	17.506	12.469	78.884	6.100	6.658
480.000	672.181	29.954	17.494	12.460	78.720	6.100	6.654
479.000	670.473	29.933	17.482	12.451	78.556	6.100	6.649
478.000	668.765	29.912	17.469	12.443	78.392	6.100	6.644
477.000	667.0572	29.891	17.457	12.434	78.228	6.100	6.640

Table A.9 Iteration Results for 0 Meters Altitude and -20°C (cont'd)

R_r	$F_{buoyancy}$ (N)	$F_{buoyancy}$ (kg)	$W_{GONDOLA}$	$W_{balloonet}$	W_{tail_system}	$V_{ballonet\_filled}$	W_{tail_cone}
3.372	6817.950	695.000	165.500	29.589	40.128	160.000	3.600
3.370	6804.314	693.610	165.500	29.589	40.075	159.000	3.600
3.368	6790.678	692.220	165.500	29.589	40.021	158.000	3.600
3.366	6777.042	690.830	165.500	29.589	39.968	157.000	3.600
3.363	6763.406	689.440	165.500	29.589	39.914	156.000	3.600
3.361	6749.771	688.050	165.500	29.589	39.861	155.000	3.600
3.359	6736.135	686.660	165.500	29.589	39.807	154.000	3.600
3.357	6722.499	685.270	165.500	29.589	39.753	153.000	3.600
3.354	6708.863	683.880	165.500	29.589	39.699	152.000	3.600
3.352	6695.227	682.490	165.500	29.589	39.645	151.000	3.600
3.350	6681.591	681.100	165.500	29.589	39.592	150.000	3.600
3.347	6667.955	679.710	165.500	29.589	39.538	149.000	3.600
3.345	6654.319	678.320	165.500	29.589	39.484	148.000	3.600
3.343	6640.683	676.930	165.500	29.589	39.430	147.000	3.600
3.341	6627.047	675.540	165.500	29.589	39.376	146.000	3.600
3.338	6613.412	674.150	165.500	29.589	39.322	145.000	3.600
3.336	6599.776	672.760	165.500	29.589	39.268	144.000	3.600
3.334	6586.140	671.370	165.500	29.589	39.214	143.000	3.600
3.331	6572.504	669.980	165.500	29.589	39.160	142.000	3.600
3.329	6558.868	668.590	165.500	29.589	39.105	141.000	3.600
3.327	6545.232	667.200	165.500	29.589	39.051	140.000	3.600
3.324	6531.596	665.810	165.500	29.589	38.997	139.000	3.600
3.322	6517.960	664.420	165.500	29.589	38.943	138.000	3.600
3.320	6504.324	663.030	165.500	29.589	38.888	137.000	3.600

Table A.10 Iteration Results for 1000 Meters Altitude and -30°C

W_{solar_sys}	$W_{propulsion\_system}$	$W_{ballonet\_system}$	$A_{ControlSurfaces}$	$W_{access\&maintenance}$	$A_{balloon}$	$W_{balloon}$	W_{nose_group}
53.000	10.500	183.669	8.189	0.730	513.872	72.970	30.300
53.000	10.500	182.385	8.179	0.729	513.186	72.872	30.300
53.000	10.500	181.101	8.168	0.728	512.500	72.775	30.300
53.000	10.500	179.817	8.157	0.727	511.814	72.678	30.300
53.000	10.500	178.533	8.146	0.726	511.127	72.580	30.300
53.000	10.500	177.249	8.135	0.725	510.440	72.482	30.300
53.000	10.500	175.966	8.124	0.724	509.752	72.385	30.300
53.000	10.500	174.681	8.113	0.723	509.064	72.287	30.300
53.000	10.500	173.397	8.102	0.722	508.376	72.189	30.300
53.000	10.500	172.113	8.091	0.721	507.687	72.091	30.300
53.000	10.500	170.829	8.080	0.720	506.997	71.994	30.300
53.000	10.500	169.545	8.069	0.719	506.307	71.896	30.300
53.000	10.500	168.261	8.058	0.718	505.616	71.797	30.300
53.000	10.500	166.977	8.047	0.717	504.925	71.699	30.300
53.000	10.500	165.693	8.036	0.716	504.234	71.601	30.300
53.000	10.500	164.409	8.025	0.715	503.542	71.503	30.300
53.000	10.500	163.125	8.014	0.714	502.850	71.405	30.300
53.000	10.500	161.841	8.003	0.713	502.157	71.306	30.300
53.000	10.500	160.557	7.992	0.712	501.463	71.208	30.300
53.000	10.500	159.273	7.981	0.711	500.770	71.109	30.300
53.000	10.500	157.989	7.970	0.710	500.075	71.011	30.300
53.000	10.500	156.705	7.959	0.709	499.381	70.912	30.300
53.000	10.500	155.421	7.947	0.708	498.685	70.813	30.300
53.000	10.500	154.137	7.936	0.707	497.990	70.715	30.300
53.000	10.500	152.853	7.925	0.706	497.293	70.616	30.300
53.000	10.500	151.569	7.914	0.705	496.597	70.517	30.300
53.000	10.500	150.285	7.903	0.704	495.899	70.418	30.300

Table A.11 Iteration Results for 1000 Meters Altitude and -30°C (cont'd)

V_{hull}	W_{total}	$L_{airship}$	R_{major}	r_{major}	W_{Helium}	$W_{suspension\_system}$	$D_{airship}$
500.000	637.997	30.364	17.733	12.631	82.000	6.100	6.745
499.000	636.398	30.344	17.722	12.622	81.836	6.100	6.740
498.000	634.798	30.323	17.710	12.614	81.672	6.100	6.736
497.000	633.198	30.303	17.698	12.605	81.508	6.100	6.731
496.000	631.597	30.283	17.686	12.597	81.344	6.100	6.727
495.000	629.997	30.262	17.674	12.588	81.180	6.100	6.722
494.000	628.397	30.242	17.662	12.580	81.016	6.100	6.718
493.000	626.796	30.222	17.650	12.571	80.852	6.100	6.713
492.000	625.196	30.201	17.638	12.563	80.688	6.100	6.709
491.000	623.595	30.181	17.626	12.554	80.524	6.100	6.704
490.000	621.995	30.160	17.614	12.546	80.360	6.100	6.699
489.000	620.394	30.140	17.602	12.537	80.196	6.100	6.695
488.000	618.793	30.119	17.590	12.529	80.032	6.100	6.690
487.000	617.192	30.098	17.578	12.520	79.868	6.100	6.686
486.000	615.590	30.078	17.566	12.512	79.704	6.100	6.681
485.000	613.989	30.057	17.554	12.503	79.540	6.100	6.677
484.000	612.388	30.037	17.542	12.494	79.376	6.100	6.672
483.000	610.786	30.016	17.530	12.486	79.212	6.100	6.667
482.000	609.185	29.995	17.518	12.477	79.048	6.100	6.663
481.000	607.583	29.974	17.506	12.469	78.884	6.100	6.658
480.000	605.981	29.954	17.494	12.460	78.720	6.100	6.654
479.000	604.379	29.933	17.482	12.451	78.556	6.100	6.649
478.000	602.777	29.912	17.469	12.443	78.392	6.100	6.644
477.000	601.175	29.891	17.457	12.434	78.228	6.100	6.640
476.000	599.573	29.870	17.445	12.425	78.064	6.100	6.635
475.000	597.971	29.849	17.433	12.416	77.900	6.100	6.630
474.000	596.368	29.828	17.420	12.408	77.736	6.100	6.626

Table A.12 Iteration Results for 1000 Meters Altitude and -30°C (cont'd)

R_r	$F_{buoyancy}$ (N)	$F_{buoyancy}$ (kg)	$W_{GONDOLA}$	$W_{balloonet}$	W_{tail_system}	$V_{ballonet\_filled}$	W_{tail_cone}
3.372	6298.020	642.000	165.500	29.589	40.128	120.000	3.600
3.370	6285.424	640.716	165.500	29.589	40.075	119.000	3.600
3.368	6272.828	639.432	165.500	29.589	40.021	118.000	3.600
3.366	6260.232	638.148	165.500	29.589	39.968	117.000	3.600
3.363	6247.636	636.864	165.500	29.589	39.914	116.000	3.600
3.361	6235.0398	635.580	165.500	29.589	39.861	115.000	3.600
3.359	6222.444	634.296	165.500	29.589	39.807	114.000	3.600
3.357	6209.848	633.012	165.500	29.589	39.753	113.000	3.600
3.354	6197.252	631.728	165.500	29.589	39.699	112.000	3.600
3.352	6184.656	630.444	165.500	29.589	39.645	111.000	3.600
3.350	6172.060	629.160	165.500	29.589	39.592	110.000	3.600
3.347	6159.464	627.876	165.500	29.589	39.538	109.000	3.600
3.345	6146.868	626.592	165.500	29.589	39.484	108.000	3.600
3.343	6134.271	625.308	165.500	29.589	39.430	107.000	3.600
3.341	6121.675	624.024	165.500	29.589	39.376	106.000	3.600
3.338	6109.079	622.740	165.500	29.589	39.322	105.000	3.600
3.336	6096.483	621.456	165.500	29.589	39.268	104.000	3.600
3.334	6083.887	620.172	165.500	29.589	39.214	103.000	3.600
3.331	6071.291	618.888	165.500	29.589	39.160	102.000	3.600
3.329	6058.695	617.604	165.500	29.589	39.105	101.000	3.600
3.327	6046.099	616.320	165.500	29.589	39.0511	100.000	3.600
3.324	6033.503	615.036	165.500	29.589	38.997	99.000	3.600
3.322	6020.907	613.752	165.500	29.589	38.943	98.000	3.600
3.320	6008.311	612.468	165.500	29.589	38.888	97.000	3.600
3.318	5995.715	611.184	165.500	29.589	38.834	96.000	3.600
3.316	5983.119	609.900	165.500	29.589	38.779	95.000	3.600
3.313	5970.523	608.616	165.500	29.589	38.725	94.000	3.600

APPENDIX B

DRAWINGS

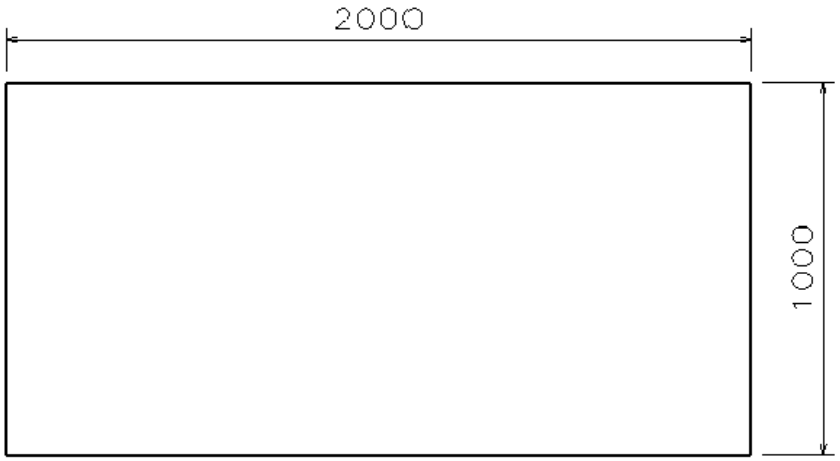

Figure B.1 Top View of the Gondola

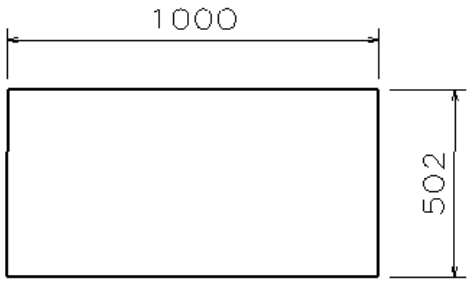

Figure B 2 Side View of the Gondola

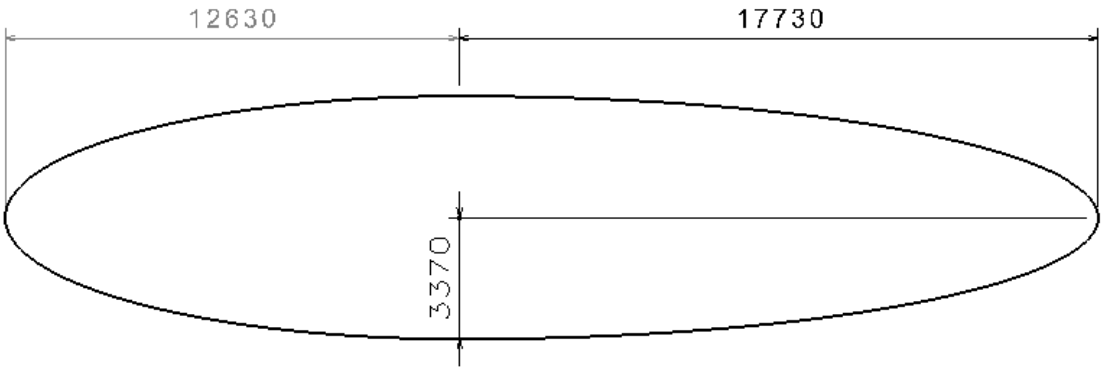

Figure B.3 Side View of the Airship Hull

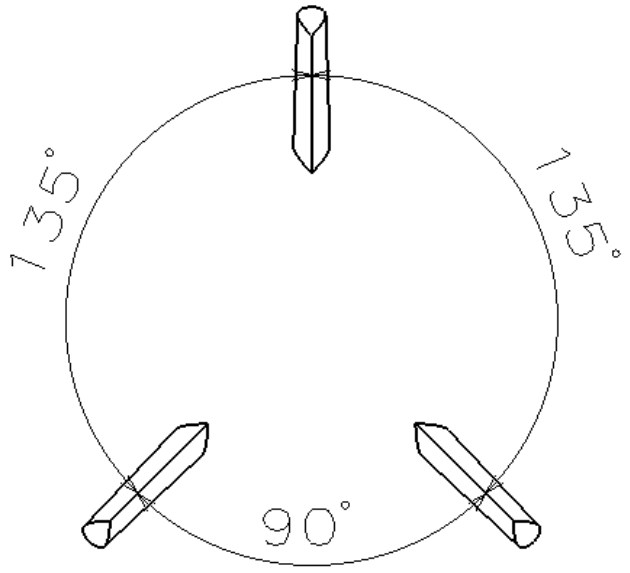

Figure B.4 Rear View of Tail (1)

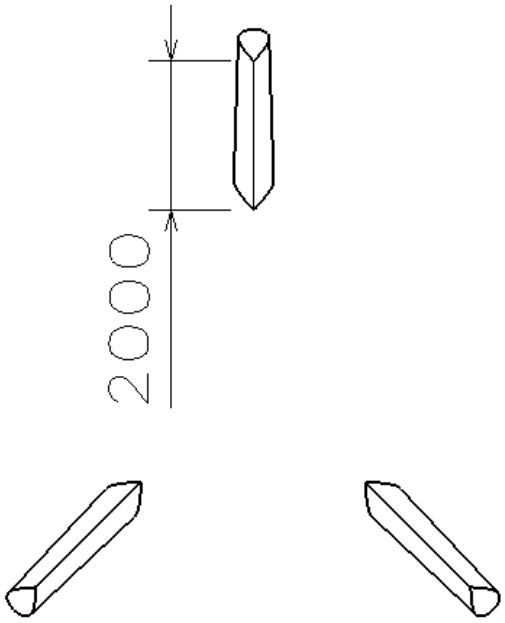

Figure B.5 Rear View of Tail (2)

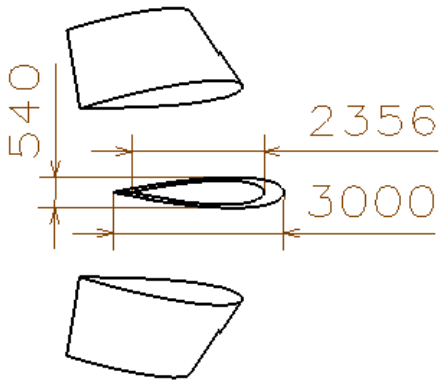

Figure B 6 Top View of Tail

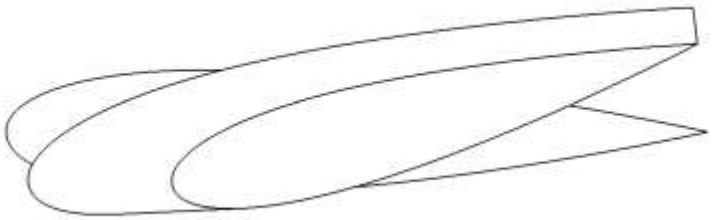

Figure B.7 Top View of the all-moving vertical tail for 15° tail incident angle

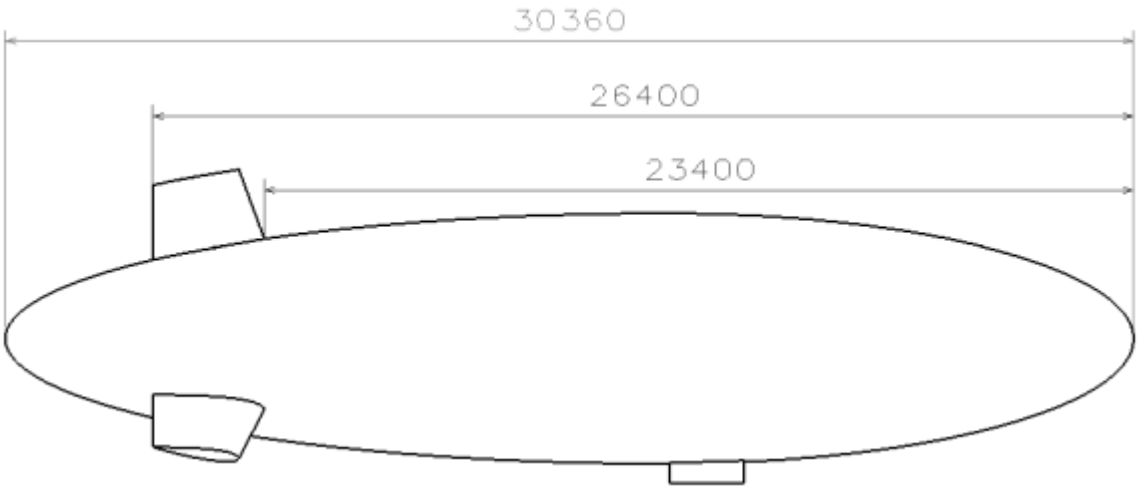

Figure B.8 Side View of the Airship System for 0° tail incident angle

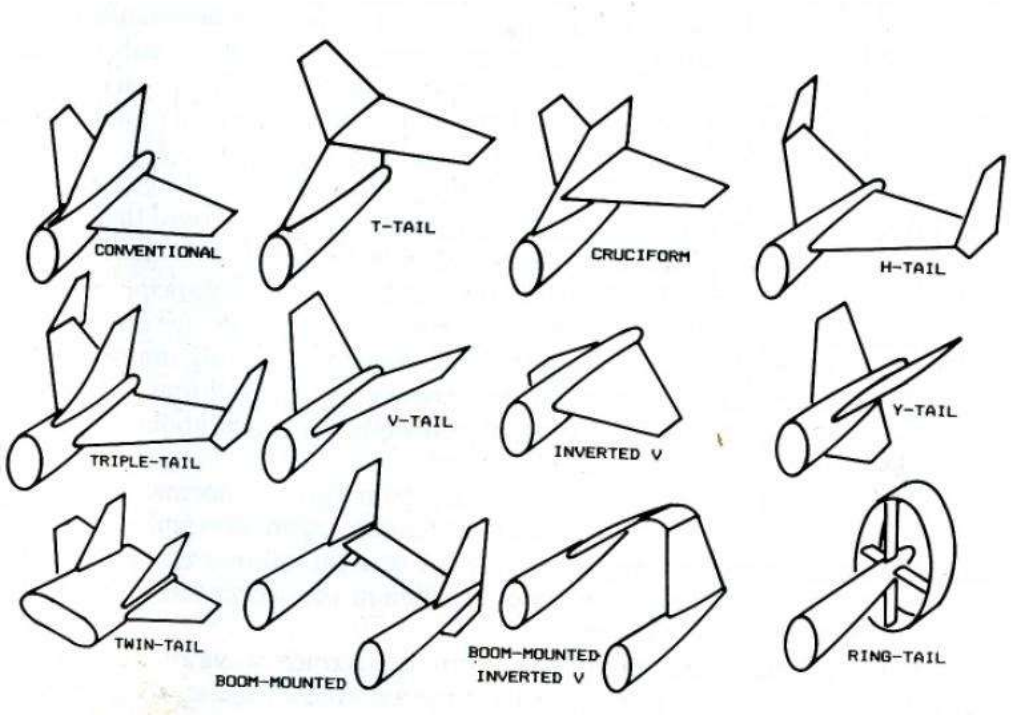

Figure B.9 Tail Types